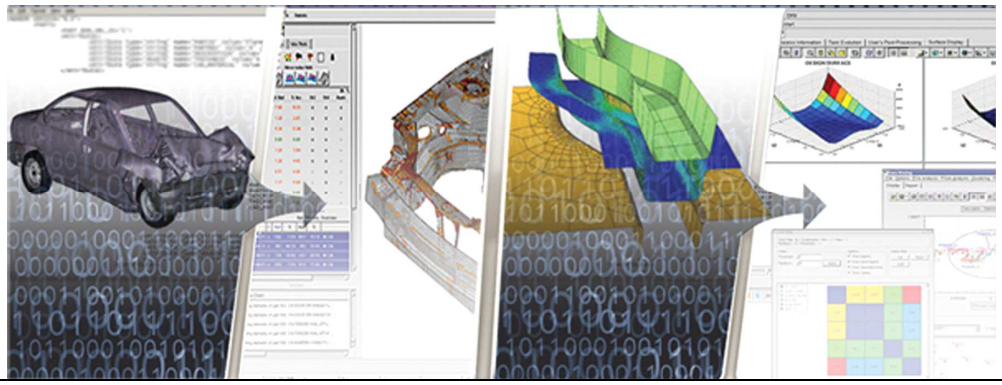

RADIOSS THEORY MANUAL

Version 2017 – January 2017

Large Displacement Finite Element Analysis
Chapter 5

Altair Engineering, Inc., World Headquarters: 1820 E. Big Beaver Rd., Troy MI 48083-2031 USA
Phone: +1.248.614.2400 • Fax: +1.248.614.2411 • www.altair.com • info@altair.com

CONTENTS

Chapter 5

ELEMENT LIBRARY

5.0 ELEMENT LIBRARY

RADIOSS element library contains elements for one, two or three dimensional problems. Some new elements have been developed and implemented in recent versions. Most of them use the assumed strain method to avoid some locking problems. For the elements using reduced integration schema, the physical stabilization method is used to control efficiently the hourglass deformations. Another point in these new elements is the use of co-rotational coordinate system. For the new solid elements, as the assumed strains are often defined in the specific directions, the use of global system combined with Jaumman's stress derivation contributes to commutative error especially when solid undergoes large shear strains.

The RADIOSS finite element library can be classified into the following categories of elements:

- Solid elements : 8- and 20-node bricks, 4- and 10-node tetrahedrons,
- Solid-shells : 8- , 16- and 20-node hexahedrons, 6-node pentahedral element,
- 2 dimensional elements : 4-node quadrilaterals for plane strain and axisymmetrical analysis,
- Shell elements : 4-node quadrilaterals and 3-node triangles,
- One dimensional elements: rivet, springs, bar and beams.

The implementation of these elements will now be detailed. Expression of nodal forces will be developed as, for explicit codes they represent the discretization of the momentum equations. Stiffness matrices, which are central to implicit finite element approaches, are not developed here.

5.1 Solid Hexahedron Elements

RADIOSS brick elements have the following properties:

- BRICK8: 8-node linear element with reduced or full integration,
- HA8: 8-node linear element with various number of integration points going from 2x2x2 to 9x9x9,
- HEPH: 8-node linear element with reduced integration point and physical stabilization of hourglass modes,
- BRICK20: 20-node quadratic element with reduced or full integration schemes.

For all elements, a lumped mass approach is used and the elements are isoparametric, i.e. the same shape functions are used to define element geometry and element displacements

The fundamental theory of each element is described in this chapter.

5.1.1 Shape functions for linear bricks

Shape functions define the geometry of an element in its computational (intrinsic) domain. As was seen in Chapter 3, physical coordinates are transformed into simpler computational intrinsic coordinates so that integration of values is numerically more efficient.

Figure 5.1.1 8 Node Brick Element

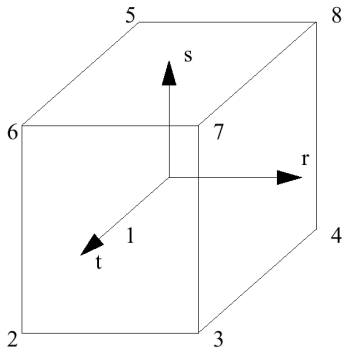

Where: $r \equiv \xi$, $s \equiv \eta$, $t \equiv \zeta$

The shape functions of an 8 node brick element, shown in Figure 5.1.1, are given by:

$$\Phi_1 = \frac{1}{8}(1-\xi)(1-\eta)(1-\zeta)$$ EQ. 5.1.1.1

$$\Phi_2 = \frac{1}{8}(1-\xi)(1-\eta)(1+\zeta)$$ EQ. 5.1.1.2

$$\Phi_3 = \frac{1}{8}(1+\xi)(1-\eta)(1+\zeta)$$ EQ. 5.1.1.3

$$\Phi_4 = \frac{1}{8}(1+\xi)(1-\eta)(1-\zeta)$$ EQ. 5.1.1.4

$$\Phi_5 = \frac{1}{8}(1-\xi)(1+\eta)(1-\zeta)$$ EQ. 5.1.1.5

$$\Phi_6 = \frac{1}{8}(1-\xi)(1+\eta)(1+\zeta)$$ EQ. 5.1.1.6

$$\Phi_7 = \frac{1}{8}(1+\xi)(1+\eta)(1+\zeta)$$ EQ. 5.1.1.7

$$\Phi_8 = \frac{1}{8}(1+\xi)(1+\eta)(1-\zeta)$$ EQ. 5.1.1.8

The element velocity field is related by:

$$v_i = \sum_{I=1}^{8} \Phi_I . v_{iI}$$ EQ. 5.1.1.9

where the v_{iI} are the nodal velocities.

5.1.2 Strain rate

The relationship between the physical coordinate and computational intrinsic coordinates system for a brick element is given by the matrix equation:

$$\begin{bmatrix} \frac{\partial \Phi_I}{\partial \xi} \\ \frac{\partial \Phi_I}{\partial \eta} \\ \frac{\partial \Phi_I}{\partial \zeta} \end{bmatrix} = \begin{bmatrix} \frac{\partial x}{\partial \xi} & \frac{\partial y}{\partial \xi} & \frac{\partial z}{\partial \xi} \\ \frac{\partial x}{\partial \eta} & \frac{\partial y}{\partial \eta} & \frac{\partial z}{\partial \eta} \\ \frac{\partial x}{\partial \zeta} & \frac{\partial y}{\partial \zeta} & \frac{\partial z}{\partial \zeta} \end{bmatrix} . \begin{bmatrix} \frac{\partial \Phi_I}{\partial x} \\ \frac{\partial \Phi_I}{\partial y} \\ \frac{\partial \Phi_I}{\partial z} \end{bmatrix} = F_\xi . \begin{bmatrix} \frac{\partial \Phi_I}{\partial x} \\ \frac{\partial \Phi_I}{\partial y} \\ \frac{\partial \Phi_I}{\partial z} \end{bmatrix} \qquad \text{EQ. 5.1.2.1}$$

Hence:

$$\begin{bmatrix} \frac{\partial \Phi_I}{\partial x_i} \end{bmatrix} = F_\xi^{-1} . \begin{bmatrix} \frac{\partial \Phi_I}{\partial \xi} \end{bmatrix} \qquad \text{EQ. 5.1.2.2}$$

where F_ξ is the Jacobian matrix.

The element strain rate is defined as:

$$\dot{\varepsilon}_{ij} = \frac{1}{2}\left(\frac{\partial v_i}{\partial x_j} + \frac{\partial v_j}{\partial x_i} \right) \qquad \text{EQ. 5.1.2.3}$$

Relating the element velocity field to its shape function gives:

$$\frac{\partial v_i}{\partial x_j} = \sum_{I=1}^{8} \frac{\partial \Phi_I}{\partial x_j} \cdot v_{iI} \qquad \text{EQ. 5.1.2.4}$$

Hence, the strain rate can be described directly in terms of the shape function:

$$\dot{\varepsilon}_{ij} = \frac{1}{2}\left(\frac{\partial v_i}{\partial x_j} + \frac{\partial v_j}{\partial x_i} \right) = \sum_{I=1}^{8} \frac{\partial \Phi_I}{\partial x_j} \cdot v_{iI} \qquad \text{EQ. 5.1.2.5}$$

As was seen in section 2.4.1, volumetric strain rate is calculated separately by volume variation.

For one integration point:

$$\frac{\partial \Phi_1}{\partial x_j} = -\frac{\partial \Phi_7}{\partial x_j}; \quad \frac{\partial \Phi_2}{\partial x_j} = -\frac{\partial \Phi_8}{\partial x_j}; \quad \frac{\partial \Phi_3}{\partial x_j} = -\frac{\partial \Phi_5}{\partial x_j}; \quad \frac{\partial \Phi_4}{\partial x_j} = -\frac{\partial \Phi_6}{\partial x_j} \qquad \text{EQ. 5.1.2.6}$$

F.E Method is used only for deviatoric strain rate calculation in A.L.E and Euler formulation.

Volumetric strain rate is computed separately by transport of density and volume variation.

5.1.3 Assumed strain rate

Using Voigt convention, the strain rate of EQ. 5.1.2.5 can be written as:

$$\{\dot{\varepsilon}\} = [B]\{v\} = \sum_{I=1}^{8} [B_I]\{v_I\} \qquad \text{EQ. 5.1.3.1}$$

With,

$$\{\dot{\varepsilon}\}=\left\langle \dot{\varepsilon}_{xx} \quad \dot{\varepsilon}_{yy} \quad \dot{\varepsilon}_{zz} \quad 2\dot{\varepsilon}_{xy} \quad 2\dot{\varepsilon}_{yz} \quad 2\dot{\varepsilon}_{xz} \right\rangle^t$$

$$[B_I]=\begin{bmatrix} \frac{\partial \Phi_I}{\partial x} & 0 & 0 & 0 & \frac{\partial \Phi_I}{\partial x} & \frac{\partial \Phi_I}{\partial y} \\ 0 & \frac{\partial \Phi_I}{\partial y} & 0 & \frac{\partial \Phi_I}{\partial x} & 0 & \frac{\partial \Phi_I}{\partial z} \\ 0 & 0 & \frac{\partial \Phi_I}{\partial z} & \frac{\partial \Phi_I}{\partial y} & \frac{\partial \Phi_I}{\partial z} & 0 \end{bmatrix}^t$$

It is useful to take the Belytschko-Bachrach's mix form [27] of the shape functions written by:

$$\Phi_I(x,y,z,\xi,\eta,\zeta)=\Delta_I+b_{xI}\cdot x+b_{yI}\cdot y+b_{zI}\cdot z+\sum_{\alpha=1}^{4}\gamma_I^\alpha\phi_\alpha \qquad \text{EQ. 5.1.3.2}$$

Where,

$$b_{iI}=\frac{\partial \Phi_I}{\partial x_i}(\xi=\eta=\zeta=0);$$

$$\gamma_I^\alpha=\frac{1}{8}\left[\Gamma_I^\alpha-\left(\sum_{J=1}^{8}\Gamma_J^\alpha x_J\right)b_{xI}-\left(\sum_{J=1}^{8}\Gamma_J^\alpha y_J\right)b_{yI}-\left(\sum_{J=1}^{8}\Gamma_J^\alpha z_J\right)b_{zI}\right];$$

$$\langle\phi\rangle=\langle\eta\zeta \quad \xi\zeta \quad \xi\eta \quad \xi\eta\zeta\rangle$$

The derivation of the shape functions is given by:

$$\frac{\partial \Phi_I}{\partial x_i}=b_{iI}+\sum_{\alpha=1}^{4}\gamma_I^\alpha\frac{\partial\phi_\alpha}{\partial x_i} \qquad \text{EQ. 5.1.3.3}$$

It is decomposed by a constant part which is directly formulated with the Cartesian coordinates, and a non-constant part which is to be approached separately. For the strain rate, only the non-constant part is modified by the assumed strain. You can see in the following that the non-constant part or the high order part is just the hourglass terms.

You now have the decomposition of the strain rate:

$$\{\dot{\varepsilon}\}=\sum_{I=1}^{8}[B_I]\{v_I\}=\sum_{I=1}^{8}\left([B_I]^0+[B_I]^H\right)\{v_I\}=\{\dot{\varepsilon}\}^0+\{\dot{\varepsilon}\}^H \qquad \text{EQ. 5.1.3.4}$$

with:

$$[B_I]^0=\begin{bmatrix} b_{xI} & 0 & 0 \\ 0 & b_{yxI} & 0 \\ 0 & 0 & b_{zI} \\ b_{yxI} & b_{xI} & 0 \\ b_{zI} & 0 & b_{xI} \\ 0 & b_{zI} & b_{yxI} \end{bmatrix};[B_I]^H=\begin{bmatrix} \sum_{\alpha=1}^{4}\gamma_I^\alpha\frac{\partial\phi_\alpha}{\partial x} & 0 & 0 & 0 & \sum_{\alpha=1}^{4}\gamma_I^\alpha\frac{\partial\phi_\alpha}{\partial x} & \sum_{\alpha=1}^{4}\gamma_I^\alpha\frac{\partial\phi_\alpha}{\partial y} \\ 0 & \sum_{\alpha=1}^{4}\gamma_I^\alpha\frac{\partial\phi_\alpha}{\partial y} & 0 & \sum_{\alpha=1}^{4}\gamma_I^\alpha\frac{\partial\phi_\alpha}{\partial x} & 0 & \sum_{\alpha=1}^{4}\gamma_I^\alpha\frac{\partial\phi_\alpha}{\partial z} \\ 0 & 0 & \sum_{\alpha=1}^{4}\gamma_I^\alpha\frac{\partial\phi_\alpha}{\partial z} & \sum_{\alpha=1}^{4}\gamma_I^\alpha\frac{\partial\phi_\alpha}{\partial y} & \sum_{\alpha=1}^{4}\gamma_I^\alpha\frac{\partial\phi_\alpha}{\partial z} & 0 \end{bmatrix}^t$$

Belytschko and Bindeman [65] ASQBI assumed strain is used:

$$\{\dot{\varepsilon}\} = \sum_{I=1}^{8} \left([B_I]^0 + [\bar{B}_I]^H \right) \{v_I\} \qquad \text{EQ. 5.1.3.5}$$

with

$$[\bar{B}_I]^H = \begin{bmatrix} X_I^{1234} & -\bar{\nu}Y_I^3 - \nu Y_I^{24} & -\bar{\nu}Z_I^2 - \nu Z_I^{34} \\ -\bar{\nu}X_I^3 - \nu X_I^{14} & Y_I^{1234} & -\bar{\nu}Z_I^1 - \nu Z_I^{34} \\ -\bar{\nu}X_I^2 - \nu X_I^{14} & -\bar{\nu}Y_I^1 - \nu Y_I^{24} & Z_I^{1234} \\ Y_I^{12} & X_I^{12} & 0 \\ Z_I^{13} & 0 & X_I^{13} \\ 0 & Z_I^{23} & Y_I^{23} \end{bmatrix}$$

where $X_I^{13} = \gamma_I^1 \frac{\partial \phi_1}{\partial x} + \gamma_I^3 \frac{\partial \phi_3}{\partial x}$; $Y_I^{13} = \gamma_I^1 \frac{\partial \phi_1}{\partial y} + \gamma_I^3 \frac{\partial \phi_3}{\partial y}$; $\bar{\nu} = \frac{\nu}{1-\nu}$;

To avoid shear locking, some hourglass modes are eliminated in the terms associated with shear so that no shear strain occurs during pure bending. E.g.: Y_I^3, X_I^3 in $\dot{\varepsilon}_{xy}$ terms and all fourth hourglass modes in shear terms are also removed since this mode is non-physical and is stabilized by other terms in $[\bar{B}_I]^H$.

The terms with Poisson coefficient are added to obtain an isochoric assumed strain field when the nodal velocity is equivoluminal. This avoids volumetric locking as $\nu = 0.5$. In addition, these terms enable the element to capture transverse strains which occurs in a beam or plate in bending. The plane strain expressions are used since this prevents incompatibility of the velocity associated with the assumed strains.

5.1.3.1 Incompressible or quasi-incompressible cases

(Flag for new solid element: Icpr =0,1,2)

For incompressible or quasi- incompressible materials, the new solid elements have no volume locking problem due to the assumed strain. Another way to deal with this problem is to decompose the stress field into the spherical part and the deviatory part and use reduced integration for spherical part so that the pressure is constant. This method has the advantage on the computation time, especially for the full integrated element. For some materials which the incompressibility can be changed during computation (for example: elastoplastic material, which becomes incompressible as the growth of plasticity), the treatment is more complicated. Since the elastoplastic material with large strain is the most frequently used, the constant pressure method has been chosen for RADIOSS usual solid elements. The flag Icpr has been introduced for new solid elements.

- Icpr =0: assumed strain with ν terms is used.
- Icpr =1: assumed strain without ν terms and with a constant pressure method is used. The method is recommended for incompressible (initial) materials.
- Icpr =2: assumed strain with ν terms is used, where ν is variable in function of the plasticity state. The formulation is recommended for elastoplastic materials.

5.1.4 Internal force calculation

Internal forces are computed using the generalized relation:

$$f_{iI}^{\text{int}} = \int_{\Omega} \sigma_{ij} \frac{\partial \Phi_I}{\partial x_j} d\Omega \qquad \text{EQ. 5.1.4.1}$$

However, to increase the computational speed of the process, some simplifications are applied.

5.1.4.1 Reduced Integration Method

This is the default method for computing internal forces. A one point integration scheme with constant stress in the element is used. Due to the nature of the shape functions, the amount of computation can be substantially reduced:

$$\frac{\partial \Phi_1}{\partial x_j} = -\frac{\partial \Phi_7}{\partial x_j}; \quad \frac{\partial \Phi_2}{\partial x_j} = -\frac{\partial \Phi_8}{\partial x_j}; \quad \frac{\partial \Phi_3}{\partial x_j} = -\frac{\partial \Phi_5}{\partial x_j}; \quad \frac{\partial \Phi_4}{\partial x_j} = -\frac{\partial \Phi_6}{\partial x_j} \qquad \text{EQ. 5.1.4.2}$$

Hence, the value $\frac{\partial \Phi_I}{\partial x_j}$ is taken at the integration point and the internal force is computed using the relation:

$$F_{iI} = \sigma_{ij}\left(\frac{\partial \Phi_I}{\partial x_j}\right)_0 \Omega \qquad \text{EQ. 5.1.4.3}$$

The force calculation is exact for the special case of the element being a parallelepiped.

5.1.4.2 Full Integration Method

The final approach that can be used is the full generalized formulation found in EQ. 5.1.4.1. A classical eight point integration scheme, with non-constant stress, but constant pressure is used to avoid locking problems. This is computationally expensive, having eight deviatoric stress tensors, but will produce accurate results with no hourglass.

When assumed strains are used with full integration (HA8 element), the reduced integration of pressure is no more necessary, as the assumed strain is then a free locking problem.

5.1.4.3 Improved Integration Method for ALE

This is an ALE method for computing internal forces (flag INTEG). A constant stress in the element is used.

The value $\int_\Omega \frac{\partial \Phi_I}{\partial x_j} d\Omega$ is computed with Gauss points.

5.1.5 Hourglass modes

Hourglass modes are element distortions that have zero strain energy. Thus, no stresses are created within the element. There are 12 hourglass modes for a brick element, 4 modes for each of the 3 coordinate directions. Γ represents the hourglass mode vector, as defined by Flanagan-Belytschko [12]. They produce linear strain modes, which cannot be accounted for using a standard one point integration scheme.

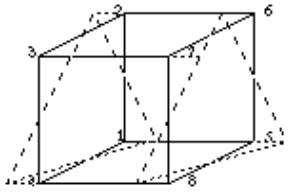

$$\Gamma^1 = (+1,-1,+1,-1,+1,-1,+1,-1)$$

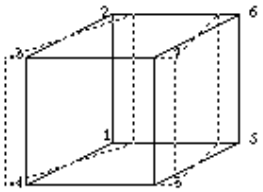

$$\Gamma^2 = (+1,+1,-1,-1,-1,-1,+1,+1)$$

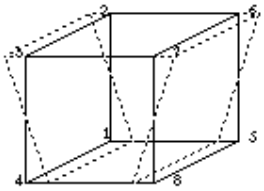

$$\Gamma^3 = (+1,-1,-1,+1,-1,+1,+1,-1)$$

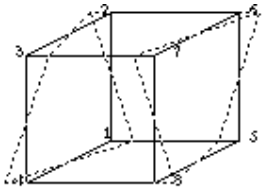

$$\Gamma^4 = (+1,-1,+1,-1,-1,+1,-1,+1)$$

To correct this phenomenon, it is necessary to introduce anti-hourglass forces and moments. Two possible formulations are presented hereafter.

5.1.5.1 Kosloff & Frasier Formulation [10]

The Kosloff-Frasier hourglass formulation uses a simplified hourglass vector. The hourglass velocity rates are defined as:

$$\frac{\partial q_i^\alpha}{\partial t} = \sum_{I=1}^{8} \Gamma_I^\alpha \cdot v_{iI} \qquad \text{EQ. 5.1.5.1}$$

where:

- Γ is the non-orthogonal hourglass mode shape vector,
- v is the node velocity vector,
- *i* is the direction index, running from 1 to 3,
- *I* is the node index, from 1 to 8,
- α is the hourglass mode index, from 1 to 4.

This vector is not perfectly orthogonal to the rigid body and deformation modes.

All hourglass formulations except the physical stabilization formulation for solid elements in RADIOSS use a viscous damping technique. This allows the hourglass resisting forces to be given by:

$$f_{iI}^{hgr} = \frac{1}{4}\rho c h \left(\sqrt[3]{\Omega}\right)^2 \sum_\alpha \frac{\partial q_i^\alpha}{\partial t} \cdot \Gamma_I^\alpha \qquad \text{EQ. 5.1.5.2}$$

where:

- ρ is the material density,
- c is the sound speed,
- h is a dimensional scaling coefficient defined in the input,
- Ω is the volume.

5.1.5.2 Flanagan-Belytschko Formulation [12]

In the Kosloff-Frasier formulation seen in section 5.1.5.1, the hourglass base vector Γ_I^α is not perfectly orthogonal to the rigid body and deformation modes that are taken into account by the one point integration scheme. The mean stress/strain formulation of a one point integration scheme only considers a fully linear velocity field, so that the physical element modes generally contribute to the hourglass energy. To avoid this, the idea in the Flanagan-Belytschko formulation is to build an hourglass velocity field which always remains orthogonal to the physical element modes. This can be written as:

$$v_{iI}^{Hour} = v_{iI} - v_{iI}^{Lin} \qquad \text{EQ. 5.1.5.3}$$

The linear portion of the velocity field can be expanded to give:

$$v_{iI}^{Hour} = v_{iI} - \left(\overline{v_{iI}} + \frac{\partial v_{iI}}{\partial x_j} \cdot \left(x_j - \overline{x_j} \right) \right) \qquad \text{EQ. 5.1.5.4}$$

Decomposition on the hourglass vectors base gives [12]:

$$\frac{\partial q_i^\alpha}{\partial t} = \Gamma_I^\alpha \cdot v_{iI}^{Hour} = \left(v_{iI} - \frac{\partial v_{il}}{\partial x_j} \cdot x_j \right) \cdot \Gamma_I^\alpha \qquad \text{EQ. 5.1.5.5}$$

where:

$\frac{\partial q_i^\alpha}{\partial t}$ are the hourglass modal velocities,

Γ_I^α is the hourglass vectors base.

Remembering that $\frac{\partial v_i}{\partial x_j} = \frac{\partial \Phi_j}{\partial x_j} \cdot v_{iJ}$ and factorizing EQ. 5.1.5.5 gives:

$$\frac{\partial q_i^\alpha}{\partial t} = v_{iI} \cdot \left(\Gamma_I^\alpha - \frac{\partial \Phi_j}{\partial x_j} x_j \Gamma_I^\alpha \right) \qquad \text{EQ. 5.1.5.6}$$

$$\gamma_I^\alpha = \Gamma_I^\alpha - \frac{\partial \Phi_j}{\partial x_j} x_j \Gamma_J^\alpha \qquad \text{EQ. 5.1.5.7}$$

is the hourglass shape vector used in place of Γ_I^α in EQ. 5.1.5.2.

5.1.5.3 physical hourglass formulation HEPH

You also try to decompose the internal force vector as follows:

$$\left\{f_I^{\text{int}}\right\}=\left\{\left(f_I^{\text{int}}\right)^0\right\}+\left\{\left(f_I^{\text{int}}\right)^H\right\} \qquad \text{EQ. 5.1.5.8}$$

In elastic case, you have:

$$\begin{aligned}\left\{f_I^{\text{int}}\right\}&=\int_\Omega [B_I]^t [C]\sum_{j=1}^{8}[B_J]\{v^J\}d\Omega \\ &=\int_\Omega \left([B_I]^0+[\overline{B}_I]^H\right)^t [C]\sum_{j=1}^{8}\left([B_J]^0+[\overline{B}_J]^H\right)\{v^J\}d\Omega\end{aligned} \qquad \text{EQ. 5.1.5.9}$$

The constant part $\left\{\left(f_I^{\text{int}}\right)^0\right\}=\int_\Omega \left([B_I]^0\right)^t [C]\sum_{j=1}^{8}[B_J]^0\{v^J\}d\Omega$ is evaluated at the quadrature point just like other one-point integration formulations mentioned before, and the non-constant part (Hourglass) will be calculated as following:

Taking the simplification of $\frac{\partial x_i}{\partial \xi_j}=0;(i\neq j)$ (that is the Jacobian matrix of EQ. 5.1.2.1 is diagonal), you have:

$$\left(f_{iI}^{\text{int}}\right)^H=\sum_{\alpha=1}^{4}Q_{i\alpha}\gamma_I^\alpha \qquad \text{EQ. 5.1.5.10}$$

with 12 generalized hourglass stress rates $\dot{Q}_{i\alpha}$ calculated by:

$$\begin{aligned}\dot{Q}_{ii}&=\mu\left[\left(H_{jj}+H_{kk}\right)\dot{q}_i^i+H_{ij}\dot{q}_j^j+H_{ik}\dot{q}_k^k\right] \\ \dot{Q}_{jj}&=\mu\left[\frac{1}{1-\nu}H_{ii}\dot{q}_i^j+\overline{\nu}H_{ij}\dot{q}_j^i\right] \\ \dot{Q}_{i4}&=2\mu\frac{1+\nu}{3}H_{ii}\dot{q}_j^4\end{aligned} \qquad \text{EQ. 5.1.5.11}$$

and

$$\begin{aligned}H_{ii}&=\int_\Omega\left(\frac{\partial\phi_j}{\partial x_i}\right)^2 d\Omega=\int_\Omega\left(\frac{\partial\phi_k}{\partial x_i}\right)^2 d\Omega=3\int_\Omega\left(\frac{\partial\phi_4}{\partial x_i}\right)^2 d\Omega \\ H_{ij}&=\int_\Omega\frac{\partial\phi_i}{\partial x_j}\frac{\partial\phi_j}{\partial x_i}d\Omega\end{aligned} \qquad \text{EQ. 5.1.5.12}$$

Where i,j,k are permuted between 1 to 3 and $\dot{q}_i^\alpha$ has the same definition than in EQ. 5.1.5.6.

Extension to non-linear materials has been done simply by replacing shear modulus μ by its effective tangent values which is evaluated at the quadrature point. For the usual elastoplastic materials, use a more sophistic procedure which is described in the following section.

5.1.5.3.1 Advanced elasto-plastic hourglass control

With one-point integration formulation, if the non-constant part follows exactly the state of constant part for the case of elasto-plastic calculation, the plasticity will be under-estimated due to the fact that the constant equivalent stress is often the smallest one in the element and element will be stiffer. Therefore, defining a yield criterion for the non-constant part seems to be a good idea to overcome this drawback.

Plastic yield criterion:

The von Mises type of criterion is written by:

$$f = \sigma_{eq}^2(\xi,\eta,\zeta) - \sigma_y^2 = 0 \qquad \text{EQ. 5.1.5.13}$$

for any point in the solid element, where σ_y is evaluated at the quadrature point.

As only one criterion is used for the non-constant part, two choices are possible:

1. taking the mean value, i.e.: $f = f(\overline{\sigma}_{eq}); \overline{\sigma}_{eq} = \frac{1}{\Omega}\int_{\Omega} \sigma_{eq} d\Omega$
2. taking the value by some representative points, for example: eight Gausse points

The second choice has been used in this element.

Elastro-plastic hourglass stress calculation:

The incremental hourglass stress is computed by:

- Elastic increment

  $(\sigma_i)_{n+1}^{trH} = (\sigma_i)_n^H + [C]\{\dot{\varepsilon}\}^H \Delta t$

- Check the yield criterion
- If $f \geq 0$, the hourglass stress correction will be done by un radial return

  $(\sigma_i)_{n+1}^H = P((\sigma_i)_{n+1}^{trH}, f)$

5.1.6 Stability

The stability of the numerical algorithm depends on the size of the time step used for time integration (section 4.5). For brick elements, RADIOSS uses the following equation to calculate the size of the time step:

$$h \leq k \frac{l}{c\left(\alpha + \sqrt{\alpha^2 + 1}\right)} \qquad \text{EQ. 5.1.6.1}$$

This is the same form as the Courant condition for damped materials. The characteristic length of a particular element is computed using:

$$l = \frac{Element\ Volume}{Largest\ Side\ Surface} \qquad \text{EQ. 5.1.6.2}$$

For a 6-sided brick, this length is equal to the smallest distance between two opposite faces.

The terms inside the parentheses in the denominator are specific values for the damping of the material:

- $\alpha = \frac{2\nu}{\rho c l}$
- ν effective kinematic viscosity,

- $c = \sqrt{\frac{1\partial p}{\rho \partial \rho}}$ for fluid materials,
- $c = \sqrt{\frac{K}{\rho} + \frac{4}{3}\frac{\mu}{\rho}} = \sqrt{\frac{\lambda + 2\mu}{\rho}}$ for a solid elastic material,
- K is the bulk modulus,
- λ , μ are Lame moduli.

The scaling factor *k=0.90*, is used to prevent strange results that may occur when the time step is equal to the Courant condition. This value can be altered by the user.

5.1.7 Shock waves

Shocks are non-isentropic phenomena, i.e. entropy is not conserved, and necessitates a special formulation.

The missing energy is generated by an artificial bulk viscosity q as derived by von Neumann and Richtmeyer [9]. This value is added to the pressure and is computed by:

$$q = q_a{}^2 \rho l^2 \left(\frac{\partial \varepsilon_{kk}}{\partial t} \right)^2 - q_b \rho l c \frac{\partial \varepsilon_{kk}}{\partial t} \qquad \text{EQ. 5.1.7.1}$$

where

- l is equal to $\sqrt[3]{\Omega}$ or to the characteristic length,
- Ω is the volume,
- $\frac{\partial \varepsilon_{kk}}{\partial t}$ is the volumetric compression strain rate tensor,
- c is the speed of sound in the medium.

The values of q_a and q_b are adimensional scalar factors defined as:

- q_a is a scalar factor on the quadratic viscosity to be adjusted so that the Hugoniot equations are verified. This value is defined by the user. The default value is 1.10.
- q_b is a scalar factor on the linear viscosity that damps out the oscillations behind the shock. This is user specified. The default value is 0.05.

Default values are adapted for velocities lower than Mach 2. However for viscoelastic materials (law 34, 35, 38) or honeycomb (law 28), very small values are recommended, i.e. 10^{-20}.

5.1.8 Element degeneration

Element degeneration is the collapsing of an element by one or more edges. For example: making an eight node element into a seven node element by giving nodes 7 and 8 the same node number.

The use of degenerated elements for fluid applications is not recommended. The use of degenerated elements for assumed strain formulation is not recommended. If they cannot be avoided, any two nodes belonging to a same edge can be collapsed, with some examples shown below.

For solid elements, it is recommended that element symmetry be maintained.

For 4 node elements, it is recommended that the special tetrahedron element be used.

Some examples of element degeneration are shown below.

Not recommended degenerations

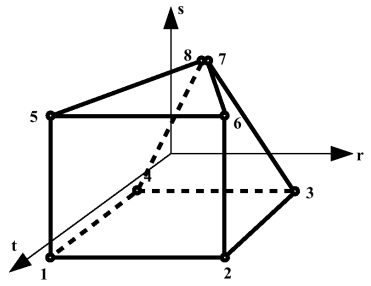

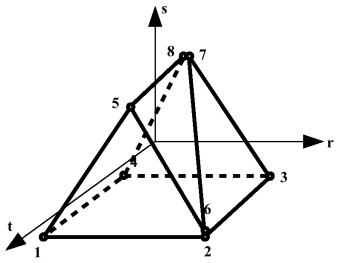

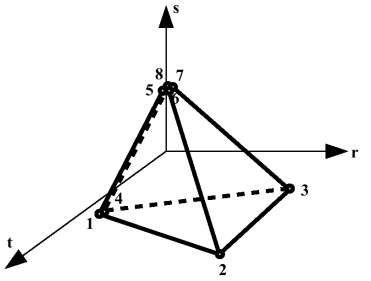

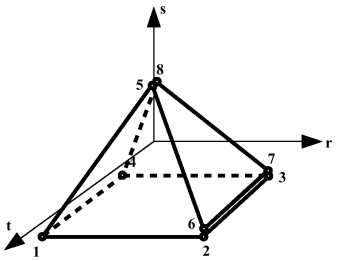

Recommended degeneration

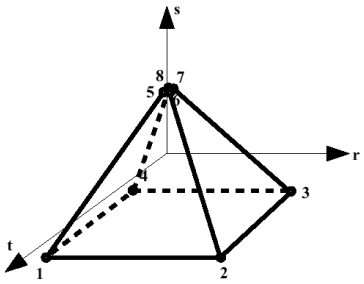

Connectivity: 1 2 3 4 5 5 5 5

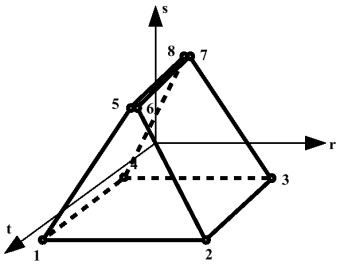

Connectivity: 1 2 3 4 5 6 6 5

5.1.9 Internal stress calculation

5.1.9.1 Global formulation

The time integration of stresses has been stated earlier (section 2.6.) as:

$$\sigma_{ij}(t+\Delta t) = \sigma_{ij}(t) + \dot{\sigma}_{ij}\Delta t \qquad \text{EQ. 5.1.9.1}$$

The stress rate is comprised of two components:

$$\dot{\sigma}_{ij} = \dot{\sigma}^{v}_{ij} + \dot{\sigma}^{r}_{ij} \qquad \text{EQ. 5.1.9.2}$$

where

- $\dot{\sigma}^{r}_{ij}$ is the stress rate due to the rigid body rotational velocity,
- $\dot{\sigma}^{v}_{ij}$ is the Jaumann objective stress tensor derivative.

The correction for stress rotation from time t to time t+ Δt is given by [2]:

$$\dot{\sigma}^{r}_{ij} = \sigma_{ik}\Omega_{kj} + \sigma_{jk}\Omega_{ki} \qquad \text{EQ. 5.1.9.3}$$

where Ω is the rigid body rotational velocity tensor (EQ. 2.4.1.11).

The Jaumann objective stress tensor derivative $\dot{\sigma}^{v}_{ij}$ is the corrected true stress rate tensor without rotational effects. The constitutive law is directly applied to the Jaumann stress rate tensor.

Deviatoric stresses and pressure (see section 2.7) are computed separately and related by:

$$\sigma_{ij} = s_{ij} - p\delta_{ij} \qquad \text{EQ. 5.1.9.4}$$

where

- s_{ij} is the deviatoric stress tensor;
- p is the pressure or mean stress - defined as positive in compression,
- δ_{ij} is the substitution tensor or unit matrix.

5.1.9.2 Co-rotational Formulation

A co-rotational formulation for bricks is a formulation where rigid body rotations are directly computed from the element's node positions. Objective stress and strain tensors are computed in the local (co-rotational) frame. Internal forces are computed in the local frame and then rotated to the global system.

So, when co-rotational formulation is used, EQ. 5.1.10.2 $\dot{\sigma}_{ij} = \dot{\sigma}^{v}_{ij} + \dot{\sigma}^{r}_{ij}$ reduces to:

$$\dot{\sigma}_{ij} = \dot{\sigma}^{v}_{ij} \qquad \text{EQ. 5.1.9.5}$$

where $\dot{\sigma}^{v}_{ij}$ is the Jaumann objective stress tensor derivative expressed in the co-rotational frame.

The following illustrates orthogonalization, when one of the r, s, t directions is orthogonal to the two other directions.

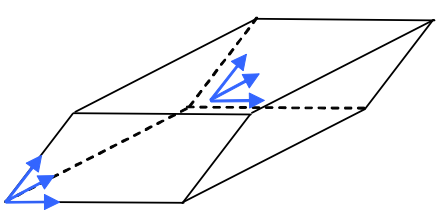

Isoparametric frames

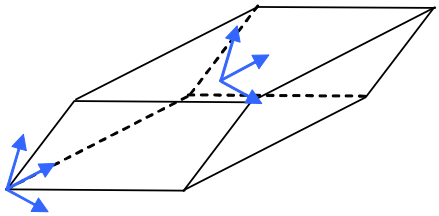

Local (co-rotational)

When large rotations occur, this formulation is more accurate than the global formulation, for which the stress rotation due to rigid body rotational velocity is computed in an incremental way.

Co-rotational formulation avoids this kind of problem.

Let us consider the following test:

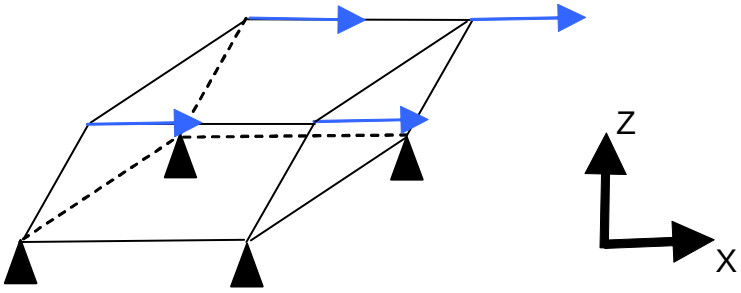

Fix constant velocity on the top of the

The increment of the rigid body rotation vector during time step Δt is:

$$\Delta\Omega = \Delta t/2 \cdot \begin{bmatrix} \left(\partial v_x/\partial y - \partial v_y/\partial x\right) = 0 \\ \left(\partial v_x/\partial z - \partial v_z/\partial x\right) = \partial v_x/\partial z \\ \left(\partial v_y/\partial x - \partial v_x/\partial y\right) = 0 \end{bmatrix} \qquad \text{EQ. 5.1.9.6}$$

So, $\Delta\Omega_y = \alpha\Delta T/2$ where $\alpha = v/h$ equals the imposed velocity on the top of the brick divided by the height of the brick (constant value).

Due to first order approximation, the increment of stress σ_{xx} due to the rigid body motion is:

$$\Delta\sigma_{xx}^r = \Delta\Omega_y\left(\tau_{xz} + \tau_{zx}\right) = 2\Delta\Omega_y\tau_{xz} = \alpha\Delta T\tau_{xz} \qquad \text{EQ. 5.1.9.7}$$

Increment of stress σ_{zz} due to the rigid body motion:

$$\Delta\sigma_{zz}^r = -\Delta\Omega_y\left(\tau_{xz} + \tau_{zx}\right) = -2\Delta\Omega_y\tau_{xz} = -\alpha\Delta T\tau_{xz} \qquad \text{EQ. 5.1.9.8}$$

Increment of shear stress τ_{xz} due to the rigid body motion:

$$\Delta\tau_{xz}^r = \Delta\Omega_y\left(\sigma_{zz} - \sigma_{xx}\right) = 2\Delta\Omega_y\sigma_{zz} = \alpha\Delta T\sigma_{zz} \qquad \text{EQ. 5.1.9.9}$$

Increment of shear strain:

$$\Delta\gamma_{xz} = \Delta T\left(\partial v_x/\partial z + \partial v_z/\partial x\right) = \alpha\Delta T \qquad \text{EQ. 5.1.9.10}$$

Increment of stress σ_{zz} due to strain:

$$\Delta\sigma_{zz}^v = 0 \qquad \text{EQ. 5.1.9.11}$$

and increment of shear stress due to strain is:

$$\Delta\tau_{xz}^{v} = G\Delta\gamma_{xz} = G\alpha\Delta T \qquad \text{EQ. 5.1.9.12}$$

where *G* is the shear modulus (material is linear elastic).

From EQ. 5.1.9.8 to EQ. 5.1.9.12, you have:

$$\begin{bmatrix} \Delta\tau_{xz} = \alpha\Delta T\sigma_{zz} + G\alpha\Delta T \\ \Delta\sigma_{zz} = -\alpha\Delta\tau_{xz} \end{bmatrix} \qquad \text{EQ. 5.1.9.13}$$

System EQ. 5.1.9.13 leads to:

$$\Delta\tau_{xz} / \Delta T^{2} = -\alpha^{2}\tau_{xz} \qquad \text{EQ. 5.1.9.14}$$

So, shear stress is sinusoidal and is not strictly increasing.

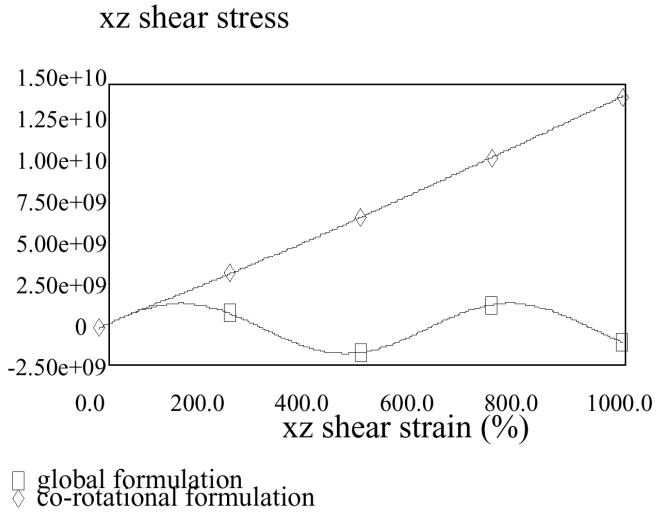

So, it is recommended to use co-rotational formulation, especially for visco-elastic materials such as foams, even if this formulation is more time consuming than the global one.

5.1.9.3 Co-rotational formulation and orthotropic material

When orthotropic material and global formulation are used, the fiber is attached to the first direction of the isoparametric frame and the fiber rotates a different way depending on the element numbering (see below).

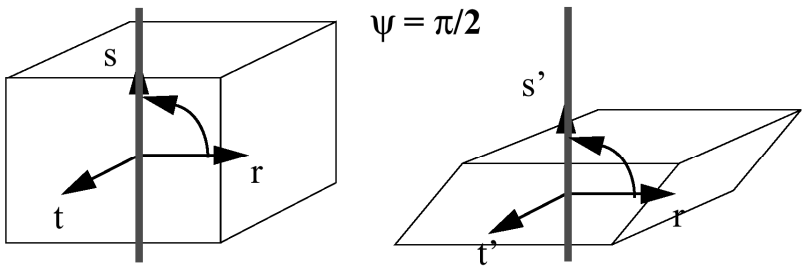

frame r, s', t' is obtained by orthogonalization of isoparametric frame

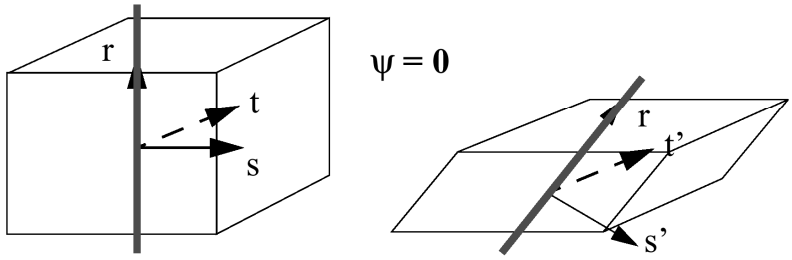

On the other hand, when the co-rotational formulation is used, the orthotropic frame keeps the same orientation with respect to the local (co-rotating) frame, and is therefore also co-rotating (see below).

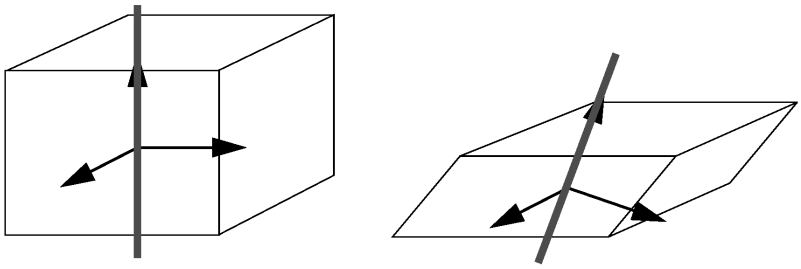

5.1.10 Deviatoric stress calculation

With the stress being separated into deviatoric and pressure (hydrostatic) stress (Section 2.7), it is the deviatoric stress that is responsible for the plastic deformation of the material. The hydrostatic stress will either shrink or expand the volume uniformly, i.e. with proportional change in shape. The determination of the deviatoric stress tensor and whether the material will plastically deform requires a number of steps.

STEP 1: Perform an Elastic Calculation

The deviatoric stress is time integrated from the previous known value using the strain rate to compute an elastic trial stress:

$$s_{ij}^{el}(t+\Delta t) = s_{ij}(t) + \dot{s}_{ij}^{r}\Delta t + 2G\left(\dot{\varepsilon}_{ij} - \frac{1}{3}\dot{\varepsilon}_{kk}\delta_{ij}\right)\Delta t \qquad \text{EQ. 5.1.10.1}$$

where *G* is the shear modulus.

This relationship is Hooke's Law, where the strain rate is multiplied by time to give strain.

STEP 2: Compute von Mises Equivalent Stress and Current Yield Stress

Depending on the type of material being modeled, the method by which yielding or failure is determined will vary. The following explanation relates to an elastoplastic material (LAW2).

The von Mises equivalent stress relates a three dimensional state of stress back to a simple case of uniaxial tension where material properties for yield and plasticity are well known and easily computed.

The von Mises stress, which is strain rate dependent, is calculated using the equation:

$$\sigma_{vm}^{e} = \sqrt{\frac{3}{2}s_{ij}^{el}s_{ij}^{el}} \qquad \text{EQ. 5.1.10.2}$$

The flow stress is calculated from the previous plastic strain:

$$\sigma_y(t) = a + b\varepsilon^{p^n}(t) \qquad \text{EQ. 5.1.10.3}$$

For material types 3, 4, 10, 21, 22, 23 and 36, EQ. 5.1.11.3 is modified according to the different modeling of the material curves.

STEP 3: Plasticity Check

The state of the deformation must be checked.

$$\sigma_{vm}^{e} - \sigma_y \leq 0$$

If this equation is satisfied, the state of stress is elastic. Otherwise, the flow stress has been exceeded and a plasticity rule must be used. This is shown in Figure 5.1.2.

Figure 5.1.2 - Plasticity Check

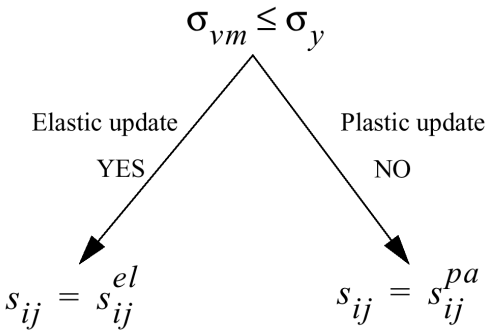

The plasticity algorithm used is due to Mendelson, [1].

STEP 4: Compute Hardening Parameter

The hardening parameter is defined as the slope of the strain-hardening part of the stress-strain curve:

$$H = \frac{d\sigma_y}{d\varepsilon^p} \qquad \text{EQ. 5.1.10.4}$$

This is used to compute the plastic strain at time *t*:

$$\dot{\varepsilon}^p \Delta t = \frac{\sigma_{vm} - \sigma_y}{3G + H} \qquad \text{EQ. 5.1.10.5}$$

This plastic strain is time integrated to determine the plastic strain at time $t + \Delta t$:

$$\varepsilon^p(t + \Delta t) = \varepsilon^p(t) + \dot{\varepsilon}^p \Delta t \qquad \text{EQ. 5.1.10.6}$$

The new flow stress is found using:

$$\sigma_y(t + \Delta t) = a + b\varepsilon^{p^n}(t + \Delta t) \qquad \text{EQ. 5.1.10.7}$$

STEP 5: Radial Return

There are many possible methods for obtaining s_{ij}^{pa} from the trial stress. The most popular method involves a simple projection to the nearest point on the flow surface, which results in the radial return method.

The radial return calculation is given in EQ. 5.1.10.8. Figure 5.1.3 is a graphic representation of radial return.

$$s_{ij}^{pa} = \frac{\sigma_y}{\sigma_{vm}} s_{ij}^{el} \qquad \text{EQ. 5.1.10.8}$$

Figure 5.1.3 - Radial Return

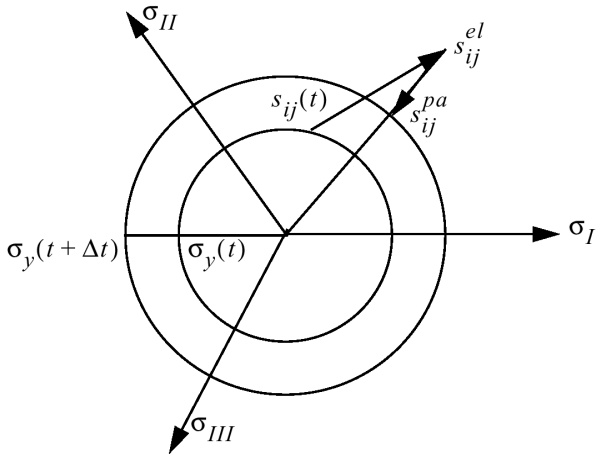

View along pure pressure axis , $\sigma_I = \sigma_{II} = \sigma_{III}$

5.2 Solid Tetrahedron Elements

5.2.1 4 node solid tetrahedron

The RADIOSS solid tetrahedron element is a 4 node element with one integration point and a linear shape function.

This element has no hourglass. But the drawbacks are the low convergence and the shear locking.

5.2.2 10 node solid tetrahedron

The RADIOSS solid tetrahedron element is a 10 nodes element with 4 integration points and a quadratic shape function as shown in Figure 5.2.1.

Figure 5.2.1 – (a) Isoparametric 10 node tetrahedron , **(b)** Nodal mass distribution

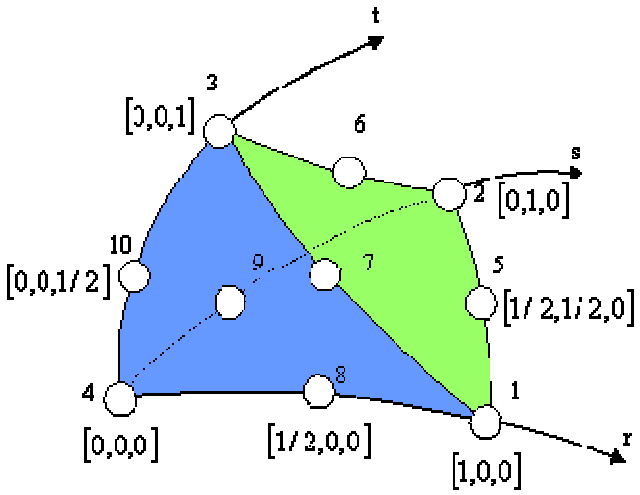

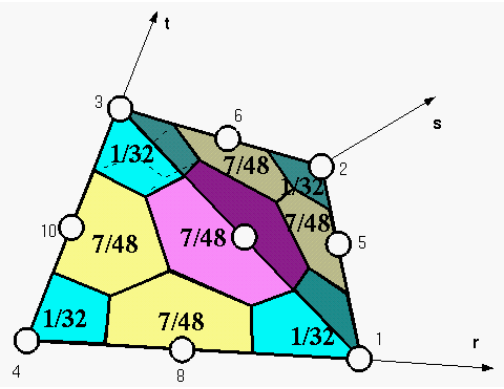

Introducing volume coordinates in an isoparametric frame:

$L_1 = r$

$L_2 = s$

$L_3 = t$

$L_4 = 1 - L_1 - L_2 - L_3$

The shape functions are expressed by:

$$\Phi_1 = (2L_1 - 1)L_1 \quad \text{EQ. 5.2.2.1}$$

$$\Phi_2 = (2L_2 - 1)L_2 \quad \text{EQ. 5.2.2.2}$$

$$\Phi_3 = (2L_3 - 1)L_3 \quad \text{EQ. 5.2.2.3}$$

$$\Phi_4 = (2L_4 - 1)L_4 \quad \text{EQ. 5.2.2.4}$$

$$\Phi_5 = 4L_1L_2 \quad \text{EQ. 5.2.2.5}$$

$$\Phi_6 = 4L_2L_3 \quad \text{EQ. 5.2.2.6}$$

$$\Phi_7 = 4L_3L_1 \quad \text{EQ. 5.2.2.7}$$

$$\Phi_8 = 4L_1L_4 \quad \text{EQ. 5.2.2.8}$$

$$\Phi_9 = 4L_2L_4 \quad \text{EQ. 5.2.2.9}$$

$$\Phi_{10} = 4L_3L_4 \quad \text{EQ. 5.2.2.10}$$

Location of the 4 integration points is expressed by [49].

	L_1	L_2	L_3	L_4
a	α	β	β	β
b	β	α	β	β
c	β	β	α	β
d	β	β	β	α

With,

$$\alpha = 0 \cdot 58541020 \text{ and } \beta = 0 \cdot 13819660$$

a, b, c, and d are the 4 integration points.

5.2.2.1 Advantages and drawbacks

This element has various advantages:

- No hourglass
- Compatible with powerful mesh generators
- Fast convergence
- No shear locking.

But there are some drawbacks too:

- Low time step
- Not compatible with ALE formulation
- No direct compatibility with contact interface and other elements.

5.2.2.2 Time step

The time step for a regular tetrahedron is computed as:

$$dt = \frac{L_c}{c}$$ EQ. 5.2.2.11

Where, L_c is the characteristic length of element depending on tetra type. The different types are shown in the following figures:

For a regular 4 node tetra as shown in Figure 5.2.2:

$$L_c = a\sqrt{\frac{2}{3}};\ L_c = 0.816a$$ EQ. 5.2.2.12

Figure 5.2.2 - 4 nodes tetra

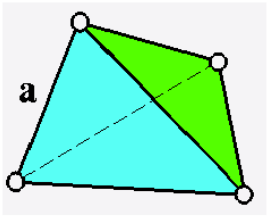

For a regular 10 node tetra as shown in Figure 5.2.3:

$$L_c = a\sqrt{\frac{5/2}{6}};\ L_c = 0.264a$$ EQ. 5.2.2.13

Figure 5.2.3 - 10 nodes tetra

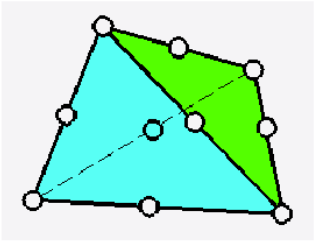

For another regular tetra obtained by the assemblage of four hexa as shown in Figure 5.2.4, the characteristic length is:

$$L_c = a\frac{\sqrt{2/3}}{4};\ L_c = 0.204a$$ EQ. 5.2.2.14

Figure 5.2.4 - Other regular tetra

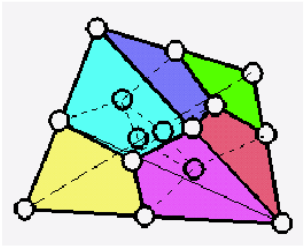

5.2.2.3 CPU cost: Time/Element/Cycle

The CPU cost is shown in Figure 5.2.5:

Figure 5.2.5 - CPU cost in TEC

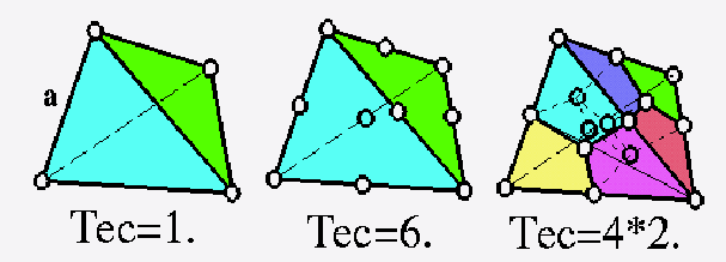

5.2.2.4 Comparison example

Below is a comparison of the 3 types of elements (8-nodes brick, 10-nodes tetra and 20-nodes brick). The results are shown in Figure 5.2.6 for a plastic strain contour.

Figure 5.2.6 - Comparison (plastic strain max = 60%)

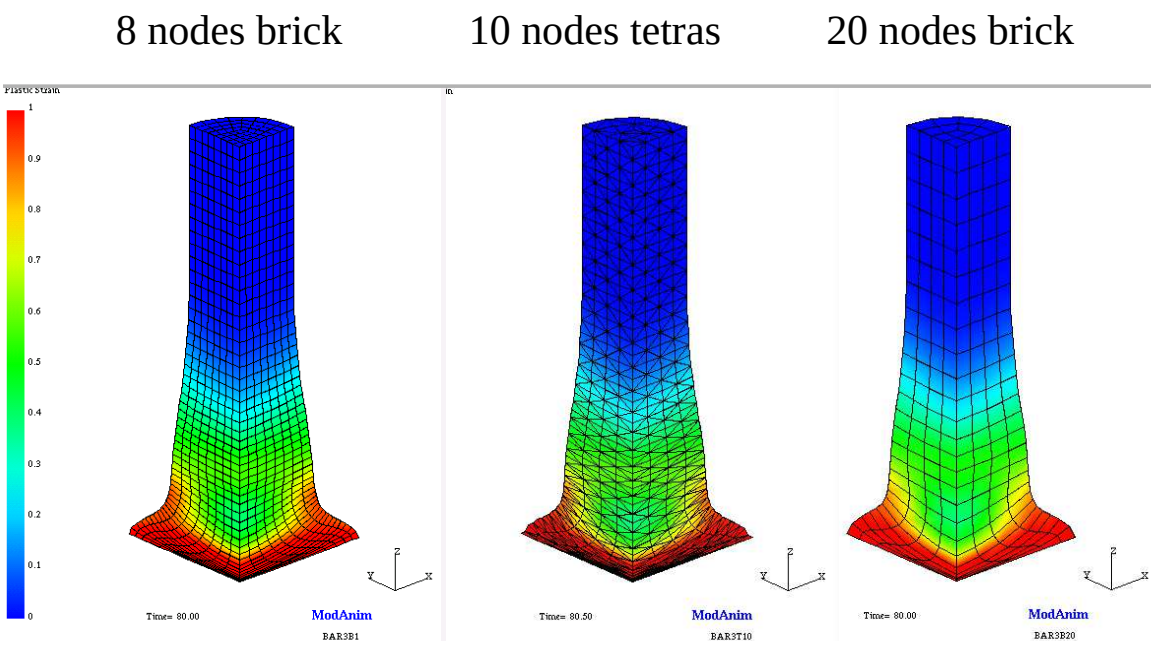

5.3 SHELL ELEMENTS

Since the degenerated continuum shell element formulation was introduced by Ahmad et al.[38], it has become dominant in commercial Finite Element codes due to its advantage of being independent of any particular shell theory, versatile and cost effective, and applicable in a reliable manner to both thin and thick shells.

In the standard 4-node shell element, full integration and reduced integration schemes have been used to compute the stiffness matrices and force vectors:

- The full integration scheme is often used in programs for static or dynamic problems with implicit time integration. It presents no problem for stability, but sometimes involves “locking” and computations are often more expensive.

- The reduced integration scheme, especially with one-point quadrature (in the mid-surface), is widely used in programs with explicit time integration such as RADIOSS and other programs applied essentially in crashworthiness studies. These elements dramatically decrease the computation time, and are very competitive if the hourglass modes (which result from the reduced integration scheme) are “well” stabilized.

5.3.1 Introduction

The historical shell element in RADIOSS is a simple bilinear Mindlin plate element coupled with a reduced integration scheme using one integration point. It is applicable in a reliable manner to both thin and moderately thick shells.

This element is very efficient if the spurious singular modes, called “hourglass modes”, which result from the reduced integration are stabilized.

The stabilization approach consists of providing additional stiffness so that the spurious singular modes are suppressed. Also, it offers the possibility of avoiding some locking problems. One of the first solutions was to generalize the formulation of Kosloff and Frazier [10] for brick element to shell element. It can be shown that the element produces accurate flexural response (thus, free from the membrane shear locking) and is equivalent to the incompatible model element of Wilson et al. [21] without the static condensation procedure. Taylor [47] extended this work to shell elements. Hughes and Liu [22] employed a similar approach and extended it to non-linear problems.

Belytschko and Tsay [23] developed a stabilized flat element based on the γ projections developed by Flanagan and Belytschko [12]. Its essential feature is that hourglass control is orthogonal to any linear field, thus preserving consistency. The stabilized stiffness is approached by a diagonal matrix and scaled by the perturbation parameters h_i which are introduced as a regulator of the stiffness for nonlinear problems. The parameters h_i are generally chosen to be as small as possible, so this approach is often called, perturbation stabilization.

The elements with perturbation stabilization have two major drawbacks:

- The parameters h_i are user-inputs and are generally problem-dependent.
- Poor behavior with irregular geometries (in-plane, out-of-plane). The stabilized stiffness (or stabilized forces) is often evaluated based on a regular flat geometry, so they generally do not pass either the Patch-test or the Twisted beam test.

Belytschko et al. [17] extended this perturbation stabilization to the 4-node shell element which has become widely used in explicit programs.

Belytschko et al. [24] improved the poor behavior exhibited in the warped configuration by adding a coupling curvature-translation term, and a particular nodal projection for the transverse shear calculation analogous to that developed by Hughes and Tezduyar [25], and MacNeal [26]. This element passes the Kirchhoff patch test and the Twisted beam test, but it cannot be extended to a general 6 DOF element due to the particular projection.

Belytschko and Bachrach [27] used a new method called “physical stabilization” to overcome the first drawback of the quadrilateral plane element. This method consists of explicitly evaluating the stabilized stiffness with the help of 'assumed strains', so that no arbitrary parameters need to be prescribed. Engelmann and Whirley [28] have applied it to the 4-node shell element. An alternative way to evaluate the stabilized stiffness explicitly is given by Liu et al. [29] based on Hughes and Liu's 4-node selected reduced integration scheme element [22], in

which the strain field is expressed explicitly in terms of natural coordinates by a Taylor-series expansion. A remarkable improvement in the one-point quadrature shell element with physical stabilization has been performed by Belytschko and Leviathan [18]. The element performs superbly for both flat and warped elements especially in linear cases, even in comparison with a similar element under a full integration scheme, and is only 20% slower than the Belytschko and Tsay element. More recently, based on Belytschko and Leviathan's element, Zhu and Zacharia [30] implemented the drilling rotation DOF in their one-point quadrature shell element; the drilling rotation is independently interpolated by the Allman function [39] based on Hughes and Brezzi's [41] mixed variational formulation.

The physical stabilization with assumed strain method seems to offer a rational way of developing a cost effective shell element with a reduced integration scheme. The use of the assumed strains based on the mixed variational principles, is powerful, not only in avoiding the locking problems (volumetric locking, membrane shear locking, as in Belytschko and Bindeman [31]; transverse shear locking, as in Dvorkin and Bathe [32]), but also in providing a new way to compute stiffness. However, as highlighted by Stolarski et al. [33], assumed strain elements generally do not have rigorous foundations; there is almost no constraint for the independent assumed strains interpolation. Therefore, a sound theoretical understanding and numerous tests are needed in order to prove the legitimacy of the assumed strain elements.

The greatest uncertainty of the one-point quadrature shell elements with physical stabilization is with respect to the nonlinear problems. All of these elements with physical stabilization mentioned above rely on the assumptions that the spin and the material properties are constant within the element. The first assumption is necessary to ensure the objectivity principle in geometrical nonlinear problems. The second was adapted in order to extend the explicit evaluation of stabilized stiffness for elastic problems to the physical nonlinear problems. It is found that the second assumption leads to a theoretical contradiction in the case of an elastoplastic problem (a classic physical nonlinear problem), and results in poor behavior in case of certain crash computations.

Zeng and Combescure [15] have proposed an improved 4-node shell element named QPPS with one-point quadrature based on the physical stabilization which is valid for the whole range of its applications (see the Chapter 5.3.12). The formulation is based largely on that of Belytschko and Leviathan.

Based on the QPPS element, Zeng and Winkelmuller have developed a new improved element named QEPH which is integrated in RADIOSS 44 version (see Chapter 5.3.13).

5.3.2 Bilinear Mindlin plate element

Most of the following explanation concerns four node plate elements, Figure 5.3.1. Section 5.3.13 explains the three node plate element, shown in Figure 5.3.2.

Figure 5.3.1 - Four Node Plate Element

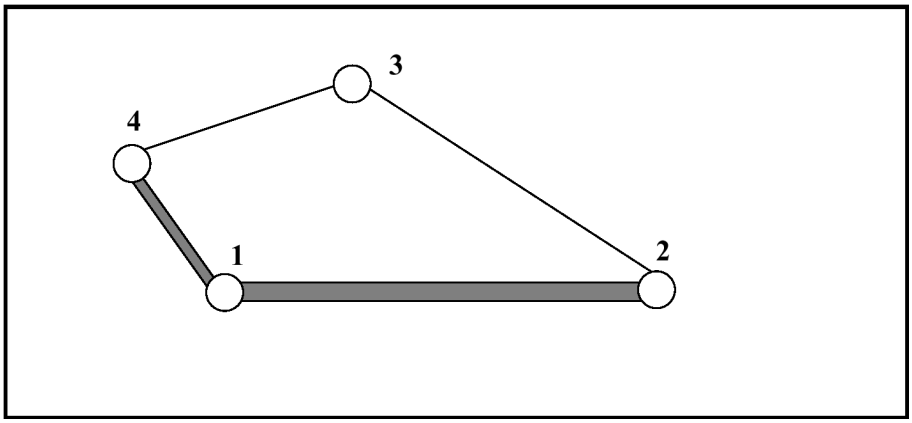

Figure 5.3.2 - Three Node Plate Element

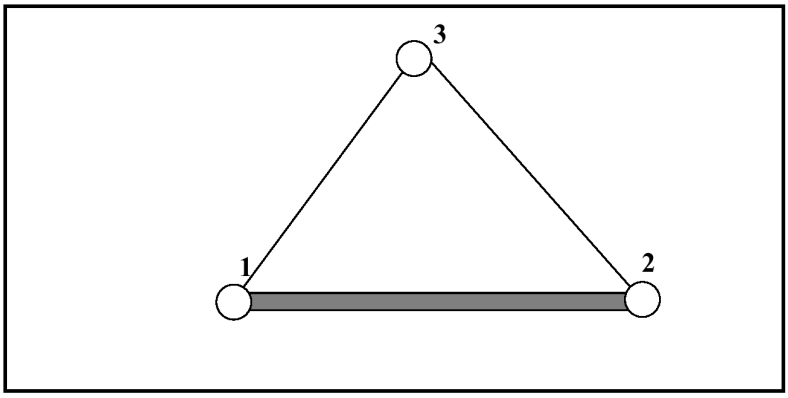

Plate theory assumes that one dimension (the thickness, z) of the structure is small compared to the other dimensions. Hence, the 3D continuum theory is reduced to a 2D theory. Nodal unknowns are the velocities (v_x, v_y, v_z) of the mid plane and the nodal rotation rates (ω_x, ω_y) as a consequence of the suppressed *z* direction. The thickness of elements can be kept constant, or allowed to be variable. This is user defined. The elements are always in a state of plane stress, i.e. $\sigma_{zz} = 0$, or there is no stress acting perpendicular to the plane of the element. A plane orthogonal to the mid-plane remains a plane, but not necessarily orthogonal as in Kirchhoff theory, (where $\varepsilon_{xz} = \varepsilon_{yz} = 0$) leading to the rotations rates $\omega_x = -\frac{\partial v_z}{\partial y}$ and $\omega_y = \frac{\partial v_z}{\partial x}$. In Mindlin plate theory, the rotations are independent variables.

5.3.3 Time step for stability

The characteristic length, *L*, for computing the critical time step, referring back to Figure 5.3.3, is defined by:

$$L_1 = \frac{area}{\max(\overline{13}, \overline{42})} \quad \text{EQ. 5.3.3.1}$$

$$L_2 = \min(\overline{12}, \overline{23}, \overline{34}, \overline{41}, \overline{13}, \overline{42}) \quad \text{EQ. 5.3.3.2}$$

$$L_c = \max(L_1, L_2) \quad \text{EQ. 5.3.3.3}$$

When the orthogonalized mode of the hourglass perturbation formulation is used, the characteristic length is defined as:

$$L_3 = \max(L_1, L_2) \quad \text{EQ. 5.3.3.4}$$

$$L_4 = 0.5\frac{(L_1 + L_2)}{\max(h_m, h_f)} \quad \text{EQ. 5.3.3.5}$$

$$L_c = \min(L_3, L_4) \quad \text{EQ. 5.3.3.6}$$

where h_m is the shell membrane hourglass coefficient and h_f is the shell out of plane hourglass coefficient, as mentioned in section 5.3.8.

5.3.4 Local reference frame

Three coordinate systems are introduced in the formulation:

- Global Cartesian fixed system $X = (X\vec{i} + Y\vec{j} + Z\vec{k})$
- Natural system (ξ, η, ζ), covariant axes x,y

- Local systems (x,y,z) defined by an orthogonal set of unit base vectors (t1,t2,n). n is taken to be normal to the mid-surface coinciding with ζ , and (t1,t2) are taken in the tangent plane of the mid-surface.

Figure 5.3.3 - Local Reference Frame

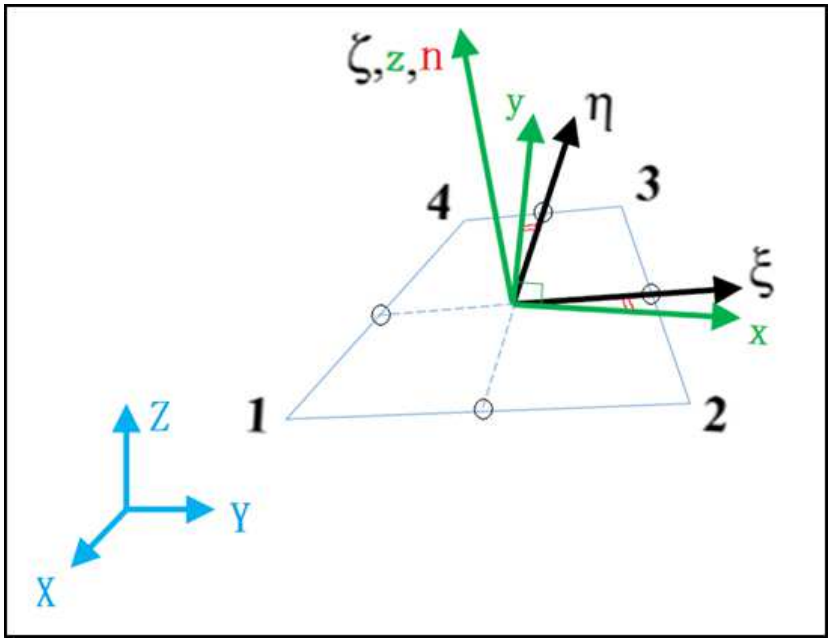

The vector normal to the plane of the element at the mid point is defined as:

$$n = \frac{x \times y}{\|x \times y\|}$$ EQ. 5.3.4.1

The vector defining the local direction is:

$$t_1 = \frac{x}{\|x\|} \quad t_2 = \frac{y}{\|y\|}$$ EQ. 5.3.4.2

Hence, the vector defining the local direction is found from the cross product of the two previous vectors:

$$t_2 = n \times t_1$$ EQ. 5.3.4.3

5.3.5 Bilinear shape functions

The shape functions defining the bilinear element used in the Mindlin plate are:

$$\Phi_I(\xi,\eta) = \frac{1}{4}(1+\xi_I\xi)(1+\eta_I\eta)$$ EQ. 5.3.5.1

or, in terms of local coordinates:

$$\Phi_I(x,y) = a_I + b_I x + c_I y + d_I xy$$ EQ. 5.3.5.2

It is also useful to write the shape functions in the Belytschko-Bachrach mix form [27]:

$$\Phi_I(x,y,\xi\eta) = \Delta_I + b_{xI} x + b_{yI} y + \gamma_I \xi\eta$$ EQ. 5.3.5.3

with

$$\Delta_I = \left[t_I - \left(t_I x^I\right) b_{xI} - \left(t_I y^I\right) b_{yI}\right];\ t = (1,1,1,1)$$

$$b_{xI} = \left(y_{24} y_{31} y_{42} y_{13}\right)/A;\quad \left(f_{ij} = \left(f_i - f_j\right)/2\right)$$

$$b_{yI} = \left(x_{42} x_{13} x_{24} x_{31}\right)/A$$

$$\gamma_I = \left[\Gamma_I - \left(\Gamma_J x^J\right) b_{xI} - \left(\Gamma_J y^J\right) b_{xI}\right]/4;\quad \Gamma = (1,-1,1,-1)$$

A is the area of the element

The velocity of the element at the mid-plane reference point is found using the relations:

$$v_x = \sum_{I=1}^{4} \Phi_I v_{xI} \qquad \text{EQ. 5.3.5.4}$$

$$v_y = \sum_{I=1}^{4} \Phi_I v_{yI} \qquad \text{EQ. 5.3.5.5}$$

$$v_z = \sum_{I=1}^{4} \Phi_I v_{zI} \qquad \text{EQ. 5.3.5.6}$$

where, v_{xI}, v_{yI}, v_{zI} are the nodal velocities in the *x,y,z* directions.

In a similar fashion, the element rotations are found by:

$$\omega_x = \sum_{I=1}^{4} \Phi_I \omega_{xI} \qquad \text{EQ. 5.3.5.7}$$

$$\omega_y = \sum_{I=1}^{4} \Phi_I \omega_{yI} \qquad \text{EQ. 5.3.5.8}$$

where ω_{xI} and ω_{yI} are the nodal rotational velocities about the x and y reference axes.

The velocity change with respect to the coordinate change is given by:

$$\frac{\partial v_x}{\partial x} = \sum_{I=1}^{4} \frac{\partial \Phi_I}{\partial x} v_{xI} \qquad \text{EQ. 5.3.5.9}$$

$$\frac{\partial v_x}{\partial y} = \sum_{I=1}^{4} \frac{\partial \Phi_I}{\partial y} v_{xI} \qquad \text{EQ. 5.3.5.10}$$

5.3.6 Mechanical properties

Shell elements behave in two ways, either membrane or bending behavior. The Mindlin plate elements that are used by RADIOSS account for bending and transverse shear deformation. Hence, they can be used to model thick and thin plates.

5.3.6.1 Membrane Behavior

The membrane strain rates for Mindlin plate elements are defined as:

$$\dot{e}_{xx} = \frac{\partial v_x}{\partial x} \qquad \text{EQ. 5.3.6.1}$$

$$\dot{e}_{yy} = \frac{\partial v_y}{\partial y}$$ EQ. 5.3.6.2

$$\dot{e}_{xy} = \frac{1}{2}\left(\frac{\partial v_x}{\partial y} + \frac{\partial v_y}{\partial x} \right)$$ EQ. 5.3.6.3

$$\dot{e}_{xz} = \frac{1}{2}\left(\frac{\partial v_x}{\partial z} + \frac{\partial v_z}{\partial x} \right) = \frac{1}{2}\left(\omega_y + \frac{\partial v_z}{\partial x} \right)$$ EQ. 5.3.6.4

$$\dot{e}_{yz} = \frac{1}{2}\left(\frac{\partial v_y}{\partial z} + \frac{\partial v_z}{\partial y} \right) = \frac{1}{2}\left(-\omega_x + \frac{\partial v_z}{\partial y} \right)$$ EQ. 5.3.6.5

where $\dot{e}_{ij}$ is the membrane strain rate.

5.3.6.2 Bending Behavior

The bending behavior in plate elements is described using the amount of curvature. The curvature rates of the Mindlin plate elements are defined as:

$$\dot{\chi}_x = \frac{\partial \omega_y}{\partial x}$$ EQ. 5.3.6.6

$$\dot{\chi}_y = -\frac{\partial \omega_x}{\partial y}$$ EQ. 5.3.6.7

$$\dot{\chi}_{xy} = \frac{1}{2}\left(\frac{\partial \omega_y}{\partial y} - \frac{\partial \omega_x}{\partial x} \right)$$ EQ. 5.3.6.8

where $\dot{\chi}_{ij}$ is the curvature rate.

5.3.6.3 Strain Rate calculation

The calculation of the strain rate of an individual element is divided into two parts, membrane and bending strain rates.

Membrane Strain rate

The vector defining the membrane strain rate is:

$$\{\dot{e}\}_m = \{\dot{e}_{x'}, \dot{e}_{y'}, 2\dot{e}_{xy}\}$$ EQ. 5.3.6.9

This vector is computed from the velocity field vector $\{v\}_m$ and the shape function gradient $\{B\}_m$:

$$\{\dot{e}\}_m = \{B\}_m \{v\}_m$$ EQ. 5.3.6.10

where

$$\{v\}_m = \{v_x^1, v_y^1, v_x^2, v_y^2, v_x^3, v_y^3, v_x^4, v_y^4\}$$ EQ. 5.3.6.11

$$[B]_m = \begin{bmatrix} \frac{\partial \Phi_1}{\partial x} & 0 & \frac{\partial \Phi_2}{\partial x} & 0 & \frac{\partial \Phi_3}{\partial x} & 0 & \frac{\partial \Phi_4}{\partial x} & 0 \\ 0 & \frac{\partial \Phi_1}{\partial y} & 0 & \frac{\partial \Phi_2}{\partial y} & 0 & \frac{\partial \Phi_3}{\partial y} & 0 & \frac{\partial \Phi_4}{\partial y} \\ \frac{\partial \Phi_1}{\partial y} & \frac{\partial \Phi_1}{\partial x} & \frac{\partial \Phi_2}{\partial y} & \frac{\partial \Phi_2}{\partial x} & \frac{\partial \Phi_3}{\partial y} & \frac{\partial \Phi_3}{\partial x} & \frac{\partial \Phi_4}{\partial y} & \frac{\partial \Phi_4}{\partial x} \end{bmatrix}$$ EQ. 5.3.6.12

Bending Strain rate

The vector defining the bending strain rate is:

$$\{\dot{e}\}_b = \{\dot{\chi}_{x'}\dot{\chi}_{y'}2\dot{\chi}_{xy'}2\dot{e}_{zx'}2\dot{e}_{yz}\} \quad \text{EQ. 5.3.6.13}$$

As with the membrane strain rate, the bending strain rate is computed from the velocity field vector. However, the velocity field vector for the bending strain rate contains rotational velocities, as well as translations:

$$\{\dot{e}\}_b = \{B\}_b\{v\}_b \quad \text{EQ. 5.3.6.14}$$

where

$$\{v\}_b = \{\omega_y^1, -\omega_x^1, \omega_y^2, -\omega_x^2, \omega_y^3, -\omega_x^3, \omega_y^4, -\omega_x^4, v_z^1, v_z^2, v_z^3, v_z^4\} \quad \text{EQ. 5.3.6.15}$$

$$[B]_b = \begin{bmatrix} \frac{\partial\Phi_1}{\partial x} & 0 & \frac{\partial\Phi_2}{\partial x} & 0 & \frac{\partial\Phi_3}{\partial x} & 0 & \frac{\partial\Phi_4}{\partial x} & 0 & 0 & 0 & 0 & 0 \\ 0 & \frac{\partial\Phi_1}{\partial y} & 0 & \frac{\partial\Phi_2}{\partial y} & 0 & \frac{\partial\Phi_3}{\partial y} & 0 & \frac{\partial\Phi_4}{\partial y} & 0 & 0 & 0 & 0 \\ \frac{\partial\Phi_1}{\partial y} & \frac{\partial\Phi_1}{\partial x} & \frac{\partial\Phi_2}{\partial y} & \frac{\partial\Phi_2}{\partial x} & \frac{\partial\Phi_3}{\partial y} & \frac{\partial\Phi_3}{\partial x} & \frac{\partial\Phi_4}{\partial y} & \frac{\partial\Phi_4}{\partial x} & 0 & 0 & 0 & 0 \\ \Phi_1 & 0 & \Phi_2 & 0 & \Phi_3 & 0 & \Phi_4 & 0 & \frac{\partial\Phi_1}{\partial x} & \frac{\partial\Phi_2}{\partial x} & \frac{\partial\Phi_3}{\partial x} & \frac{\partial\Phi_4}{\partial x} \\ 0 & \Phi_1 & 0 & \Phi_2 & 0 & \Phi_3 & 0 & \Phi_4 & \frac{\partial\Phi_1}{\partial y} & \frac{\partial\Phi_2}{\partial y} & \frac{\partial\Phi_3}{\partial y} & \frac{\partial\Phi_4}{\partial y} \end{bmatrix}$$

EQ. 5.3.6.16

Figure 5.3.4 - Strain rate calculation

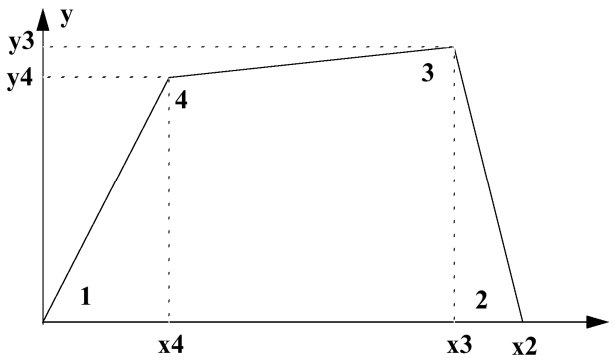

$$Px_1 = \frac{1}{2}(y_2 - y_4) \qquad Px_2 = \frac{1}{2}y_3$$

$$Py_1 = \frac{1}{2}(x_4 - x_2) \qquad Py_2 = -\frac{1}{2}x_3$$

$$\frac{\partial\Phi_1}{\partial x} = \frac{1}{S}Px_1 \qquad \frac{\partial\Phi_2}{\partial x} = \frac{1}{S}Px_2 \qquad \frac{\partial\Phi_3}{\partial x} = -\frac{1}{S}Px_1 \qquad \frac{\partial\Phi_4}{\partial x} = -\frac{1}{S}Px_2$$

$$\frac{\partial\Phi_1}{\partial y} = \frac{1}{S}Py_1 \qquad \frac{\partial\Phi_2}{\partial y} = \frac{1}{S}Py_2 \qquad \frac{\partial\Phi_3}{\partial y} = -\frac{1}{S}Py_1 \qquad \frac{\partial\Phi_4}{\partial y} = -\frac{1}{S}Py_2$$

$$\Phi_1 = \Phi_2 = \Phi_3 = \Phi_4 = \frac{1}{4}$$

5.3.6.4 Mass and Inertia

Consider a rectangular plate with sides of length *a* and *b*, surface area A = ab and thickness *t*, as shown in Figure 5.3.5.

Figure 5.3.5 - Mass Distribution

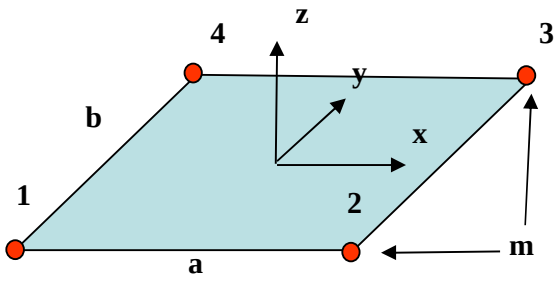

Due to the lumped mass formulation used by RADIOSS, the lumped mass at a particular node is:

$$m = \frac{1}{4}\rho A t \qquad \text{EQ. 5.3.6.17}$$

The mass moments of inertia, with respect to local element reference frame, are calculated at node *i* by:

$$I_{xx} = m\left(\frac{b^2 + t^2}{12}\right) \qquad \text{EQ. 5.3.6.18}$$

$$I_{yy} = m\left(\frac{a^2 + t^2}{12}\right) \qquad \text{EQ. 5.3.6.19}$$

$$I_{zz} = m\left(\frac{a^2 + b^2}{12}\right) \qquad \text{EQ. 5.3.6.20}$$

$$I_{xy} = -m\frac{ab}{16} \qquad \text{EQ. 5.3.6.21}$$

5.3.6.5 Inertia Stability

With the exact formula for inertia (EQS 5.3.6.18 to 5.3.6.21), the solution tends to diverge for large rotation rates. Belytschko proposed a way to stabilize the solution by setting $I_{xx} = I_{yy}$, i.e. to consider the rectangle as a square with respect to the inertia calculation only. This introduces an error into the formulation. However, if the aspect ratio is small the error will be minimal. In RADIOSS a better stabilization is obtained by:

$$I_{xx} = m\left(\frac{A}{f} + \frac{t^2}{12}\right) \qquad \text{EQ. 5.3.6.22}$$

$$I_{zz} = I_{yy} = I_{xx} \qquad \text{EQ. 5.3.6.23}$$

$$I_{xy} = 0 \qquad \text{EQ. 5.3.6.24}$$

where *f* is a regulator factor with default value *f=12* for QBAT element and *f=9* for other quadrilateral elements.

5.3.7 Internal forces

The internal force vector is given by:

$$f^{\text{int}} = \int_{\Omega e} B^t \sigma d\Omega^e \qquad \text{EQ. 5.3.7.1}$$

In elasticity it becomes:

$$f^{\text{int}} = \int_{\Omega e} B^t C B v d\Omega^e \qquad \text{EQ. 5.3.7.2}$$

It can be written as:

$$f^{\text{int}} = f^{\text{int}\,0} + f^{\text{int}\,hgr} \qquad \text{EQ. 5.3.7.3}$$

with the constant part $f^{\text{int}\,0}$ being computed with one-point quadrature and the non constant part or hourglass part $f^{\text{int}\,hgr}$ being computed by perturbation stabilization (Ishell = 1, 2 ,3 ...) or by physical stabilization (Ishell = 22).

5.3.8 Hourglass modes

Hourglass modes are element distortions that have zero strain energy. The 4 node shell element has 12 translational modes, 3 rigid body modes (1, 2, 9), 6 deformation modes (3, 4, 5, 6, 10, 11) and 3 hourglass modes (7, 8, 12).

Figure 5.3.6 - Translational Modes of Shell

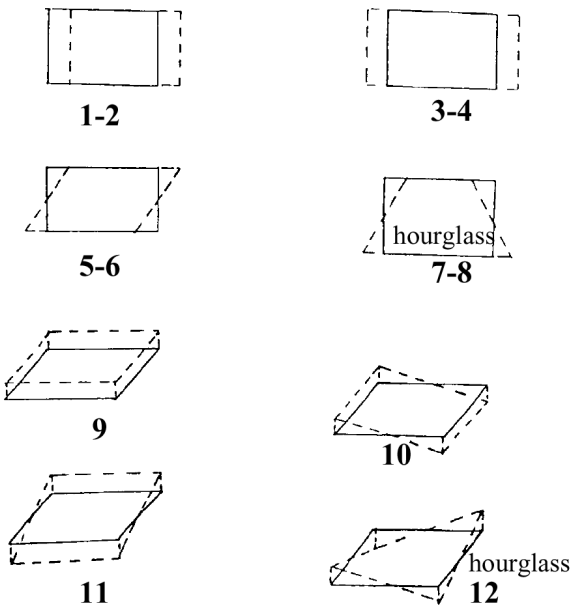

Along with the translational modes, the 4 node shell has 12 rotational modes: 4 out of plane rotation modes (1, 2, 3, 4), 2 deformation modes (5, 6), 2 rigid body or deformation modes (7, 8) and 4 hourglass modes (9, 10, 11, 12).

Figure 5.3.7 - Rotational Modes of Shell

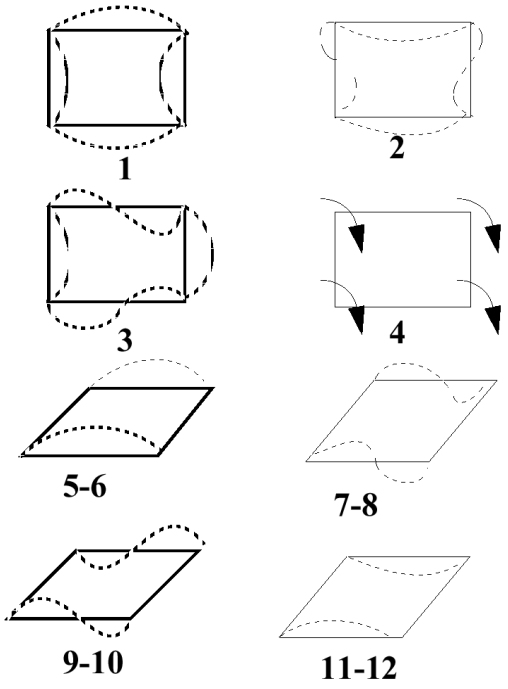

5.3.8.1 Hourglass Viscous Forces

Hourglass resistance forces are usually either viscous or stiffness related. The viscous forces relate to the rate of displacement or velocity of the elemental nodes, as if the material was a highly viscous fluid. The viscous formulation used by RADIOSS is the same as that outlined by Kosloff and Frasier [10]. Refer to section 5.1.5. An hourglass normalized vector is defined as:

$$\Gamma = (1, -1, 1, -1) \qquad \text{EQ. 5.3.8.1}$$

The hourglass velocity rate for the above vector is defined as:

$$\frac{\partial q_i}{\partial t} = \Gamma_I v_{iI} = v_{iI} - v_{i2} + v_{i3} - v_{i4} \qquad \text{EQ. 5.3.8.2}$$

The hourglass resisting forces at node *I* for in-plane modes are:

$$f_{iI}^{hgr} = \frac{1}{4}\rho c t \sqrt{h_m}\,\frac{A}{2}\frac{\partial q_i}{\partial t}\Gamma_I \qquad \text{EQ. 5.3.8.3}$$

For out of plane mode, the resisting forces are:

$$f_{iI}^{hgr} = \frac{1}{4}\rho c t^2 \sqrt{\frac{h_f}{10}}\,\frac{\partial q_i}{\partial t}\Gamma_I \qquad \text{EQ. 5.3.8.4}$$

where

i is the direction index,

I is the node index,

t is the element thickness,

c is the sound propagation speed,

A is the element area,

ρ is the material density,

h_m is the shell membrane hourglass coefficient,

h_f is the shell out of plane hourglass coefficient.

5.3.8.2 Hourglass Elastic Stiffness Forces

RADIOSS can apply a stiffness force to resist hourglass modes. This acts in a similar fashion to the viscous resistance, but uses the elastic material stiffness and node displacement to determine the size of the force. The formulation is the same as that outlined by Flanagan et al. [12]. Refer to section 5.1.5.2. The hourglass resultant forces are defined as:

$$f_{iI}^{hgr} = f_i^{hgr}\Gamma_I \qquad \text{EQ. 5.3.8.5}$$

For membrane modes:

$$f_i^{hgr}(t+\Delta t) = f_i^{hgr}(t) + \frac{1}{8}h_m E t \frac{\partial q_i}{\partial t}\Delta t \qquad \text{EQ. 5.3.8.6}$$

For out of plane modes:

$$f_i^{hgr}(t+\Delta t) = f_i^{hgr}(t) + \frac{1}{40}h_f E t^3 \frac{\partial q_i}{\partial t}\Delta t \qquad \text{EQ. 5.3.8.7}$$

where

t is the element thickness,

Δt is the time step,

E is Young's Modulus.

5.3.8.3 Hourglass Viscous Moments

This formulation is analogous to the hourglass viscous force scheme. The hourglass angular velocity rate is defined for the main hourglass modes as:

$$\frac{\partial r_i}{\partial t} = \Gamma_I \omega_{iI}^I = \omega_{i1} - \omega_{i2} + \omega_{i3} - \omega_{i4} \qquad \text{EQ. 5.3.8.8}$$

The hourglass resisting moments at node I are given by:

$$m_{iI}^{hgr} = \frac{1}{50}\sqrt{\frac{h_r}{2}}\rho c A t^2 \frac{\partial r_i}{\partial t}\Gamma_I \qquad \text{EQ. 5.3.8.9}$$

where h_r is the shell rotation hourglass coefficient.

5.3.9 Hourglass resistance

To correct this phenomenon, it is necessary to introduce anti-hourglass forces and moments. Two possible formulations are presented hereafter.

5.3.9.1 Flanagan-Belytschko Formulation [12]

Ishell=1

In the Kosloff-Frasier formulation seen in section 5.1.5.1, the hourglass base vector Γ_I^{α} is not perfectly orthogonal to the rigid body and deformation modes that are taken into account by the one point integration scheme. The mean stress/strain formulation of a one point integration scheme only considers a fully linear velocity field, so that the physical element modes generally contribute to the hourglass energy. To avoid this, the idea in the Flanagan-Belytschko formulation is to build an hourglass velocity field which always remains orthogonal to the physical element modes. This can be written as:

$$v_{iI}^{Hour} = v_{iI} - v_{iI}^{Lin} \qquad \text{EQ. 5.3.9.1}$$

The linear portion of the velocity field can be expanded to give:

$$v_{iI}^{Hour} = v_{iI} - \left(\overline{v_{iI}} + \frac{\partial v_{iI}}{\partial x_j} \cdot \left(x_j - \overline{x_j} \right) \right) \qquad \text{EQ. 5.3.9.2}$$

Decomposition on the hourglass base vectors gives [12]:

$$\frac{\partial q_i^\alpha}{\partial t} = \Gamma_I^\alpha \cdot v_{iI}^{Hour} = \left(v_{iI} - \frac{\partial v_{iI}}{\partial x_j} \cdot x_j \right) \cdot \Gamma_I^\alpha \qquad \text{EQ. 5.3.9.3}$$

where

$\frac{\partial q_i^\alpha}{\partial t}$ are the hourglass modal velocities,

Γ_I^α are the hourglass vectors, base.

Remembering that $\frac{\partial v_i}{\partial x_j} = \frac{\partial \Phi_j}{\partial x_j} \cdot v_{iJ}$ and factorizing EQ. 5.1.5.5 gives:

$$\frac{\partial q_i^\alpha}{\partial t} = v_{iI} \cdot \left(\Gamma_I^\alpha - \frac{\partial \Phi_J}{\partial x_j} x_j \Gamma_J^\alpha \right) \qquad \text{EQ. 5.3.9.4}$$

$$\gamma_I^\alpha = \Gamma_I^\alpha - \frac{\partial \Phi_J}{\partial x_j} x_j \Gamma_J^\alpha \qquad \text{EQ. 5.3.9.5}$$

is the hourglass shape vector used in place of Γ_I^α in EQ. 5.1.5.2.

Figure 5.3.8 - Flanagan Belytschko Hourglass formulation

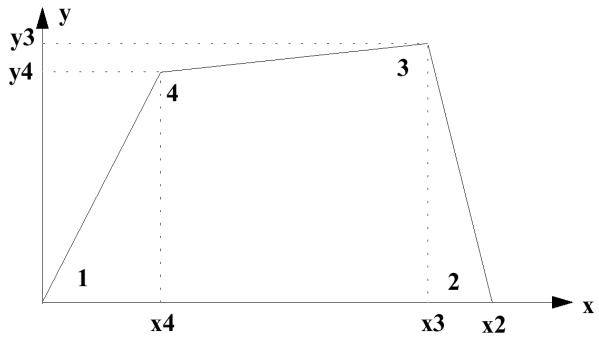

$$Px_1 = \frac{1}{2}(y_2 - y_4) \qquad Px_2 = \frac{1}{2}y_3$$

$$Py_1 = \frac{1}{2}(x_4 - x_2) \qquad Py_2 = -\frac{1}{2}x_3$$

$$hx = \frac{(-x_2 + x_3 - x_4)}{S} \qquad hy = \frac{(-y_2 + y_3 - y_4)}{S}$$

$$\Gamma_1 = 1 - Px_1 hx - Py_1 hy$$

$$\Gamma_2 = -1 + Px_2 hx + Py_2 hy$$

$$\Gamma_3 = 1 - Px_1 hx - Py_1 hy$$

$$\Gamma_4 = -1 + Px_2 hx + Py_2 hy$$

5.3.9.2 Elastoplastic Hourglass Forces

Ishell=3

The same formulation as elastic hourglass forces is used (section 5.3.8.2 and Flanagan et al. [12]) but the forces are bounded with a maximum force depending on the current element mean yield stress. The hourglass forces are defined as:

$$f_{iI}^{hgr} = f_i^{hgr}\Gamma_I \qquad \text{EQ. 5.3.9.6}$$

For in plane mode:

$$f_i^{hgr}(t+\Delta t) = f_i^{hgr}(t) + \frac{1}{8}h_m Et\frac{\partial q_i}{\partial t}\Delta t \qquad \text{EQ. 5.3.9.7}$$

$$f_i^{hgr}(t+\Delta t) = \min\left(f_i^{hgr}(t+\Delta t),\quad \frac{1}{2}h_m\sigma_y t\sqrt{A}\right) \qquad \text{EQ. 5.3.9.8}$$

For out of plane mode:

$$f_i^{hgr}(t+\Delta t) = f_i^{hgr}(t) + \frac{1}{40}h_f Et^3\frac{\partial q_i}{\partial t}\Delta t \qquad \text{EQ. 5.3.9.9}$$

$$f_i^{hgr}(t+\Delta t) = \min\left(f_i^{hgr}(t+\Delta t), \frac{1}{4}h_f\sigma_y t^2\right) \qquad \text{EQ. 5.3.9.10}$$

where:

t is the element thickness,

σ_y is the yield stress,

A is the element area.

5.3.9.3 Physical Hourglass Forces

Ishell=22, 24

The hourglass forces are given by:

$$f^{\text{int}\,hgr} = \int_{\Omega e} B^{Ht}CB^H v d\Omega^e \qquad \text{EQ. 5.3.9.11}$$

For in-plane membrane rate-of-deformation, with $\Phi = \xi\eta$ and γ_I defined in EQ 5.3.5.3:

$$\left[\left(B_I^m\right)^H\right] = \begin{bmatrix} \gamma_I\phi,x & 0 & 0 \\ 0 & \gamma_I\phi,y & 0 \\ \gamma_I\phi,y & \gamma_I\phi,x & 0 \end{bmatrix} \qquad \text{EQ. 5.3.9.12}$$

For bending:

$$\left[\left(B_I^b\right)^H\right] = \begin{bmatrix} 0 & \gamma_I\phi,x \\ -\gamma_I\phi,y & 0 \\ -\gamma_I\phi,x & \gamma_I\phi,y \end{bmatrix} \qquad \text{EQ. 5.3.9.13}$$

It is shown in [16] that the non-constant part of the membrane strain rate does not vanish when a warped element undergoes a rigid body rotation. Thus, a modified matrix [$\left(B_I^m\right)^H$] is chosen using $z_\gamma = \gamma_I z^I$ as a measure of the warping:

$$\left[\left(B_I^m\right)^H\right]=\begin{bmatrix}\gamma_I\phi_{,x} & 0 & z_\gamma b_{xI}\phi_{,x} \\ 0 & \gamma_I\phi_{,y} & z_\gamma b_{yI}\phi_{,y} \\ \gamma_I\phi_{,y} & \gamma_I\phi_{,x} & z_\gamma\left(b_{xI}\phi_{,y}+b_{yI}\phi_{,x}\right)\end{bmatrix} \quad \text{EQ. 5.3.9.14}$$

This matrix is different from the Belytschko-Leviathan [17] correction term added at rotational positions, which couples translations to curvatures as follows:

$$\left[\left(B_I^m\right)^H\right]=\begin{bmatrix}\gamma_I\phi_{,x} & 0 & 0 & 0 & -\frac{1}{4}z_\gamma\phi_{,x} \\ 0 & \gamma_I\phi_{,y} & 0 & \frac{1}{4}z_\gamma\phi_{,y} & 0 \\ \gamma_I\phi_{,y} & \gamma_I\phi_{,x} & 0 & \frac{1}{4}z_\gamma\phi_{,x} & -\frac{1}{4}z_\gamma\phi_{,y}\end{bmatrix} \quad \text{EQ. 5.3.9.15}$$

This will lead to "membrane locking" (the membrane strain will not vanish under a constant bending loading). According to the general formulation, the coupling is presented in terms of bending and not in terms of membrane, yet the normal translation components in (B_I^m) do not vanish for a warped element due to the tangent vectors $t_i(\xi,\eta)$ which differ from $t_i(0,0)$.

5.3.9.4 Full integrated formulation

Ishell=12

The element is based on the Q4γ24 shell element developed in [40] by Batoz and Dhatt. The element has 4 nodes with 5 local degrees-of-freedom per node. Its formulation is based on the Cartesian shell approach where the middle surface is curved. The shell surface is fully integrated with four Gauss points. Due to an in-plane reduced integration for shear, the element shear locking problems are avoided. The element without hourglass deformations is based on Mindlin-Reissner plate theory where the transversal shear deformation is taken into account in the expression of the internal energy. The reader is invited to consult the reference for more details.

5.3.9.5 Shell membrane damping

The shell membrane damping, *dm*, is only used for law 25, 27, 19, 32 and 36. The Shell membrane damping factor is a factor on the numerical VISCOSITY and not a physical viscosity. Its effect is shown in the formula of the calculation of forces in a shell element:

dm = *dm* read in D00 input (Shell membrane damping factor parameter) then:

$$dm=\sqrt{2}\cdot dm_{D00}\cdot\rho_0\cdot c\cdot\sqrt{AREA} \quad \text{EQ. 5.3.9.16}$$

Effect in the force vector (*F*) calculation:

$$F_{1new}=F_{1old}+dm\left(\dot{\varepsilon}_{11}+\frac{\dot{\varepsilon}_{22}}{2}\right) \quad \text{EQ. 5.3.9.17}$$

$$F_{2new}=F_{2old}+dm\left(\dot{\varepsilon}_{22}+\frac{\dot{\varepsilon}_{11}}{2}\right) \quad \text{EQ. 5.3.9.18}$$

$$F_{3new}=F_{3old}+dm\frac{\dot{\varepsilon}_{12}}{3} \quad \text{EQ. 5.3.9.19}$$

Where: ρ_0 is the density

AREA is the area of the shell element surface

dt is the time step

c is the sound speed

In order to calibrate the *dm* value so that it represents the physical viscosity, one should obtain the same size for all shell elements (Cf. AREA factor), then scale the physical viscosity value to the element size.

5.3.10 Stress and strain calculation

The stress and strain for a shell element can be written in vector notation. Each component is a stress or strain feature of the element. The generalized strain ε can be written as:

$$\{\varepsilon\} = \{e_x, e_y, e_{xy}, k_x, k_y, k_{xy}\} \quad \text{EQ. 5.3.10.1}$$

where

e_{ij} is the membrane strain,

χ_{ij} is the bending strain or curvature.

The generalized stress Σ can be written as:

$$\{\Sigma\} = \{N_x, N_y, N_{xy}, M_x, M_y, M_{xy}\} \quad \text{EQ. 5.3.10.2}$$

where: $N_x = \int_{-t/2}^{t/2} \sigma_x dz$ $\quad M_x = -\int_{-t/2}^{t/2} \sigma_x z dz$

$N_y = \int_{-t/2}^{t/2} \sigma_y dz$ $\quad M_y = -\int_{-t/2}^{t/2} \sigma_y z dz$

$N_{xy} = \int_{-t/2}^{t/2} \sigma_{xy} dz$ $\quad M_{xy} = -\int_{-t/2}^{t/2} \sigma_{xy} z dz$

$N_{yz} = \int_{-t/2}^{t/2} \sigma_{yz} dz$ $\quad N_{xz} = \int_{-t/2}^{t/2} \sigma_{xz} dz$

5.3.10.1 Isotropic Linear Elastic Stress Calculation

The stress for an isotropic linear elastic shell for each time increment is computed using:

$$\{\Sigma^{el}(t+\Delta t)\} = \{\Sigma(t)\} + \mathbf{L}\{\dot{\varepsilon}\}\Delta t \quad \text{EQ. 5.3.10.3}$$

where EQ. 5.3.10.4

$$\mathrm{L} = \begin{bmatrix} L_m & 0 \\ 0 & L_b \end{bmatrix} \quad \text{EQ. 5.3.10.5}$$

$$L_m = \begin{bmatrix} \frac{Et}{1-\nu^2} & \frac{-\nu Et}{1-\nu^2} & 0 \\ \frac{-\nu Et}{1-\nu^2} & \frac{Et}{1-\nu^2} & 0 \\ 0 & 0 & \frac{Et}{1+\nu} \end{bmatrix} \quad \text{EQ. 5.3.10.6}$$

$$L_b = \begin{bmatrix} \frac{Et^3}{12(1-\nu^2)} & \frac{-\nu Et^3}{12(1-\nu^2)} & 0 \\ \frac{-\nu Et^3}{12(1-\nu^2)} & \frac{Et^3}{12(1-\nu^2)} & 0 \\ 0 & 0 & \frac{Et^3}{12(1+\nu)} \end{bmatrix}$$ EQ. 5.3.10.7

E is the Young's or Elastic Modulus,

ν is Poisson's Ratio,

t is the shell thickness.

5.3.10.2 Isotropic Linear Elastic-Plastic Stress Calculation

An incremental step-by-step method is usually used to resolve the nonlinear problems due to elasto-plastic material behavior. The problem is presented by the resolution of the following equation:

$$\dot{\boldsymbol{\sigma}} = \mathbf{C} : (\dot{\varepsilon} - \dot{\varepsilon}_p)$$ EQ. 5.3.10.8

$$f(\sigma, \sigma_y) = \sigma_{eq}^2 - \sigma_y^2 = 0 \quad ; \quad \dot{\sigma}_y = H\dot{\varepsilon}^p$$ EQ. 5.3.10.9

$$\dot{f} = 0$$ EQ. 5.3.10.10

and $\dot{\varepsilon}_p = \frac{\partial f}{\partial \sigma}\dot{\lambda}$ EQ. 5.3.10.11

f is the yield surface function for plasticity for associative hardening. The equivalent stress σ_{eq} may be expressed in form:

$$\sigma_{eq}^2 = \{\sigma\}^t [A] \{\sigma\}$$ EQ. 5.3.10.12

with $\{\sigma\} = \begin{Bmatrix} \sigma_{xx} \\ \sigma_{yy} \\ \sigma_{xy} \end{Bmatrix}$ and $[A] = \begin{bmatrix} 1 & -\frac{1}{2} & 0 \\ -\frac{1}{2} & 1 & 0 \\ 0 & 0 & 3 \end{bmatrix}$ for von Mises criteria.

The normality law (EQ. 5.3.10.11) for associated plasticity is written as:

$$\{\dot{\varepsilon}_p\} = \frac{\partial f}{\partial(\sigma)}\dot{\lambda} = 2[A]\{\sigma\}\dot{\lambda} = \frac{\dot{\varepsilon}^p}{\sigma_y}[A]\{\sigma\}$$ EQ. 5.3.10.13

Where $\dot{\varepsilon}^p$ is the equivalent plastic deformation.

EQ. 5.3.10.8 is written in an incremental form:

$$\{\sigma\}_{n+1} = \{\sigma\}_n + \{d\sigma\} = \{\sigma\}_n + [C](\{d\varepsilon\} - \{d\varepsilon_p\}) = \{\sigma^*\} - \frac{d\varepsilon^p}{\sigma_y^{n+1}}[C][A]\{\sigma\}_{n+1}$$ EQ. 5.3.10.14

Where $\{\sigma^*\}$ represents stress components obtained by an elastic increment and [*C*] the elastic matrix in plane stress. The equations EQ. 5.3.10.8 to 14 lead to obtain the nonlinear equation:

$$f(d\varepsilon^p) = 0 \qquad \text{EQ. 5.3.10.15}$$

that can be resolved by an iterative algorithm as Newton-Raphson method.

To determine the elastic-plastic state of a shell element, a number of steps have to be performed to check for yielding and defining a plasticity relationship. Stress-strain and force-displacement curves for a particular ductile material are shown in Figure 5.3.9.

Figure 5.3.9 - Material Curve

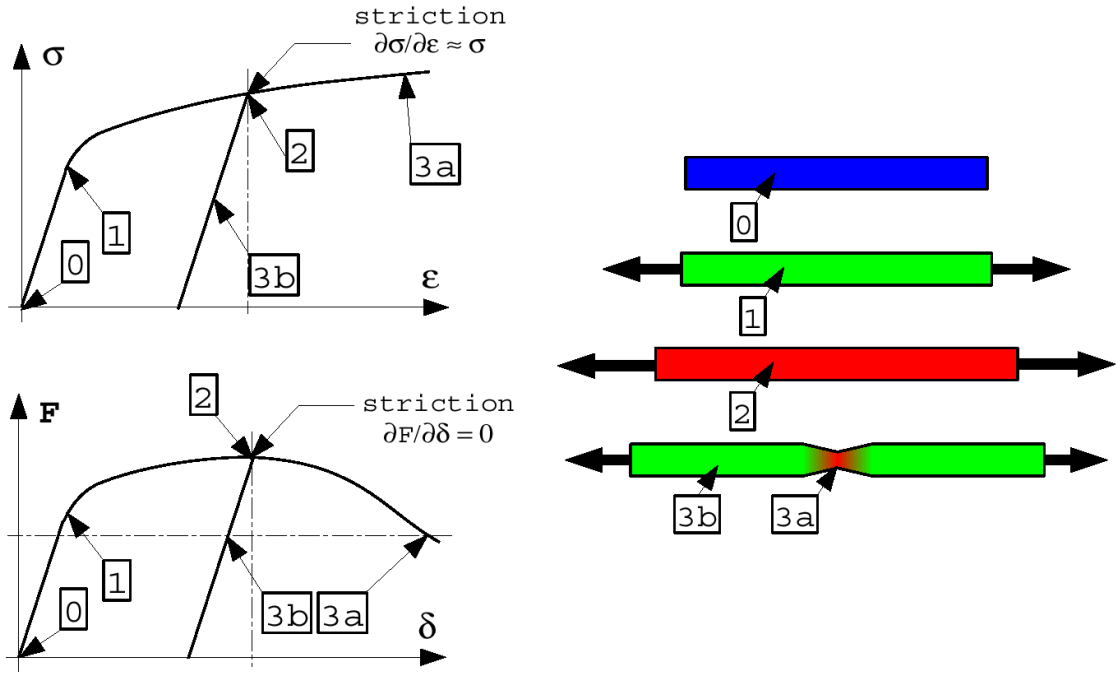

The steps involved in the stress calculation are as follows.

1. Strain calculation at integration point z

The overall strain on an element due to both membrane and bending forces is:

$$\varepsilon_x = e_x - z\chi_x \qquad \text{EQ. 5.3.10.16}$$

$$\varepsilon_y = e_y - z\chi_y \qquad \text{EQ. 5.3.10.17}$$

$$\varepsilon_{xy} = e_{xy} - z\chi_{xy} \qquad \text{EQ. 5.3.10.18}$$

$$\{\varepsilon\} = \{\varepsilon_x, \varepsilon_y, \varepsilon_{xy}\} \qquad \text{EQ. 5.3.10.19}$$

2. Elastic stress calculation

The stress is defined as:

$$\{\sigma\} = \{\sigma_x, \sigma_y, \sigma_{xy}\} \qquad \text{EQ. 5.3.10.20}$$

It is calculated using explicit time integration and the strain rate:

$$\left\{\sigma^{el}\left(t+\Delta t\right)\right\}=\left\{\sigma\left(t\right)\right\}+\mathbf{L}\left\{\dot{\varepsilon}\right\}\Delta t \qquad \text{EQ. 5.3.10.21}$$

$$\mathrm{L}=\begin{bmatrix} \frac{E}{1-\nu^2} & \frac{\nu E}{1-\nu^2} & 0 \\ \frac{\nu E}{1-\nu^2} & \frac{E}{1-\nu^2} & 0 \\ 0 & 0 & \frac{E}{1+\nu} \end{bmatrix}$$

The two shear stresses acting across the thickness of the element are calculated by:

$$\sigma_{yz}^{el}\left(t+\Delta t\right)=\sigma_{yz}\left(t\right)+\alpha\frac{E}{1+\nu}\dot{e}_{yz}\Delta t \qquad \text{EQ. 5.3.10.22}$$

$$\sigma_{xz}^{el}\left(t+\Delta t\right)=\sigma_{xz}\left(t\right)+\alpha\frac{E}{1+\nu}\dot{e}_{xz}\Delta t$$

where α is the shear factor. Default is Reissner's value of 5/6.

3. von Mises yield criterion

The von Mises yield criterion for shell elements is defined as:

$$\sigma_{vm}^2=\sigma_x^2+\sigma_y^2-\sigma_x\sigma_y+3\sigma_{xy}^2 \qquad \text{EQ. 5.3.10.23}$$

For type 2 simple elastic-plastic material, the yield stress is calculated using:

$$\sigma_{yield}\left(t\right)=a+b\varepsilon^{p^n}\left(t\right) \qquad \text{EQ. 5.3.10.24}$$

This equation will vary according to the type of material being modeled.

4. Plasticity Check

The element's state of stress must be checked to see if it has yielded. These values are compared with the von Mises and Yield stresses calculated in the previous step. If the von Mises stress is greater than the yield stress, then the material will be said to be in the plastic range of the stress-strain curve.

Figure 5.3.10 - Plasticity Check

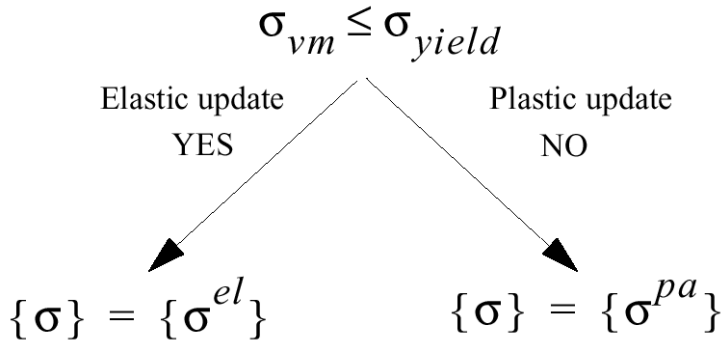

5. Compute plastically admissible stresses

If the state of stress of the element is in the plastic region, there are two different analyses that can be used as described in the next paragraph. The scheme used is defined in the shell property set, card 2 of the input.

6. Compute thickness change

The necking of the shells undergoing large strains in hardening phase can be taken into account by computing normal strain ε_{zz} in an incremental process. The incompressibility hypothesis in plasticity gives:

$$d\varepsilon_{zz}^{p} = -\left(d\varepsilon_{xx}^{p} + d\varepsilon_{yy}^{p}\right) \quad \text{EQ. 5.3.10.25}$$

where the components of membrane strain $d\varepsilon_{xx}^{p}$ and $d\varepsilon_{yy}^{p}$ are computed by EQ. 5.3.10.13 as:

$$\begin{Bmatrix} d\varepsilon_{xx}^{p} \\ d\varepsilon_{yy}^{p} \end{Bmatrix} = \frac{d\varepsilon^{p}}{\sigma_{y}} [A]_{2\times 2} \begin{Bmatrix} \sigma_{xx} \\ \sigma_{yy} \end{Bmatrix} \quad \text{EQ. 5.3.10.26}$$

The plan stress condition $d\sigma_{zz} = 0$ allows to resolve for $d\varepsilon_{zz}$:

$$d\varepsilon_{zz} = -\frac{\upsilon}{1-\upsilon}\left(d\varepsilon_{xx} + d\varepsilon_{yy}\right) + \frac{1-2\upsilon}{1-\upsilon} d\varepsilon_{zz}^{p} \quad \text{EQ. 5.3.10.27}$$

5.3.10.3 Plastically Admissible Stresses

Radial return

Iplas=2

When the shell plane stress plasticity flag is set to 0 on card 1 of the shell property type definition, a radial return plasticity analysis is performed. Thus, Step 5 of the stress computation is:

The hardening parameter is calculated using the material stress-strain curve:

$$\sigma_{yield}(t) = a + b\varepsilon^{p^{n}}(t) \quad \text{EQ. 5.3.10.28}$$

$$\dot{\varepsilon}^{p}\Delta t = \frac{\sigma_{vm} - \sigma_{yield}}{E}$$

where $\dot{\varepsilon}^{p}$ is the plastic strain rate.

The plastic strain, or hardening parameter, is found by explicit time integration:

$$\varepsilon^{p}(t + \Delta t) = \varepsilon^{p}(t) + \dot{\varepsilon}^{p}\Delta t \quad \text{EQ. 5.3.10.29}$$

Finally, the plastic stress is found by the method of radial return. In case of plane stress this method is approximated because it cannot verify simultaneously the plane stress condition and the flow rule. The following return gives a plane stress state:

$$\sigma_{ij}^{pa} = \frac{\sigma_{yield}}{\sigma_{vm}} \sigma_{ij}^{el} \quad \text{EQ. 5.3.10.30}$$

Iterative algorithm

Iplas=1

If flag 1 is used on card 1 of the shell property type definition, an incremental method is used. Step 5 is performed using the incremental method described by Mendelson [1]. It has been extended to plane stress situations. This method is more computationally expensive, but provides high accuracy on stress distribution, especially when one is interested in residual stress or elastic return. This method is also recommended when variable thickness is being used. After some calculations, the plastic stresses are defined as:

$$\sigma_x^{pa} = \frac{\sigma_x^{el} + \sigma_y^{el}}{2\left(1+\frac{\Delta r}{1-\nu}\right)} + \frac{\sigma_x^{el} - \sigma_y^{el}}{2\left(1+\frac{3\Delta r}{1+\nu}\right)}$$ EQ. 5.3.10.31

$$\sigma_y^{pa} = \frac{\sigma_x^{el} + \sigma_y^{el}}{2\left(1+\frac{\Delta r}{1-\nu}\right)} - \frac{\sigma_x^{el} - \sigma_y^{el}}{2\left(1+\frac{3\Delta r}{1+\nu}\right)}$$ EQ. 5.3.10.32

$$\sigma_{xy}^{pa} = \frac{\sigma_{xy}^{el}}{1+\frac{3\Delta r}{1+\nu}}$$ EQ. 5.3.10.33

where $$\Delta r = \frac{E\Delta\varepsilon^p}{2\sigma_{yield}\left(t+\Delta t\right)}$$ EQ. 5.3.10.34

The value of $\boldsymbol{\Delta\varepsilon^P}$ must be computed to determine the state of plastic stress. This is done by an iterative method. To calculate the value of $\boldsymbol{\Delta\varepsilon^P}$, the von Mises yield criterion for the case of plane stress is introduced:

$$\sigma_x^2 + \sigma_y^2 - \sigma_x\sigma_y + 3\sigma_{xy}^2 = \sigma_{yield}^2\left(t+\Delta t\right)$$ EQ. 5.3.10.35

and the values of σ_x, σ_y, σ_{xy} and σ_{yield} are replaced by their expression as a function of $\boldsymbol{\Delta\varepsilon^P}$ (EQS 5.3.8.31 to 5.3.8.34), with for example:

$$\sigma_{yield}\left(t+\Delta t\right) = a + b\varepsilon^{p^n}\left(t+\Delta t\right)$$ EQ. 5.3.10.36

and:

$$\varepsilon^p\left(t+\Delta t\right) = \varepsilon^p\left(t\right) + \Delta\varepsilon^p$$ EQ. 5.3.10.37

The nonlinear equation 5.3.10.35 is solved iteratively for $\boldsymbol{\Delta\varepsilon^P}$ by Newton's method using three iterations. This is sufficient to obtain $\boldsymbol{\Delta\varepsilon^P}$ accurately.

5.3.10.4 Plastic plane stress with Hill's criterion

In the case of Hill's orthotropic criterion, the equivalent stress is given by:

$$\sigma_{eq}^2 = A_1\sigma_{xx}^2 + A_2\sigma_{yy}^2 - A_3\sigma_{xx}\sigma_{yy} + A_{12}\sigma_{xy}^2$$ EQ. 5.3.10.38

with $$\left[A\right] = \begin{bmatrix} A_1 & -\frac{A_3}{2} & 0 \\ & A_2 & 0 \\ sym & & A_{12} \end{bmatrix}$$

EQ. 5.3.10.14 is then written as:

$$\left[B\right]\left\{\sigma\right\}_{n+1} = \left\{\sigma^*\right\}$$ EQ. 5.3.10.39

$$[B]=\begin{bmatrix} 1+\left(A_1-\frac{A_3}{2}\upsilon\right)dR & \left(A_2\upsilon-\frac{A_3}{2}\right)dR & 0 \\ \left(A_1\upsilon-\frac{A_3}{2}\right)dR & 1+\left(A_2-\frac{A_3}{2}\upsilon\right)dR & 0 \\ 0 & 0 & 1+\frac{1-\upsilon}{2}A_{12}dR \end{bmatrix};\quad dR=\frac{d\varepsilon^p}{\sigma_y}\frac{E}{1-\upsilon^2}$$

Changing the stress variables to $\{\overline{\sigma}\}$:

$$\{\overline{\sigma}\}=[Q]\{\sigma\}$$ EQ. 5.3.10.40

with:

$$[Q]=\begin{bmatrix} 1 & \frac{A_1-A_2+C}{-2\left(A_2\upsilon-\frac{A_3}{2}\right)} & 0 \\ \frac{A_1-A_2+C}{2\left(A_1\upsilon-\frac{A_3}{2}\right)} & 1 & 0 \\ 0 & 0 & 1 \end{bmatrix};\ C=\sqrt{(1-\upsilon^2)(A_1-A_2)^2+[A_3-(A_1+A_2)\upsilon]^2}$$

The matrix $[\overline{B}]=[Q][B][Q]^{-1}$ is diagonal:

$$[\overline{B}]=\begin{bmatrix} 1+dR\left(A_2-\frac{A_3\upsilon}{2}-\frac{C}{J_Q}\right) & 0 & 0 \\ 0 & 1+dR\left(A_1-\frac{A_3\upsilon}{2}+\frac{C}{J_Q}\right) & 0 \\ 0 & 0 & 1+dR.A_{12}\left(\frac{1-\upsilon}{2}\right) \end{bmatrix}$$ EQ. 5.3.10.41

where $J_Q=1+\frac{(A_1-A_2+C)^2}{4\left(A_1\upsilon-\frac{A_3}{2}\right)\left(A_2\upsilon-\frac{A_3}{2}\right)}$ is the Jacobian of [Q]. EQ. 5.3.10.40 is now written as:

$$[\overline{B}]\{\overline{\sigma}\}_{n-1}=\{\overline{\sigma}^*\}$$ EQ. 5.3.10.42

This will enable to give explicitly the expression of the yield surface EQ. 5.3.10.15:

$$f_{n+1}=\left(\sigma_{eq}^{n+1}\right)^2-\left(\sigma_y^{n+1}\right)^2=\{\overline{\sigma}^*\}^t[\overline{B}]^{-t}[\overline{A}][\overline{B}]^{-1}\{\overline{\sigma}^*\}-\left(\sigma_y^{n+1}\right)^2$$

$$=\frac{\overline{A}_{11}}{\overline{B}_1^2}\overline{\sigma}_{xx}^2+\frac{\overline{A}_{22}}{\overline{B}_2^2}\overline{\sigma}_{yy}^2+\frac{A_{12}}{\overline{B}_3^2}\overline{\sigma}_{xy}^2+\frac{\overline{A}_{12}}{\overline{B}_1\overline{B}_2}\overline{\sigma}_{xx}\overline{\sigma}_{yy}-\left(\sigma_y^{n+1}\right)^2$$ EQ. 5.3.10.43

With $[\overline{A}]_{2\times2}=[Q]_{2\times2}^{-t}[A]_{2\times2}[Q]_{2\times2}^{-1}$.

The derivative of f_{n+1} is carried out in order to use the Newton-Raphson method:

$$\Delta\varepsilon_{n+1}^{p} = \Delta\varepsilon_{n}^{p} - \frac{f_{n+1}}{f'_{n+1}} \qquad \text{EQ. 5.3.10.44}$$

5.3.11 Calculation of forces and moments

5.3.11.1 Integration points throughout the thickness

The integration is performed using n equally spaced integration points throughout the thickness. The method used assumes a linear variation of stresses between integrations points:

$$N_x = t\sum_{k=1}^{n} w_k^N \sigma_{xk}^{pa} \qquad \text{EQ. 5.3.11.1}$$

$$M_x = t^2\sum_{k=1}^{n} w_k^M \sigma_{xk}^{pa} \qquad \text{EQ. 5.3.11.2}$$

Table 5.3.1 compares the coefficients used to the classical Newton quadrature in case of 3 integration points.

w^N for 3 integration points			
Coefficients	**w_1**	**w_2**	**w_3**
RADIOSS	0.250	0.500	0.250
Simpson	0.166	0.666	0.166

w^M for 3 integration points			
Coefficients	**w_1**	**w_2**	**w_3**
RADIOSS	-0.083	0.	0.083
Simpson	-0.083	0.	0.083

Lobatto Integration Scheme		
Number of Points	**Position**	**Weight**
2	±1.0000000000	1.0000000000
3	±1.0000000000 0.0000000000	0.3333333333 1.3333333333
4	±1.0000000000 ±0.4472135955	0.1666666666 0.8333333333
5	±1.0000000000 ±0.6546536707 0.0000000000	0.1000000000 0.5444444444 0.7111111111

Gauss Integration Scheme		
Number of Points	**Position**	**Weight**
1	±0.0000000000	2.0000000000
2	$\pm 1/\sqrt{3}$	1.0000000000
3	0.0000000000 $\pm\sqrt{3/5}$	8/9 5/9
4	$\pm\sqrt{\frac{3-2\sqrt{6/5}}{7}}$ $\pm\sqrt{\frac{3+2\sqrt{6/5}}{7}}$	$\frac{1}{2}+\frac{1}{6\sqrt{6/5}}$ $\frac{1}{2}-\frac{1}{6\sqrt{6/5}}$

5.3.11.2 Global plasticity algorithm

In the case of global plasticity, the forces and moments are computed directly. The algorithm is activated by specifying the number of integration points through the thickness as zero. The first step is an obvious elastic calculation:

$$\{\Sigma^{el}\} = \{\Sigma(t)\} + \mathbf{L}\{\dot{E}\}\Delta t \qquad \text{EQ. 5.3.11.3}$$

The yield criterion used is the uncoupled Iliouchine form [13]:

$$F = \frac{\overline{N}^2}{t^2} + \frac{16\overline{M}^2}{t^4} - \sigma_{yield}^2 \le 0 \qquad \text{EQ. 5.3.11.4}$$

with

$$\overline{N}^2 = N_x^2 + N_y^2 - N_x N_y + 3N_{xy}^2 \qquad \text{EQ. 5.3.11.5}$$

$$\overline{M}^2 = M_x^2 + M_y^2 - M_x M_y + 3M_{xy}^2 \qquad \text{EQ. 5.3.11.6}$$

where

$$N_x = \int_{-t/2}^{t/2} \sigma_x^{pa} dz \qquad M_x = \int_{-t/2}^{t/2} \sigma_x^{pa} z dz$$

$$N_y = \int_{-t/2}^{t/2} \sigma_y^{pa} dz \qquad M_y = \int_{-t/2}^{t/2} \sigma_y^{pa} z dz$$

$$N_{xy} = \int_{-t/2}^{t/2} \sigma_{xy}^{pa} dz \qquad M_{xy} = \int_{-t/2}^{t/2} \sigma_{xy}^{pa} z dz$$

An extension of Iliouchine criterion for isotropic hardening is developed here. The yield surface can be expressed as:

$$f = \begin{Bmatrix} \{N\} \\ \{M\} \end{Bmatrix}^t [F] \begin{Bmatrix} \{N\} \\ \{M\} \end{Bmatrix} - \left(\sigma_y^0 \beta\right)^2 = 0 \qquad \text{EQ. 5.3.11.7}$$

$$\text{with: } [F] = \begin{bmatrix} \frac{1}{h^2}[A] & \frac{1}{2\sqrt{3}\left(s\gamma h \frac{h^2}{6}\right)}[A] \\ sym & \frac{1}{\left(\gamma \frac{h^2}{6}\right)^2}[A] \end{bmatrix} \qquad \text{EQ. 5.3.11.8}$$

$$\text{and } s = \frac{\left|\{N\}^t [A] \{M\}\right|}{\{N\}^t [A] \{M\}} \qquad \text{EQ. 5.3.11.9}$$

Where β and γ are scalar material characteristic constants, function of plastic deformation. They can be identified by the material hardening law in pure traction and pure bending:

$$\text{In pure traction: } f = \frac{N^2}{h^2} - \left(\sigma_y^0 \beta\right)^2 = 0 \rightarrow \beta = \frac{\sigma_y\left(\varepsilon^p\right)}{\sigma_y^0} \qquad \text{EQ. 5.3.11.10}$$

$$\text{In pure bending: } f = \frac{M^2}{\left(\gamma h^2/6\right)^2} - \left(\sigma_y^0 \beta\right)^2 = 0 \rightarrow \gamma = \frac{M}{\sigma_y h^2/6} \qquad \text{EQ. 5.3.11.11}$$

If no hardening law in pure bending is used, γ is simply computed by $\gamma = \frac{\sigma_y / E + \frac{3}{2}\varepsilon^p}{\sigma_y / E + \varepsilon^p}$ varying between 1.0 and 1.5.

The plasticity flow is written using the normality law:

$$\begin{Bmatrix}\{d\varepsilon_p\}\\ \{d\mathrm{X}_p\}\end{Bmatrix} = d\lambda\frac{\partial f}{\partial\begin{Bmatrix}\{N\}\\ \{M\}\end{Bmatrix}} = 2d\lambda[F]\begin{Bmatrix}\{N\}\\ \{M\}\end{Bmatrix}$$ EQ. 5.3.11.12

The equivalent plastic deformation ε^P is proportional to the plastic work. Its expression is the same as in the case of traction:

$$\sigma_y^0\beta d\varepsilon^p = \begin{Bmatrix}\{d\varepsilon_p\}\\ \{d\chi_p\}\end{Bmatrix}^t\begin{Bmatrix}\{N\}\\ \{M\}\end{Bmatrix} = 2d\lambda\left(\sigma_y^0\beta\right)^2$$ EQ.5.3.11.13

This leads to:

$$d\varepsilon^p = 2d\lambda\sigma_y^0\beta \text{ and } d\beta = \frac{H}{\sigma_y^0}d\varepsilon^p$$ EQ. 5.3.11.14

where *H* is the plastic module. The derivative of function *f* in EQ. 5.3.11.7 is discontinuous when $\{N\}^t\{A\}\{M\}$=0. This can be treated when small steps are used by putting s=0 as explained in [87].

Then the derivative of *f* with respect to $d\varepsilon^P$ ($\frac{\partial f}{\partial d\varepsilon^P}$) is carried out. The derived equation is nonlinear in internal efforts and is resolved by Newton-Raphson:

$$\begin{Bmatrix}\{N\}\\ \{M\}\end{Bmatrix}_{n+1} = \begin{Bmatrix}\{N\}\\ \{M\}\end{Bmatrix}_* - 2d\lambda[D][F]\begin{Bmatrix}\{N\}\\ \{M\}\end{Bmatrix}_{n+1}$$ EQ. 5.3.11.15

where [*D*] is the elastic stiffness matrix and:

$$\begin{Bmatrix}\{N\}\\ \{M\}\end{Bmatrix}_* = \begin{Bmatrix}\{N\}\\ \{M\}\end{Bmatrix}_n - [D]\begin{Bmatrix}\{d\varepsilon\}\\ \{d\chi\}\end{Bmatrix}$$ EQ. 5.3.11.16

5.3.12 QPH, QPPS, QEPH and QBAT shell formulations

QPH shell is the Belytschko Leviathan [17] shell for linear models or quasi-static analysis is identical to a QPPS shell analysis, only one difference being explained in section 5.3.12.2.

The QPPS shell is a new One-point Quadrature, General Nonlinear Quadrilateral Shell Element with Physical Stabilization. This shell is a Belytschko Leviathan [17] shell modified by Zeng and Combescure [15].

The physical stabilization is applied which enables the explicit evaluation of the stabilizing forces based on the general degenerated shell formulation and which does not require any input parameters. An optimized choice of the moduli is made in order to compute the stabilized forces for nonlinear material so that element's behavior is improved with respect to similar physical stabilization elements. The cost efficiency of the element is demonstrated by numerical examples, as compared with a fully-integrated 4-node element.

The QEPH shell is a new improved element with respect to QPH,QPPS. The improvements will be explained in section 5.3.12.2. As the QEPH is very efficient, it replaces QPH,QPPS in the applications.

The QBAT shell is a new fully-integrated 4-node element based on Q4γ24 shell of Batoz and Dhatt [40] as discussed in section 5.3.9.4.

The general formulation of the degenerated continuum quadrilateral shell (for which all these elements used) is given in the section 5.3.12.1. The difficulties in evaluating the stabilized stiffness are also described. Section 5.3.12.2 presents the detailed formulations for the one-point quadrature shell element based on the general formulation, and compares it with that of Belytschko and Leviathan.

5.3.12.1 Formulations for a general degenerated 4-node shell

The following formulations of degenerated quadrilateral shells are based on the successful full integration element MITC4 developed by Dvorkin-Bathe [32] and Q4γ24 developed by Batoz and Dhatt [40]; they are suitable for both thin and thick shells and are applicable to linear and nonlinear problems. Their main feature is that a classical displacement method is used to interpolate the in-plane strains (membrane, bending), and a mix/collocation (or assumed strain) method is used to interpolate the out-plane strains (transverse shear). Certain conditions are also specified:

- They are based on the Reissner-Mindlin model,
- In-plane strains are linear, out-plane strains(transverse shear) are constant throughout the thickness,
- Thickness is constant in the element (the normal and the fiber directions are coincident),
- 5 DOF in the local system (i.e. the nodal normal vectors are not constant from one element to another).

A - Notational conventions

- A bold letter denotes a vector or a tensor.
- An upper case index denotes a node number; a lower case index denotes a component of vector or tensor.
- The Einstein convention applies only for the repeated index where one is subscript and another is superscript, e.g.:
  $N_I x^I = \sum N_I x^I$.
- {} denotes a vector and [ ] denotes a matrix.

B - Geometry and kinematics

Figure 5.3.11 - Coordinate systems

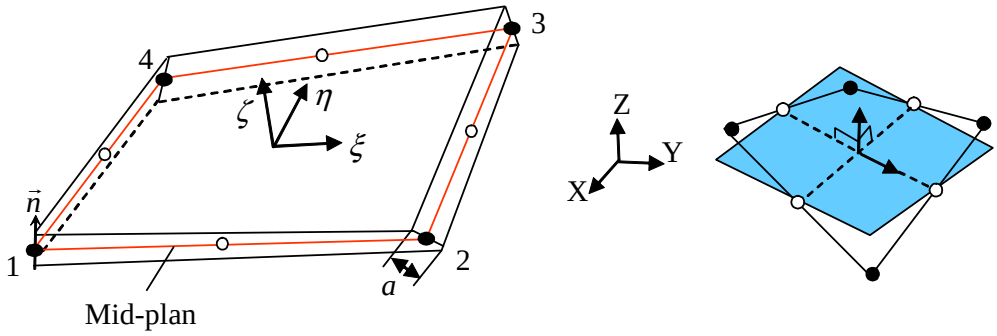

The geometry of the 4-node degenerated shell element, as shown in the Fig 5.3.11., is defined by its mid-surface with coordinates denoted by $\mathrm{X}p$ interpolated by the node coordinates X^I (I=1,4):

$$\mathrm{X}p(\xi,\eta) = N_I \mathrm{X}^I \qquad \text{EQ. 5.3.12.1}$$

where $N_I(\xi,\eta)$ are the bilinear isoparametric shape functions, given by:

$$N_I(\xi,\eta) = (1+\xi_I\xi)(1+\eta_I\eta)/4 \qquad \text{EQ. 5.3.12.2}$$

A generic point q within the shell is derived from point p on the mid-surface and its coordinate along the normal (fiber):

$$\mathrm{Xq}(\xi,\eta,\zeta) = \mathrm{Xp} + \mathrm{z}\cdot\mathrm{n} \quad \text{with} \quad z = \tfrac{a\zeta}{2}$$ EQ. 5.3.12.3

where *a* is the shell thickness.

The transformation between the Cartesian system and the Natural system is given by the differential relation (in matrix form):

$$\{dXq\} = \left([F_0] + z\left[\{n,_\xi\} \quad \{n,_\eta\} \quad \{0\}\right]\right)\{d\xi\} = [F]\{d\xi\}$$ EQ. 5.3.12.4

with

$$[\mathrm{F_0}] = \left[\{\mathrm{g_1}\}\{\mathrm{g_2}\}\tfrac{a}{2}\{\mathrm{n}\}\right]; \mathrm{g_1}(\xi,\eta) = \mathrm{X_{p,\xi}} = \mathrm{N_{I,\xi}X^I}, \mathrm{g_2}(\xi,\eta) = \mathrm{X_{p,\eta}} = \mathrm{N_{I,\eta}X^I}$$

F is the gradient tensor which is related to the Jacobian tensor $[J] = [F]^t$.

With 5 DOF at each node I (three translational velocities $v^I \rightarrow v_i^I$ and two rotational velocities $\left(\omega^I \rightarrow \omega_i^I\right)$, the velocity interpolation is given by the Mindlin model:

$$\mathrm{v_q}(\xi,\eta,\zeta) = \mathrm{v_p} + \mathrm{z}\beta = \mathrm{N_I}(\xi,\eta)\left(\mathrm{v^I} + \mathrm{z}\beta^{\mathrm{I}}\right)$$ EQ. 5.3.12.5

$$\beta = \omega \times \mathrm{n}$$

where β and ω are the rotational velocity vectors of the normal: $\beta = \beta_1 \mathrm{t_1} + \beta_2 \mathrm{t_2} = \omega_2 \mathrm{t_1} - \omega_1 \mathrm{t_2}$

and $(\mathrm{t_1}, \mathrm{t_2}, \mathrm{n})$ is base of the local coordinate system.

EQ. 5.3.12.5 can be written also by:

$$\mathrm{v_i} = \mathrm{N_I v_i^I} + \mathrm{z}\left(-\mathrm{N_I}\omega_1^{\mathrm{I}}\mathrm{t}_{2\mathrm{i}}^{\mathrm{I}} + \mathrm{N_I}\omega_2^{\mathrm{I}}\mathrm{t}_{1\mathrm{i}}^{\mathrm{I}}\right); \quad \mathrm{i} = 1,3$$

This velocity interpolation is expressed in the global system, but ω^{I} must be defined first in the local nodal coordinate system to ensure Mindlin's kinematic condition.

C - Strain-rate construction

The in-plane rate-of-deformation is interpolated by the usual displacement method.

The rate-of-deformation tensor (or velocity-strains) $\mathbf{D} = \left(\mathbf{L}_t + \mathbf{L}_{\mathrm{t}}^{\mathrm{T}}\right)/2$ is defined by the velocity gradient tensor *L*:

$$\{dv_q\} = [L_\zeta]\{d\xi\} = [L_\zeta][F]^{-1}\{dXq\} = [L]\{dXq\} = [Q][L_t][Q]^T\{dXq\}$$ EQ. 5.3.12.6

with $[Q] = [\{t_1\}\{t_2\}\{n\}]$.

The Reissner-Mindlin conditions $\varepsilon_\zeta = 0$ and $\sigma_\zeta = 0$ requires that the strain and stress tensors are computed in the local coordinate system (at each quadrature point).

After the linearization of L_t with respect to *z*, the in-plane rate-of-deformation terms are given by:

$$[L_t]_{2\times 2} = [L_{s0}] + z[L_{s1}]$$

with the membrane terms:

$$[L_{s0}] = [C_1][C_0]$$

the bending terms:

$$[L_{s1}] = 2H[L_{s0}] + [C_1]\begin{bmatrix} g^2 \cdot n,_\eta & -g^1 \cdot n,_\eta \\ -g^2 \cdot n,_\xi & g^1 \cdot n,_\xi \end{bmatrix}[C_0] + \begin{bmatrix} t_1 \cdot \beta,_\xi & t_1 \cdot \beta,_\eta \\ t_1 \cdot \beta,_\xi & t_1 \cdot \beta,_\eta \end{bmatrix} \quad \text{EQ. 5.3.12.7}$$

where the contravariant vectors $g^\alpha(\alpha = 1,2)$, dual to g_α, satisfy the orthogonality condition: $g^\alpha \cdot g_\beta = \delta_\beta^\alpha$ (Kronecker delta symbol); $H(\xi,\eta)$ is the average curvature: $2H = -(g^1 \cdot n,_\xi + g^2 \cdot n,_\eta)$

$$[C_0] = \begin{bmatrix} t_1 \cdot g^1 & t_2 \cdot g^1 \\ t_1 \cdot g^2 & t_2 \cdot g^2 \end{bmatrix} \text{ and } [C_1] = \begin{bmatrix} t_1 \cdot v_p,_\xi & t_1 \cdot v_p,_\eta \\ t_2 \cdot v_p,_\xi & t_2 \cdot v_p,_\eta \end{bmatrix} \quad \text{EQ. 5.3.12.8}$$

The curvature-translation coupling is presented in the bending terms for a warped element (the first two terms in last EQ.)

The out-plane rate-of-deformation (transverse shear) is interpolated by the "assumed strain" method, which is based on the Hu-Washizu variation principle.

If the out-plane rate-of-deformation is interpolated in the same manner for a full integration scheme, it will lead to "shear locking". It is known that the transverse shear strains energy cannot vanish when it is subjected to a constant bending moment. Dvorkin-Bathe's [32] mix/collocation method has been proved very efficient in overcoming this problem. This method consists in interpolating the transverse shear from the values of the covariant components of the transverse shear strains at 4 mid-side points. i.e.:

$$\gamma_\xi = \left[(1-\eta)\gamma_\xi^{A1} + (1+\eta)\gamma_\xi^{A2}\right]/2 \quad \text{EQ. 5.3.12.9}$$

$$\gamma_\eta = \left[(1-\xi)\gamma_\eta^{B1} + (1+\xi)\gamma_\eta^{B2}\right]/2 \quad \text{EQ. 5.3.12.10}$$

Where $\gamma_\xi^{A\alpha}, \gamma_\eta^{B\alpha}$ are the values of the covariant components at 4 mid-side points which vanish under a constant bending moment (see Figure 5.3.12).

Figure 5.3.12 - Covariant components at 4 mid-side

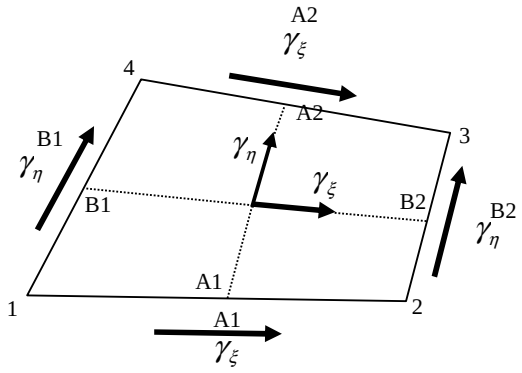

D - Special case for one-point quadrature and the difficulties in stabilization

The formulations described above are general for both the full integration and reduced integration schemes. For a one-point quadrature element, you have the following particularities:

The quadrature point is often chosen at $(\xi = 0, \eta = 0)$. The derivatives of the shape functions are:

$$N_{I,\xi} = (\xi_I + h_I\eta)/4 \quad N_{I,\eta} = (\eta_I + h_I\xi)/4 \quad \text{EQ. 5.3.12.11}$$

Where $h_I = (1 \quad -1 \quad 1 \quad -1)$.

This implies that all the terms computed at the quadrature point are the constant parts with respect to (ξ,η), and the stabilizing terms (hourglass) are the non-constant parts.

The constant parts can be derived directly from the general formulations at the quadrature point without difficulty. The difficulties in stabilization lie in correctly computing the internal force vector (or stiffness matrices):

$$f^{\text{int}} = \int_{\Omega} \overline{B}^{t} \cdot \sigma \quad d\Omega = f^{\text{int}}(\xi = \eta = 0) + f^{\text{int}}_{stab} \qquad \text{EQ. 5.3.12.12}$$

It would be ideal if the integration term f^{int}_{stab} could be evaluated explicitly. But such is not the case, and the main obstacles are the following:

For a non-coplanar element, the normal varies at each point so that it is difficult to write the non-constant part of strains explicitly. For a physically nonlinear problem, the non-constant part of stress is not generally in an explicit form. Thus, simplification becomes necessary.

5.3.12.2 Fully-integrated shell element QBAT

QBAT is a fully-integrated shell element based on the general formulation described above. In the surface of each element, 4 Gauss points are used to evaluate the nodal forces.

The main modifications with respect to Q4γ24 shell element [40] are the following:

- Reduced integration for in-plane shear (constant) to avoid locking.
- Co-rotational coordinate system is used and the stresses are evaluated in 4 local systems at each Gauss points..

5.3.12.3 The new one-point quadrature shell element

In this section, a one-point quadrature shell element formulation will be developed from the general formulation described in the previous section. It is based on the Physical Stabilization method which explicitly computes the stabilization terms in making some simplifications.

The following formulations will be written in the local coordinate system [$\mathbf{t}_1$ $\mathbf{t}_2$ $\mathbf{n}$] (the circumflex in the co-rotational system notation has been omitted for convenience).

A - Kinematic approximation

The velocity interpolation using the nodal tangent vectors ($\mathrm{t}_1^{\mathrm{I}}, \mathrm{t}_2^{\mathrm{I}}$) complicates the strain computation, especially for transverse shear which is used mainly as a penalty function. To be consistent with the one-point quadrature approach, the kinematic approximation is performed by:

$$v_i = N_I \left[v_i^I + z\left(-\delta_{i2}\overline{\omega}_1^I + \delta_{i1}\overline{\omega}_2^I \right) \right] \qquad \text{EQ. 5.3.12.13}$$

where $\overline{\omega}_i^I$ (i=1,2) is the nodal rotation velocity around $\mathrm{t}_{\mathrm{i}}^{\mathrm{I}}$. $\overline{\omega}_i^I$ can be computed by a projection scheme by :

$$\overline{\omega}^I = \omega^I - \left(\omega^I \cdot n^I\right) n^I = P\left(n^I\right)\omega^I \qquad \text{EQ. 5.3.12.14}$$

The projection consists in eliminating the nodal drilling rotations in order to reinforce Mindlin's kinematic condition at the nodes. It has been pointed out [18] that without this projection, the element is too flexible and cannot pass the Twisted Beam test.

This projection has a drawback of changing the invariance property to rigid body motion, i.e.: a warped element being invariant to rigid body rotation will now strains under to rigid body rotation if the drill projection is applied. To overcome this problem, a full projection proposed by Belytschko-Leviathan [66] which free either drilling rotation or rigid motion should be used. This full projection is only used for QEPH element.

B - In-plane strain-rate construction

Constant part

It is useful to write the shape functions in Belytschko-Bachrach's mixed form:

$$N_I(x,y,\xi\eta) = \Delta_I + b_{xI}^x + b_{yI}^y + \gamma_I\phi \qquad \text{EQ. 5.3.12.15}$$

with: $\Delta_I = \left[t_I - \left(t_I x^I\right) b_{xI} - \left(t_I y^I\right) b_{yI}\right]; \quad t_I = (1,1,1,1)$

$$b_{xI} = \left(y_{24}y_{31}y_{42}y_{13}\right)/A; b_{yI} = \left(x_{42}x_{13}x_{24}x_{31}\right)/A \quad (fij = (fi - fj)/2)$$

$$\gamma_I = \left[h_I - \left(h_J x^J\right) b_{xI} - \left(h_J y^J\right) b_{yI}\right]/4 \; ; \phi = \xi\eta \quad ;$$

A is the area of element.

The derivation of the shape functions is given by:

$$N_{I,\alpha} = b_{\alpha I} + \gamma_I \phi_{,\alpha} (\alpha = x, y)$$

where:

$$\begin{aligned} \phi_{,x} &= \eta\xi_{,x} + \xi\eta_{,x} = J_{11}^{-1}\eta + J_{12}^{-1}\xi \\ \phi_{,y} &= \eta\xi_{,y} + \xi\eta_{,y} = J_{21}^{-1}\eta + J_{22}^{-1}\xi \end{aligned} \qquad \text{EQ. 5.3.12.16}$$

The advantage of this shape function form is that a linear field expressed with Cartesian coordinates and a bilinear field expressed with Natural coordinates is decomposed so that the constant part is directly formulated with the Cartesian coordinates, and the non-constant part is to be approached separately.

The in-plane rate-of-deformation (decomposed on membrane and bending) is given by:

$$\{D\} = \{D^m\} + z\{D^b\} = [B_I]\{v_n^I\} \qquad \text{EQ. 5.3.12.17}$$

with:

$$\lfloor B_I \rfloor = \left[B_I^m\right] + z\left[B_I^b\right]; \quad < v_n^I > = < v_x^I v_y^I v_z^I \varpi_x^I \varpi_y^I > .$$

The development of the general formulations leads to the constant part, denoted by superscript 0, of the matrix $[B_I]$:

$$\left[\left(B_I^m\right)^0\right] = \begin{bmatrix} b_{xI} & 0 & 0 \\ 0 & b_{yI} & 0 \\ b_{yI} & b_{xI} & 0 \end{bmatrix} \qquad \left[\left(B^b\right)^0\right] = 2H\left[\left(B_I^m\right)^0\right] + \begin{bmatrix} b_{xI}^c & 0 & 0 & 0 & b_{xI} \\ 0 & b_{yI}^c & 0 & -b_{yI} & 0 \\ b_{yI}^c & b_{xI}^c & 0 & -b_{xI} & b_{yI} \end{bmatrix} \qquad \text{EQ. 5.3.12.18}$$

with

$$< b_{xI}^c > = 4z_\gamma / A^2 < b_{y2} \; ; b_{y1} \; ; b_{y4} \; ; b_{y3} >$$

$$< b_{yI}^c > = 4z_\gamma / A^2 < b_{x4} \; ; b_{x3} \; ; b_{x2} \; ; b_{x1} >$$

The parameter $z_\gamma = \gamma_I z^I$ is a measure of the warping of the element.

The first term $2H\left[\left(B_I^m\right)^0\right]$ is neglectable. You have verified that the order of $2H\left[\left(B_I^m\right)^0\right]$ is ε times the second term of $\left[\left(B^b\right)^0\right]$ with $\varepsilon = 2\bar{x}_{34}/\bar{y}_{34}$ $\left(\bar{f}_{ij} = \left(f_i + f_j\right)/2\right)$, which vanishes when the element is rectangular. Thus, this term is not used in the program.

The constant part of the in-plane rate-of-deformation formulation without the *H* term is consistent with the result of Belytschko's family shell element [24], [17], though this part has been obtained in a very different manner. Letellier has given the same result in his thesis [43], and studies were also made of the quadratic terms with respect to *z*.

Non-constant part

The main simplification for the non-constant part formulation, in order to overcome the difficulties described above, is the following:

The element is considered to be flat.

In this case, the Jacobian matrix is written as:

$$[J] = [F_0]^t = \begin{bmatrix} x_{,\xi} & y_{,\xi} & 0 \\ x_{,\eta} & y_{,\eta} & 0 \\ 0 & 0 & a\bar{J}_0/2\bar{J} \end{bmatrix} = \begin{bmatrix} [\bar{J}] & 0 \\ 0 & a\bar{J}_0/2\bar{J} \end{bmatrix} \qquad \text{EQ. 5.3.12.19}$$

with the determinant $\bar{J}$ of the in-plane Jacobian:

$$\bar{J} = \det[\bar{J}] = \bar{J}_0 + \bar{J}_1\xi + \bar{J}_2\eta \qquad \text{EQ. 5.3.12.20}$$

and:

$$\bar{J}_0 = \left[\left(\xi_I x^I\right)\left(\eta_I y^I\right) - \left(\eta_I x^I\right)\left(\xi_I y^I\right)\right]/16 = A/4$$

$$\bar{J}_1 = \left[\left(\xi_I x^I\right)\left(h_I y^I\right) - \left(h_I x^I\right)\left(\xi_I y^I\right)\right]/16$$

$$\bar{J}_2 = \left[\left(h_I x^I\right)\left(\eta_I y^I\right) - \left(\eta_I x^I\right)\left(h_I y^I\right)\right]/16$$

The inverse of the in-plane Jacobian matrix can be expressed explicitly:

$$[J] = \begin{bmatrix} \xi_{,x} & \eta_{,x} \\ \xi_{,y} & \eta_{,y} \end{bmatrix} = \frac{1}{J}\begin{bmatrix} y_{,\eta} & -y_{,\xi} \\ -x_{,\eta} & x_{,\xi} \end{bmatrix} = \frac{1}{4\bar{J}}\begin{bmatrix} (\eta_I + h_I\xi)y^I & (\xi_I + h_I\eta)y^I \\ (\eta_I + h_I\xi)x^I & (\xi_I + h_I\eta)x^I \end{bmatrix} \qquad \text{EQ. 5.3.12.21}$$

You can now write the non-constant part, denoted by superscript *H*, of the matrix [B_I] for in-plane rate-of-deformation:

$$\left[\left(B_I^m\right)^H\right] = \begin{bmatrix} \gamma_I\phi_{,x} & 0 & 0 \\ 0 & \gamma_I\phi_{,y} & 0 \\ \gamma_I\phi_{,y} & \gamma_I\phi_{,x} & 0 \end{bmatrix}; \quad \left[\left(B_I^b\right)^H\right] = \begin{bmatrix} 0 & \gamma_I\phi_{,x} \\ -\gamma_I\phi_{,y} & 0 \\ -\gamma_I\phi_{,x} & \gamma_I\phi_{,y} \end{bmatrix} \qquad \text{EQ. 5.3.12.22}$$

It is shown in [16] that the non-constant part of membrane rate-strain does not vanish when a warped element undergoes a rigid body rotation. Thus, a modified matrix $\left[\left(B_I^m\right)^H\right]$ is chosen:

$$\left[\left(B_I^m\right)^H\right] = \begin{bmatrix} \gamma_I\phi_{,x} & 0 & z_\gamma b_{xI}\phi_{,x} \\ 0 & \gamma_I\phi_{,y} & z_\gamma b_{yI}\phi_{,y} \\ \gamma_I\phi_{,y} & \gamma_I\phi_{,x} & z_\gamma\left(b_{xI}\phi_{,y} + b_{yI}\phi_{,x}\right) \end{bmatrix} \qquad \text{EQ. 5.3.12.23}$$

This matrix is different from the Belytschko-Leviathan correction term added at rotational positions, which couples translations to curvatures as follows:

$$\left[\left(B_I^m\right)^H\right]=\begin{bmatrix} \gamma_I\phi,_x & 0 & 0 & 0 & -\frac{1}{4}z_\gamma\phi,_x \\ 0 & \gamma_I\phi,_y & 0 & \frac{1}{4}z_\gamma\phi,_y & 0 \\ \gamma_I\phi,_y & \gamma_I\phi,_x & 0 & \frac{1}{4}z_\gamma\phi,_x & -\frac{1}{4}z_\gamma\phi,_y \end{bmatrix} \qquad \text{EQ. 5.3.12.24}$$

This will lead to 'membrane locking' (the membrane strain will not vanish under a constant bending loading). According to the general formulation, the coupling is presented in the bending terms not in the membrane terms, yet the normal translation components in $(B_I^m)_{i3}$ do not vanish for a warped element due to the tangent vectors $\mathbf{t}_i(\xi,\eta)$ which differ from $\mathbf{t}_i(0,0)$.

C - Out-plane strain-rate construction

The out-plane rate-of-deformation (transverse shear) is interpolated by the Dvorkin-Bathe method, whose closed form is given by Belytschko-Leviathan:

$$\begin{Bmatrix} D_{xz} \\ D_{yz} \end{Bmatrix}=[B_{Ic}]\begin{Bmatrix} v_z^I \\ \varpi_x^I \\ \varpi_y^I \end{Bmatrix} \qquad \text{EQ. 5.3.12.25}$$

where: $[B_{Ic}](\zeta,\eta)=\left[B_{Ic}{}^{\eta}\right](\eta)+\left[B_{Ic}{}^{\xi}\right](\xi)$

$$\left(B_{Ic}^{\eta}\right)^0=\frac{1}{16A}\begin{bmatrix} 4\eta_I y^I\xi_I & -(\xi_J+h_J\eta_I)\eta_k y^k y^J & (\xi_J+h_J\eta_I)\eta_k y^k x^J \\ -4\eta_I x^I\xi_I & (\xi_J+h_J\eta_I)\eta_k x^k y^J & -(\xi_J+h_J\eta_I)\eta_k x^k x^J \end{bmatrix}$$

$$\left(B_{Ic}^{\xi}\right)^0=\frac{1}{16A}\begin{bmatrix} -4\xi_I y^I\eta_I & (\eta_J+h_J\xi_I)\xi_k y^k y^J & -(\eta_J+h_J\xi_I)\xi_k y^k x^J \\ 4\xi_I y^I\eta_I & -(\eta_J+h_J\xi_I)\xi_k x^k y^J & (\eta_J+h_J\xi_I)\xi_k x^k x^J \end{bmatrix} \qquad \text{EQ. 5.3.12.26}$$

and $\left(B_{Ic}{}^{\eta}\right)^H=\eta_I\left(B_{Ic}{}^{\eta}\right)^0\eta;\left(B_{Ic}{}^{\xi}\right)^H=\xi_I\left(B_{Ic}{}^{\xi}\right)^0\xi$

The straightforward form of $[B_{Ic}]$ is obtained using one additional simplification:

$$\xi_{,x}(\xi,\eta)=\xi_{,x}(0,0)\eta_{,x}(\xi,\eta)=\eta_{,x}(0,0)$$

which is true for a parallelogram element. Although this simplification is not necessary, it is justified by the fact that the transverse shear terms serve mainly as a penalty function.

D - Explicit integration of the nodal internal force vector

Elastic case

The elementary nodal force vector is computed by:

$$\left\{f_I^{\text{int}}\right\}=\int_{ve}[B_I]^t[C][B_J]\{v_n^J\}dv^e$$

Taking advantage of substantial orthogonality between:

- the constant in-plane fields along with the non-constant ones
- the membrane and the bending
- the in-plane fields and the out-plane fields
- the decomposed non-constant out-plane fields

resulting in:

$$\left\{f_I^{\text{int}}\right\} = \left\{\left(f_I^{\text{int}}\right)^0\right\} + \left\{\left(f_I^{\text{int}}\right)^H\right\}$$

With $\left\{\left(f_I^{\text{int}}\right)^0\right\}$ the constant part being computed with one-point quadrature, and

$$\left\{\left(f_I^{\text{int}}\right)^H\right\} = \int_{ve}\left[\left(B_I\right)^H\right]^t[C]\left[\left(B_J\right)^H\right]\left\{v_n^J\right\}dv^e$$

It can be shown in the last equation that only the following scalar functions need to be integrated:

$$H_{xx} = \int A_e\phi_{,x}\phi_{,x}dA_e, H_{xy} = \int A_e\phi_{,x}\phi_{,y}dA_e, H_{yy} = \int A_e\phi_{,y}\phi_{,y}dA_e \qquad \text{EQ. 5.3.12.27}$$

These can be evaluated explicitly.

Defining 6 hourglass generalized rate-of-deformation $\dot{q}$ by:

$$\text{membrane}: \begin{cases} \dot{q}_x^m = \gamma_I v_x^I + z^1 b_{xI} v_z^I \\ \dot{q}_y^m = \gamma_I v_y^I + z^1 b_{yI} v_z^I \end{cases} \qquad \text{EQ. 5.3.12.28}$$

$$\text{bending}: \begin{cases} \dot{q}_x^b = \gamma_I \varpi_y^I \\ \dot{q}_y^b = \gamma_I \varpi_x^I \end{cases} \qquad \text{EQ. 5.3.12.29}$$

$$\text{shear}: \begin{cases} \dot{q}_x^s = 4h_I v_z^I - \left[\left(\xi_I y^I\right)\eta_I + \left(h_I y^I\right)t_I\right]\varpi_x^I + \left[\left(\xi_I x^I\right)\eta_I + \left(h_I x^I\right)t_I\right]\varpi_y^I \\ \dot{q}_y^s = 4h_I v_z^I - \left[\left(\eta_I y^I\right)\xi_I + \left(h_I y^I\right)t_I\right]\varpi_x^I + \left[\left(\eta_I x^I\right)\xi_I + \left(h_I x^I\right)t_I\right]\varpi_y^I \end{cases} \qquad \text{EQ. 5.3.12.30}$$

The rate-of-deformations will be written explicitly.

The rate form of the constitutive relation is written as (stress plane for in-plane terms):

$$\dot{\sigma} = C{:}D$$

With the assumption: **the spin is constant within the element**, the objectivity principle will be satisfied. The incremental computation is performed with the hourglass generalized rate-of-deformation $\dot{q}$, i.e.:

$$(q)_{n+1} = (q)_n + \dot{q}_{n+\frac{1}{2}}\Delta t$$

Noting that if $\phi_{,\alpha}$ is considered as constant over a time step, it is equivalent to the incremental stress computation.

Physical nonlinear case

You will now consider an elastoplastic problem.

The elementary nodal internal force vector is now computed by:

$$\left\{f_I^{\text{int}}\right\} = \int_{ve}[B_I]^t\{\sigma\}dv^e$$

The constitutive relation is written by either a tangent form: $\dot{\sigma} = C^t{:}D$, or a projection form: $\sigma = P\left(\sigma^e,...\right)$,

where $C^t\left(\sigma\ ,...\right)$ is the history-dependent tangent tensor ; $\left\{\sigma_{n+1}^e\right\} = \{\sigma_n\} + [C]\{D_{n+1/2}\}\Delta t$ is the trial stress, and the function *P* consists of projecting the trial stress on the updated yield surface.

The decomposed form of the last equation is written:

$$\left\{f_I^{\text{int}}\right\} = \left\{\left(f_I^{\text{int}}\right)^0\right\} + \left\{\left(f_I^{\text{int}}\right)^H\right\}$$

The constant part is computed by integration at each integration point through the thickness.

The stabilization part will be approached by relying on two hypotheses:

- Keep the same orthogonalities as in the elastic case, and

Use the unidimensional tangent modulus $E_t(\zeta)$ to evaluate the non-constant rate-stress, i.e.:

$$\{\dot{\sigma}\}^H = (E_t(\zeta)/E)[C]\{D\}^H \quad \text{EQ. 5.3.12.31}$$

where *E* is the Young's modulus and $[C]$ is the matrix of elastic moduli.

Thus, the elastic case easily extends to the nonlinear case.

The incremental computation with the hourglass generalized rate-of-deformation $\dot{q}$ becomes:

$$membrane: (q^m)_{n+1} = (q^m)_n + \lambda_m \dot{q}^m_{n+1/2}\Delta t \quad \text{EQ. 5.3.12.32}$$

$$bending: (q^b)_{n+1} = (q^b)_n + \lambda_b \dot{q}^b_{n+1/2}\Delta t \quad \text{EQ. 5.3.12.33}$$

$$shear: (q^s)_{n+1} = (q^s)_n + \dot{q}^s_{n+1/2}\Delta t \quad \text{EQ. 5.3.12.34}$$

Where $E_t(\zeta)$ is obtained by the constant stress incremental computation along the thickness and $E_t(\zeta) = E$ in the elastic zone, and $\lambda_m = \overline{E_t}/E; \overline{E_t}$ is the average value of $E_t(\zeta)$ and $\lambda_b = \min E_t(\zeta)/E$.

For the QPH shell, λm = 1

The key orthogonalities has been maintained without any significant deterioration in performance, although the first two orthogonalities might have been slightly violated. In fact, it is simply due to these orthogonalities that a one-point quadrature element dramatically reduces the computation cost; otherwise you return to the full integration scheme.

Most of the physical stabilization elements have incorporated the following assumption:

The material response is constant within the element.

There are two alternatives to this assumption:

- **to take the elastic matrix $[C]$ directly:**

$$\{\dot{\sigma}\} = \{\dot{\sigma}\}^0 + [C]\left\{\left(\dot{\varepsilon} - \dot{\varepsilon}^P\right)^H\right\} = \{\dot{\sigma}\}^0 + [C]\left\{\left(\dot{\varepsilon}\right)^H\right\} \rightarrow \left\{\left(\dot{\varepsilon}^P\right)^H\right\} = 0$$

which means that the plastic rate-of-deformation $\left\{\dot{\varepsilon}^P\right\}$ is constant within the element; or

- **to take the tangent matrix [C^t] ($\xi = \eta = 0 \quad , \zeta =$** constant**):**

Since the components of [C^t] are generally functions of the updated stress (precisely, the stress deviator for an elastoplastic problem with an associative flow rule, which means that *the stress is constant within the element.*

Neither of these alternatives is theoretically perfect. Let us note that the [C] option results in a contradiction with the stress computation (which yields different results for the constant part and the non-constant part); it is more expensive and the tangent form is not generally used for constant stress computations within an explicit program. Hence, the approximation based on the above assumption is not necessary.

The choice of the moduli for the nonlinear case has not been studied for Belytschko-Leviathan's element [17], and it has been shown that this choice has little effect on the result of the “Cylindrical panel test”. In [30], the elastic tangent matrix has been used for the evaluation of the stabilizing forces.

QPH,QPPS have shown often stiffer behaviors and sometimes have certain numerical problems in crash simulations.

5.3.12.4 Advanced elasto-plastic hourglass control

QEPH (Quadrilateral ElastoPlastic Physical Hourglass Control) element

With one-point integration formulation, if the non-constant part follows exactly the state of constant part for the case of elasto-plastic calculation, the plasticity will be under-estimated due to the fact that the constant equivalent stress is often the smallest one in the element and element will be stiffer. Therefore, defining a yield criterion for the non-constant part seems to be a good idea to overcome this drawback.

From EQ. 5.3.12.16 and EQ. 5.3.12.21, you have the rate of stresses of non-constant part:

$$\{\dot{\sigma}_i\}^H = [C]\{\dot{\varepsilon}\}^H = [C]\begin{Bmatrix}\phi_{,x}\dot{q}_x^\alpha\\ \phi_{,y}\dot{q}_y^\alpha\\ 0\end{Bmatrix} = \eta\begin{Bmatrix}\dot{\sigma}_{x\eta}^\alpha\\ \dot{\sigma}_{y\eta}^\alpha\\ 0\end{Bmatrix} + \xi\begin{Bmatrix}\dot{\sigma}_{x\xi}^\alpha\\ \dot{\sigma}_{y\xi}^\alpha\\ 0\end{Bmatrix} \quad \text{EQ. 5.3.12.35}$$

Where $\alpha = m, b$ corresponds to the membrane and bending terms respectively. Note that the shear terms are eliminated to avoid shear locking. The transverse shear terms can also be written as the same way:

$$\{\dot{\tau}_i\}^H = \eta\begin{Bmatrix}\dot{\tau}_{x\eta}\\ \dot{\tau}_{y\eta}\end{Bmatrix} + \xi\begin{Bmatrix}\dot{\tau}_{x\xi}\\ \dot{\tau}_{y\xi}\end{Bmatrix} \quad \text{EQ. 5.3.12.36}$$

You can now redefine 12 generalized hourglass stresses by integrating their rate ones, and the stress field can be expressed by:

Membrane, bending: $\{\sigma_i^\alpha\} = \{\sigma_i^\alpha\}^0 + \{\sigma_i^\alpha\}^H = \{\sigma_i^\alpha\}^0 + \eta\begin{Bmatrix}\sigma_{x\eta}^\alpha\\ \sigma_{y\eta}^\alpha\\ 0\end{Bmatrix} + \xi\begin{Bmatrix}\sigma_{x\xi}^\alpha\\ \sigma_{y\xi}^\alpha\\ 0\end{Bmatrix}$

Shear: $\{\tau_i\} = \{\tau_i\}^0 + \{\tau_i\}^H = \{\tau_i\}^0 + \eta\begin{Bmatrix}\dot{\tau}_{x\eta}\\ \dot{\tau}_{y\eta}\end{Bmatrix} + \xi\begin{Bmatrix}\dot{\tau}_{x\xi}\\ \dot{\tau}_{y\xi}\end{Bmatrix}$

Even the redefinition for shear is not necessary as it is not included in the plastic yield criterion, but the same stress calculation as the constant part with the updated Lagrangian formulation is always useful when large strain is involved.

Plastic yield criterion:

The von Mises type of criterion is written by:

$$f = \sigma_{eq}^2(\xi,\eta,\zeta) - \sigma_y^2 = 0 \quad \text{EQ. 5.3.12.37}$$

for any point in the solid element, where σ_y is evaluated at the quadrature point.

As only one criterion is used for the non-constant part, two choices are possible:

- taking the mean value, i.e.: $f = f(\overline{\sigma}_{eq}), \overline{\sigma}_{eq} = \frac{1}{\Omega}\int_\Omega \sigma_{eq} d\Omega$
- taking the value by some representative points, e.g. eight Gausse points

The second choice has been used in this element.

Elasto-plastic hourglass stress calculation:

The incremental hourglass stress is computed by:

- Elastic increment

$$(\sigma_i)_{n+1}^{trH} = (\sigma_i)_n^H + [C]\{\dot{\varepsilon}\}^H \Delta t$$

- Check the yield criterion
- If $f \geq 0$, the hourglass stress correction will be done by un radial return

$$(\sigma_i)_{n+1}^{H} = P\left((\sigma_i)_{n+1}^{trH}, f\right)$$

5.3.13 Three-node shell elements

As for the four node shell element, a simple linear Mindlin Plate element formulation is used. Likewise, the use of one integration point and rigid body motion given by the time evolution of the local reference frame is applied. There is no hourglass mode in case of one integration point.

5.3.13.1 Local Reference Frame

The local reference frame for the three node shell element is shown in Figure 5.3.13.

Figure 5.3.13 - Node Shell Local Reference Frame

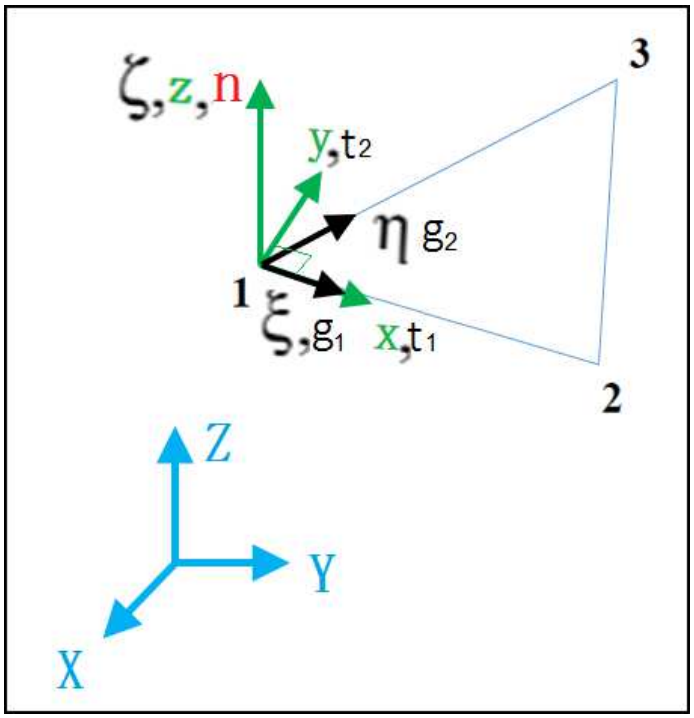

The vector normal to the plane of the element is defined as:

$$n = \frac{g_1 \times g_2}{\|g_1 \times g_2\|} \qquad \text{EQ. 5.3.13.1}$$

The vector defining the local x direction is defined as edge 1-2:

$$t_1 = \frac{g_1}{\|g_1\|} \qquad \text{EQ. 5.3.13.2}$$

Hence, the vector defining the local y direction is found from the cross product of the two previous vectors:

$$t_2 = n \times t_1$$ EQ. 5.3.13.3

5.3.13.2 Time Step

The characteristic length for computing the critical time step is defined by:

$$L = \frac{2area}{\max\left(\overline{12}, \overline{23}, \overline{31}\right)}$$ EQ. 5.3.13.4

Three Node Shell Shape Functions

The three node shell has a linear shape functions defined as:

$$\phi_1 = a_1 + b_1 x + c_1 y$$ EQ. 5.3.13.5

$$\phi_2 = a_2 + b_2 x + c_2 y$$ EQ. 5.3.13.6

$$\phi_3 = a_3 + b_3 x + c_3 y$$ EQ. 5.3.13.7

These shape functions are used to determine the velocity field in the element:

$$v_x = \sum_{I=1}^{3} \phi_I v_{xI}$$ EQ. 5.3.13.8

$$v_y = \sum_{I=1}^{3} \phi_I v_{yI}$$ EQ. 5.3.13.9

$$v_z = \sum_{I=1}^{3} \phi_I v_{zI}$$ EQ. 5.3.13.10

$$\omega_x = \sum_{I=1}^{3} \phi_I \omega_{xI}$$ EQ. 5.3.13.11

$$\omega_y = \sum_{I=1}^{3} \phi_I \omega_{yI}$$ EQ. 5.3.13.12

$$\frac{\partial v_x}{\partial x} = \sum_{I=1}^{3} \frac{\partial \phi_I}{\partial x} v_{xI}$$ EQ. 5.3.13.13

$$\frac{\partial v_x}{\partial y} = \sum_{I=1}^{3} \frac{\partial \phi_I}{\partial y} v_{xI}$$ EQ. 5.3.13.14

5.3.13.4 Membrane Behavior

The method used to calculate the membrane behavior and the membrane strain rates is exactly the same as that used for four node shell elements (see section 5.3.6.1).

5.3.13.5 Bending Behavior

The bending behavior and calculation of the bending strain rates (or curvature rates) is the exact same method used for four node shell elements (see section 5.3.6.2).

5.3.13.6 Strain Rate Calculation

The strain rate calculation for the three node shell is the same as the method used for the four node shell. However, only three nodes are accounted for. This makes the vectors and matrices smaller. The overall membrane strain rate is calculated by:

$$\{\dot{e}\}_m = \{\dot{e}_x, \dot{e}_y, 2\dot{e}_{xy}\} \quad \text{EQ. 5.3.13.15}$$

$$\{v\}_m = \{v_x^1, v_y^1, v_x^2, v_y^2, v_x^3, v_y^3\} \quad \text{EQ. 5.3.13.16}$$

$$\{\dot{e}\}_m = [B]_m \{v\}_m \quad \text{EQ. 5.3.13.17}$$

where the $[B]_m$ matrix of shape function gradients is defined as:

$$[B]_m = \begin{bmatrix} \frac{\partial \phi_1}{\partial x} & 0 & \frac{\partial \phi_2}{\partial x} & 0 & 0 & 0 \\ 0 & \frac{\partial \phi_1}{\partial y} & 0 & \frac{\partial \phi_2}{\partial y} & 0 & \frac{\partial \phi_3}{\partial y} \\ \frac{\partial \phi_1}{\partial y} & \frac{\partial \phi_1}{\partial x} & \frac{\partial \phi_2}{\partial y} & \frac{\partial \phi_2}{\partial x} & \frac{\partial \phi_3}{\partial y} & \frac{\partial \phi_3}{\partial x} \end{bmatrix} \quad \text{EQ. 5.3.13.18}$$

where $\frac{\partial \phi_3}{\partial x} = 0$ for a shell element.

The overall bending strain or curvature rate is computed by:

$$\{\dot{e}\}_b = \{\dot{k}_x, \dot{k}_y, 2\dot{k}_{xy}, 2\dot{e}_{zx}, 2\dot{e}_{yz}\} \quad \text{EQ. 5.3.13.19}$$

$$\{v\}_b = \{\omega_y^1, -\omega_x^1, \omega_y^2, -\omega_x^2 \omega_y^3, -\omega_x^3, v_z^1, v_z^2, v_z^3\} \quad \text{EQ. 5.3.13.20}$$

$$\{\dot{e}\}_b = [B]_b \{v\}_{bm} \quad \text{EQ. 5.3.13.21}$$

where:

$$[B] = \begin{bmatrix} \frac{\partial \phi_1}{\partial x} & 0 & \frac{\partial \phi_2}{\partial x} & 0 & 0 & 0 & 0 & 0 & 0 \\ 0 & \frac{\partial \phi_1}{\partial y} & 0 & \frac{\partial \phi_2}{\partial y} & 0 & \frac{\partial \phi_3}{\partial y} & 0 & 0 & 0 \\ \frac{\partial \phi_1}{\partial y} & \frac{\partial \phi_1}{\partial x} & \frac{\partial \phi_2}{\partial y} & \frac{\partial \phi_2}{\partial x} & \frac{\partial \phi_3}{\partial y} & \frac{\partial \phi_3}{\partial x} & 0 & 0 & 0 \\ \phi_1 & 0 & \phi_2 & 0 & \phi_3 & 0 & \frac{\partial \phi_1}{\partial x} & \frac{\partial \phi_2}{\partial x} & \frac{\partial \phi_3}{\partial x} \\ 0 & \phi_1 & 0 & \phi_2 & 0 & \phi_3 & \frac{\partial \phi_1}{\partial y} & \frac{\partial \phi_2}{\partial y} & \frac{\partial \phi_3}{\partial y} \end{bmatrix} \quad \text{EQ. 5.3.13.22}$$

5.3.13.7 Mass and Inertia

The three node shell element is considered as an element with a lumped mass. Its mass is defined as:

$$m = \rho A t \quad \text{EQ. 5.3.13.23}$$

where:

ρ is the material density,

t is the shell thickness,

A is the reference plane surface area.

The mass moment of inertia about all axes is the same:

$$I_{xx} = m\left(\frac{2A}{6} + \frac{t^2}{12}\right) \quad \text{EQ. 5.3.13.24}$$

$$I_{zz} = I_{yy} = I_{xx} \quad \text{EQ. 5.3.13.25}$$

$$I_{xy} = 0 \quad \text{EQ. 5.3.13.26}$$

When nodal masses need to be calculated, the distribution is determined by the shape of the element as shown in Figure 5.3.14.

Figure 5.3.14 - Mass distribution

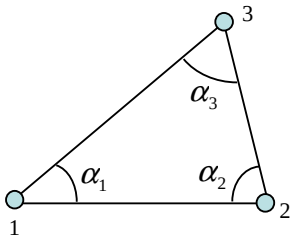

The mass and inertia at node *i* are given by:

$$m_i = \frac{\alpha_i}{\pi} m \quad ; \quad I_i = \frac{\alpha_i}{\pi} I \quad \text{EQ. 5.3.13.27}$$

5.3.14 Composite Shell Elements

There are three different element types that can be used for modeling composites. These are:

- Type 9 Element Property - Orthotropic Shell
- Type 10 Element Property - Composite Shell
- Type 11 Element Property - Composite Shell with variable layers

These elements are primarily used with the Tsai-Wu model (material law 25). They allow one global behavior or varying characteristics per layer, with varying orthotropic orientations, varying thickness and/or varying material properties, depending on which element is used. Elastic, plastic and failure modeling can be undertaken.

5.3.14.1 Transformation matrix from global to orthotropic skew

If the element reference is defined by the axes X, Y and the orthotropy directions by axes 1-2, write:

Figure 5.3.15 - Fiber orientation

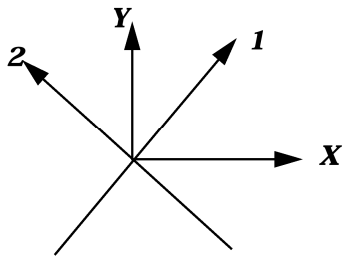

$\begin{bmatrix} c & -s \\ s & c \end{bmatrix}$ with c =cosθ and s = sinθ.

$$\begin{bmatrix} \varepsilon_{11} & \varepsilon_{12} \\ \varepsilon_{12} & \varepsilon_{22} \end{bmatrix} = \begin{bmatrix} c & s \\ -s & c \end{bmatrix} . \begin{bmatrix} \varepsilon_X & \varepsilon_{XY} \\ \varepsilon_{XY} & \varepsilon_Y \end{bmatrix} . \begin{bmatrix} c & -s \\ s & c \end{bmatrix} \quad \text{EQ. 5.3.14.1}$$

$$\begin{bmatrix} \varepsilon_{11} & \varepsilon_{12} \\ \varepsilon_{12} & \varepsilon_{22} \end{bmatrix} = \begin{bmatrix} c & s \\ -s & c \end{bmatrix} . \begin{bmatrix} c \cdot \varepsilon_X + s.\varepsilon_{XY} & -s \cdot \varepsilon_X + c.\varepsilon_{XY} \\ c \cdot \varepsilon_{XY} + s.\varepsilon_Y & -s \cdot \varepsilon_{XY} + c.\varepsilon_Y \end{bmatrix} \quad \text{EQ. 5.3.14.2}$$

$$\begin{bmatrix} \varepsilon_{11} & \varepsilon_{12} \\ \varepsilon_{12} & \varepsilon_{22} \end{bmatrix} = \begin{bmatrix} c^2 \cdot \varepsilon_X + 2cs.\varepsilon_{XY} + s^2.\varepsilon_Y & -cs \cdot \varepsilon_X + \left(c^2 - s^2\right).\varepsilon_{XY} + cs.\varepsilon_Y \\ -cs \cdot \varepsilon_X + \left(c^2 - s^2\right).\varepsilon_{XY} + cs.\varepsilon_Y & s^2.\varepsilon_X - 2cs.\varepsilon_{XY} + c^2.\varepsilon_Y \end{bmatrix} \quad \text{EQ. 5.3.14.3}$$

The strain-stress relation in orthotropy directions is written as:

$$\{\sigma\} = [C]\{\varepsilon\} \quad \text{EQ. 5.3.14.4}$$

$$[C]^{-1} = \begin{bmatrix} \frac{1}{E_{11}} & \frac{-\nu_{21}}{E_{22}} & 0 \\ \frac{-\nu_{12}}{E_{11}} & \frac{1}{E_{22}} & 0 \\ 0 & 0 & \frac{1}{G_{12}} \end{bmatrix} \quad \text{EQ. 5.3.14.5}$$

$$\langle \sigma \rangle = \langle \sigma_{11} \quad \sigma_{22} \quad \sigma_{12} \rangle \quad ; \quad \langle \varepsilon \rangle = \langle \varepsilon_{11} \quad \varepsilon_{22} \quad \varepsilon_{12} \rangle \quad \text{EQ. 5.3.14.6}$$

The computed stresses are then projected to the element reference:

$$\begin{bmatrix} \sigma_{XX} & \sigma_{XY} \\ \sigma_{XY} & \sigma_{YY} \end{bmatrix} = \begin{bmatrix} c & -s \\ s & c \end{bmatrix} . \begin{bmatrix} \sigma_{11} & \sigma_{12} \\ \sigma_{12} & \sigma_{22} \end{bmatrix} . \begin{bmatrix} c & s \\ -s & c \end{bmatrix} \quad \text{EQ. 5.3.14.7}$$

5.3.14.2 Composite modeling in RADIOSS

RADIOSS has been successfully used to predict the behavior of composite structures for crash and impact simulations in the automotive, rail and aeronautical industries.

The purpose of this chapter is to present the various options available in RADIOSS to model composites, as well as some modeling methods.

Modeling composites with shell elements

Composite materials with up to 100 layers may be modeled, each with different material properties, thickness, and fiber directions.

Lamina plasticity is taken into account using the Tsai-Wu criteria, which may also consider strain rate effects. Plastic work is used as a plasticity as well as rupture criterion.

Fiber brittle rupture may be taken into account in both orthotropic directions.

Delamination may be taken into account through a damage parameter in shear direction.

Modeling composites with solid elements

Solid elements may be used for composites.

Two material laws are available:

- Solid composite materials: one layer of composite is modeled with one solid element. Orthotropic characteristics and yield criteria are the same as shell elements (see above).

- A honeycomb material law is also available, featuring user defined yield curves for all components of the stress tensor and rupture strain.

Solid + shell elements

For sandwich plates, if the foam or the honeycomb is very thick, it is possible to combine composite shells for the plates and solid elements for the sandwich (see figure below).

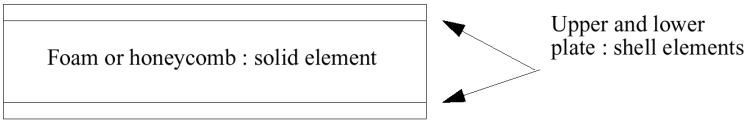

5.3.14.3 Element orientation

A global reference vector $\vec{v}$ is used to define the fiber direction. The direction in which the material properties (or fiber direction) lay is known as the direction 1 of the local coordinate system of orthotropy. It is defined by the Φ angle, which is the angle between the local direction 1 (fiber direction) and the projection of the global vector $\vec{v}$ as shown in Figure 5.3.16.

Figure 5.3.16 - Fiber Direction Orientation

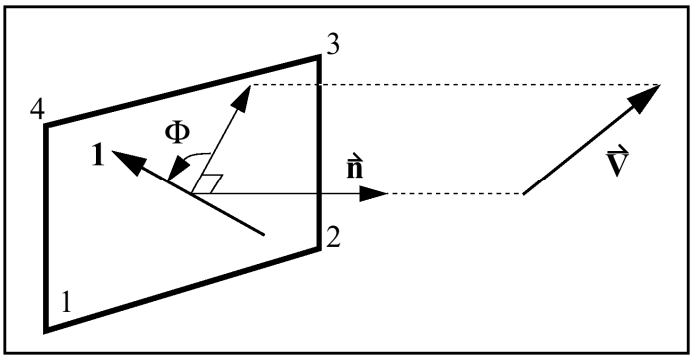

The shell normal defines the positive direction for ϕ. For elements with more than one layer, multiple ϕ angles can be defined.

The fiber direction orientation may be updated by two different ways:

1. constant orientation in local corotational reference frameconstant orientation in local isoparametric frame. The first formulation may lead to unstable models especially in the case of very thin shells (e.g. airbag modelling). In Figure 5.3.17 the difference between the two formulations is illustrated for the case of element traction and shearing.

Figure 5.3.17 - Fiber Direction Updating

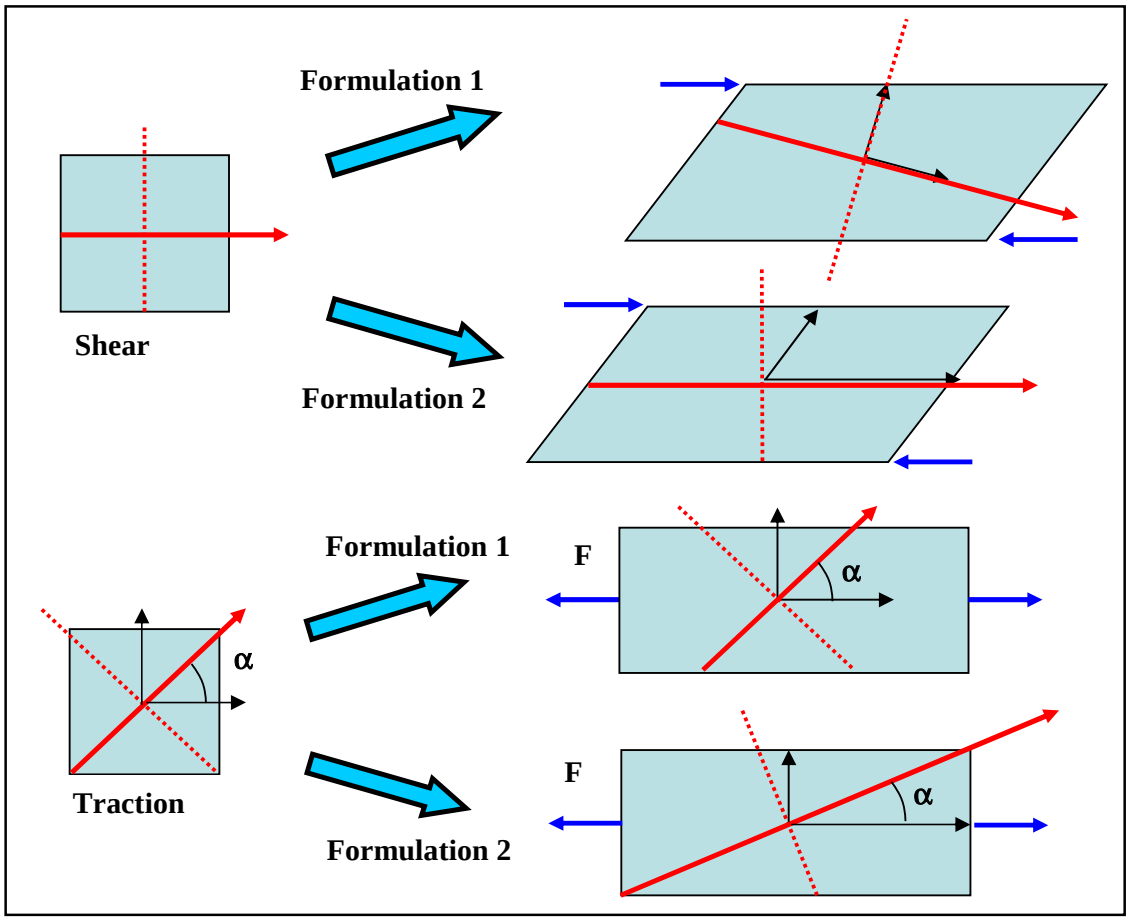

5.3.14.4 Orthotropic shells

The type 9 element property set defines orthotropic shell elements. They have the following properties:

1. Only one layer.
2. Can have up to 5 integration points[1] through the thickness.
3. One orientation.
4. One material property.

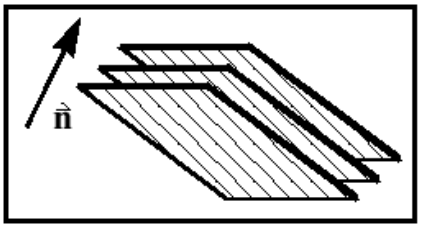

5.3.14.5 Composite shell

The type 10 element property set defines composite shell elements. They have the following properties:

1. Up to 100 layers can be modeled.
2. Constant layer thickness.
3. Constant reference vector.
4. Variable layer orientation.
5. Constant material properties.

Integration is performed with constant stress distribution for each layer.

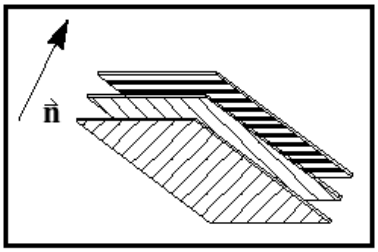

5.3.14.6 Composite shell with variable layers

The type 11 element property set defines composite shell elements that allow variable layer thicknesses and materials. They have the following properties:

1. Up to 100 layers can be modeled.
2. Variable layer thicknesses.
3. Constant reference vector.
4. Variable layer orientation.
5. Variable material properties, $m_i^{2,3}$

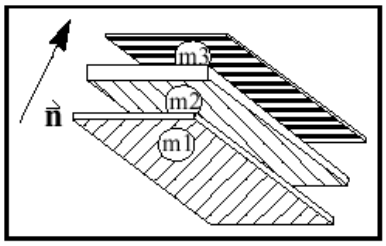

Integration is performed with constant stress distribution for each layer.

1. Same integration rule as shells.
2. Material number m_i must be defined as law type 25 or type 27 (not both) in material input cards.
3. Material given in the shell definition is only used for memory allocation, time step computation and interface stiffness. It must also be defined as law 25.

5.3.14.7 Limitations

When modeling a composite material, there are two strategies that may be applied. The first, and simplest, is to model the material in a laminate behavior. This involves using type 9 property shell elements. The second is to model each ply of the laminate using one integration point. This requires either a type 10 or 11 element.

Modeling using the type 9 element allows global behavior to be modeled. Input is simple, with only the reference vector as the extra information. A Tsai-Wu yield criterion and hardening law is easily obtained from the manufacturer or a test of the whole material.

Using the type 10 or 11 element, one model's each ply in detail, with one integration point per ply and tensile failure is described in detail for each ply. However, the input requirements are complex, especially for the type 11 element.

Delamination is the separation of the various layers in a composite material. It can occur in situations of large deformation and fatigue. This phenomenon cannot be modeled in detail using shell theory. A global criterion is available in material law 25. Delamination can affect the material by reducing the bending stiffness and buckling force.

5.3.15 Three-node triangle without rotational d.o.f. (SH3N6)

The need of simple and efficient element in nonlinear analysis of shells undergoing large rotations is evident in crash and sheet metal forming simulations. The constant-moment plate elements fit this need. One of the famous concepts in this field is that of Batoz et al. [40] known under DKT elements where DKT stands for Discrete Kirchhoff Triangle. The DKT12 element [40], [105] has a total of 12 d.o.f's. The discrete Kirchhoff plate conditions are imposed at three mid-point of each side. The element makes use of rotational d.o.f. at each edge to take into account the bending effects. A simplified three-node element without rotational d.o.f. is presented in [106]. The rotational d.o.f. is computed with the help of out-of-plane translational d.o.f. in the neighbor elements. This attractive approach is used in RADIOSS in the development of element SH3N6 which based on DKT12.

5.3.15.1 Strain computation

Consider two adjacent coplanar elements with a common edge i-j as shown in Figure 5.3.19. Due to out-of-plane displacements of nodes *m* and *k*, the elements rotate around the side i-j. The angles between final and initial positions of the elements are respectively α_m and α_k for corresponding opposite nodes *m* and *k*. Assuming, a constant curvature for both of elements, the rotation angles θ_m and θ_k related to the bending of each element around the common side are obtained by:

$$\theta_k = \frac{h_k}{2R} \quad \text{and} \quad \theta_m = \frac{h_m}{2R} \qquad \text{EQ.5.3.15.1}$$

However, for total rotation you have:

$$\theta_k + \theta_m = \alpha_k + \alpha_m \qquad \text{EQ.5.3.15.2}$$

which leads to:

$$\theta_k = \frac{(\alpha_k + \alpha_m)h_k}{(h_k + h_m)} \quad \text{and} \quad \theta_m = \frac{(\alpha_k + \alpha_m)h_m}{(h_k + h_m)} \qquad \text{EQ.5.3.15.3}$$

Figure 5.3.18 – Computation of rotational d.o.f. in SH3N6

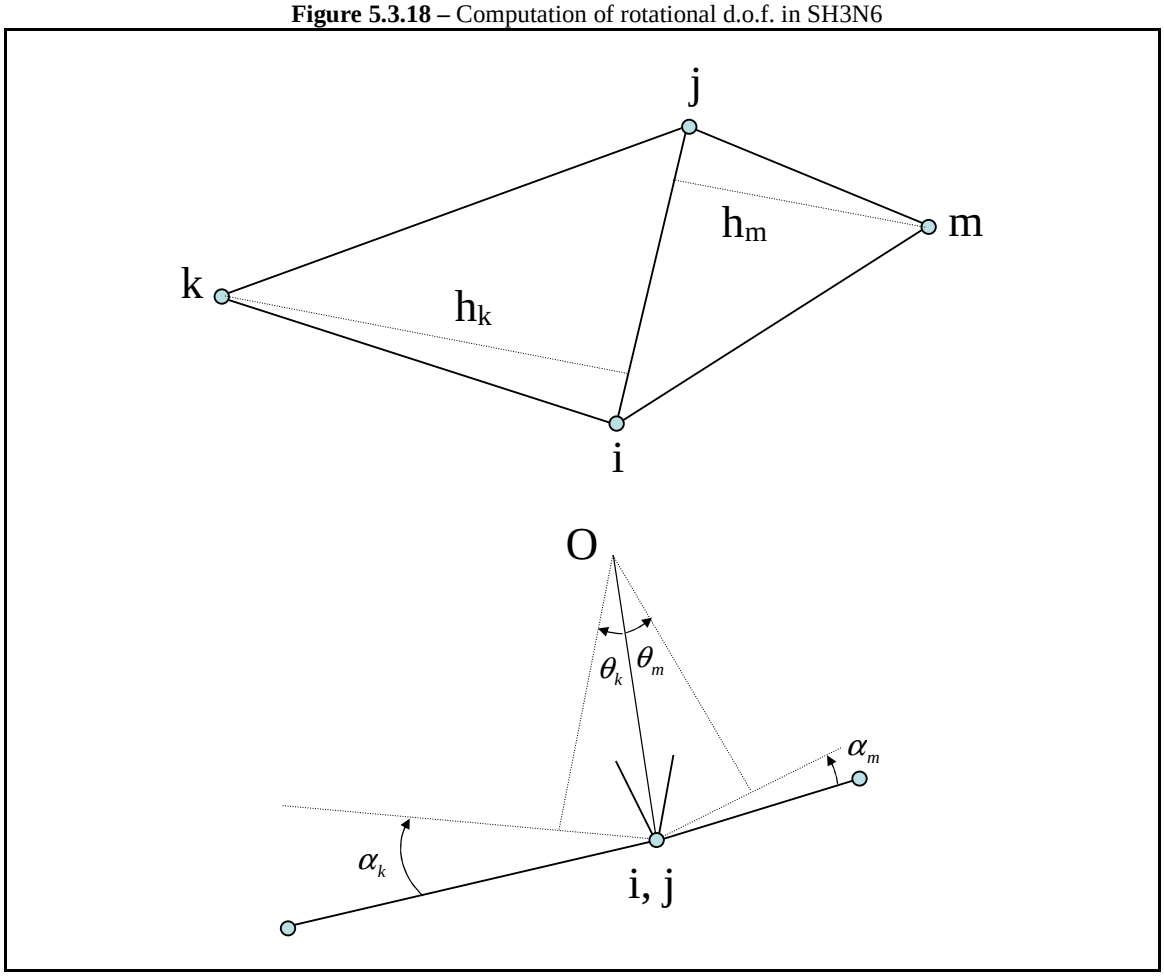

Consider the triangle element in Figure 5.3.19. The outward normal vectors at the three sides are defined and denoted n1, n2 and n3. The normal component strain due to the bending around the element side is obtained using plate assumption:

$$\begin{Bmatrix} \varepsilon_{n1} \\ \varepsilon_{n2} \\ \gamma_{n3} \end{Bmatrix} = \begin{bmatrix} \frac{2}{(h_1+h_5)} & 0 & 0 & 0 & \frac{2}{(h_1+h_5)} & 0 \\ 0 & \frac{2}{(h_2+h_6)} & 0 & 0 & 0 & \frac{2}{(h_2+h_6)} \\ 0 & 0 & \frac{2}{(h_3+h_4)} & \frac{2}{(h_3+h_4)} & 0 & 0 \end{bmatrix} \begin{Bmatrix} \alpha_1 \\ \alpha_2 \\ \alpha_3 \\ \alpha_4 \\ \alpha_5 \\ \alpha_6 \end{Bmatrix} \qquad \text{EQ.5.3.15.4}$$

The six mid-side rotations α_i are related to the out-of-plane displacements of the six apex nodes as shown in Figure 5.3.20 by the following relation:

$$\begin{Bmatrix} \alpha_1 \\ \alpha_2 \\ \alpha_3 \\ \alpha_4 \\ \alpha_5 \\ \alpha_6 \end{Bmatrix} = \begin{bmatrix} \frac{1}{h_1} & -\frac{\cos\beta_3}{h_2} & -\frac{\cos\beta_2}{h_3} & 0 & 0 & 0 \\ -\frac{\cos\beta_3}{h_1} & \frac{1}{h_2} & -\frac{\cos\beta_1}{h_3} & 0 & 0 & 0 \\ -\frac{\cos\beta_2}{h_1} & -\frac{\cos\beta_1}{h_2} & \frac{1}{h_3} & 0 & 0 & 0 \\ -\frac{\cos\gamma_2}{q_1} & -\frac{\cos\gamma_1}{q_2} & 0 & \frac{1}{h_4} & 0 & 0 \\ 0 & -\frac{\cos\psi_3}{r_2} & -\frac{\cos\psi_2}{r_3} & 0 & \frac{1}{h_5} & 0 \\ -\frac{\cos\phi_2}{s_1} & 0 & -\frac{\cos\phi_1}{s_3} & 0 & 0 & \frac{1}{h_6} \end{bmatrix} \begin{Bmatrix} w_1 \\ w_2 \\ w_3 \\ w_4 \\ w_5 \\ w_6 \end{Bmatrix} \qquad \text{EQ.5.3.15.5}$$

where $(h_1 \quad h_2 \quad h_3)$, $(q_1 \quad h_4 \quad q_2)$, $(r_2 \quad h_5 \quad r_3)$ and $(s_3 \quad h_6 \quad s_1)$ are respectively the heights of the triangles (1,2,3), (1,4,2), (2,5,3) and (3,6,1).

Figure 5.3.19 – Normal vectors definition

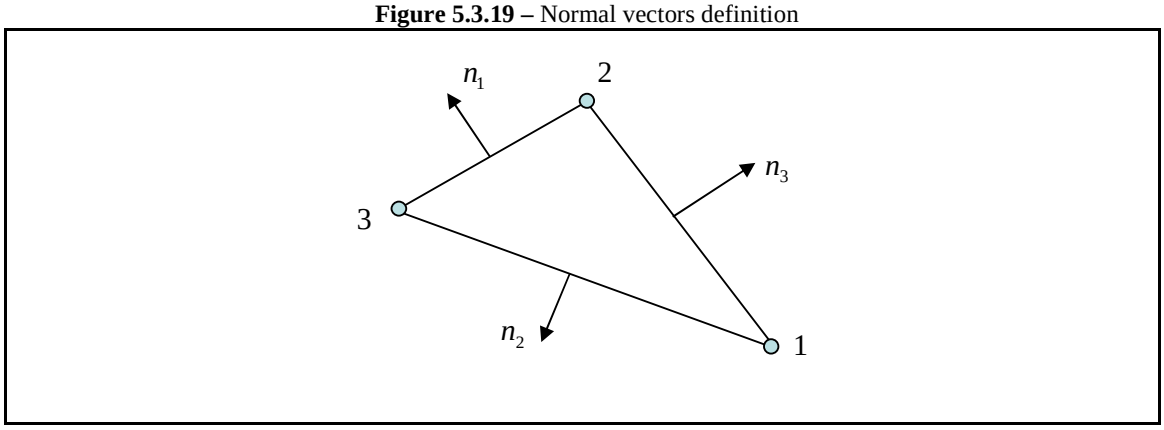

The non-null components of strain tensor in the local element reference are related to the normal components of strain by the following relation (see [40] and [106] for details):

$$\begin{Bmatrix} \varepsilon_{xx} \\ \varepsilon_{yy} \\ \gamma_{xy} \end{Bmatrix} = \begin{bmatrix} \left(\frac{y_3-y_2}{l_1}\right)^2 & \left(\frac{y_1-y_3}{l_2}\right)^2 & \left(\frac{y_2-y_1}{l_3}\right)^2 \\ \left(\frac{x_2-x_3}{l_1}\right)^2 & \left(\frac{x_3-x_1}{l_2}\right)^2 & \left(\frac{x_1-x_2}{l_3}\right)^2 \\ 2\left(\frac{y_3-y_2}{l_1}\right)\left(\frac{x_2-x_3}{l_1}\right) & 2\left(\frac{y_1-y_3}{l_2}\right)\left(\frac{x_3-x_1}{l_2}\right) & 2\left(\frac{y_2-y_1}{l_3}\right)\left(\frac{x_1-x_2}{l_3}\right) \end{bmatrix} \begin{Bmatrix} \varepsilon_{n1} \\ \varepsilon_{n2} \\ \gamma_{n3} \end{Bmatrix} \quad \text{EQ.5.3.15.6}$$

Figure 5.3.20 – Neighbor elements for a triangle

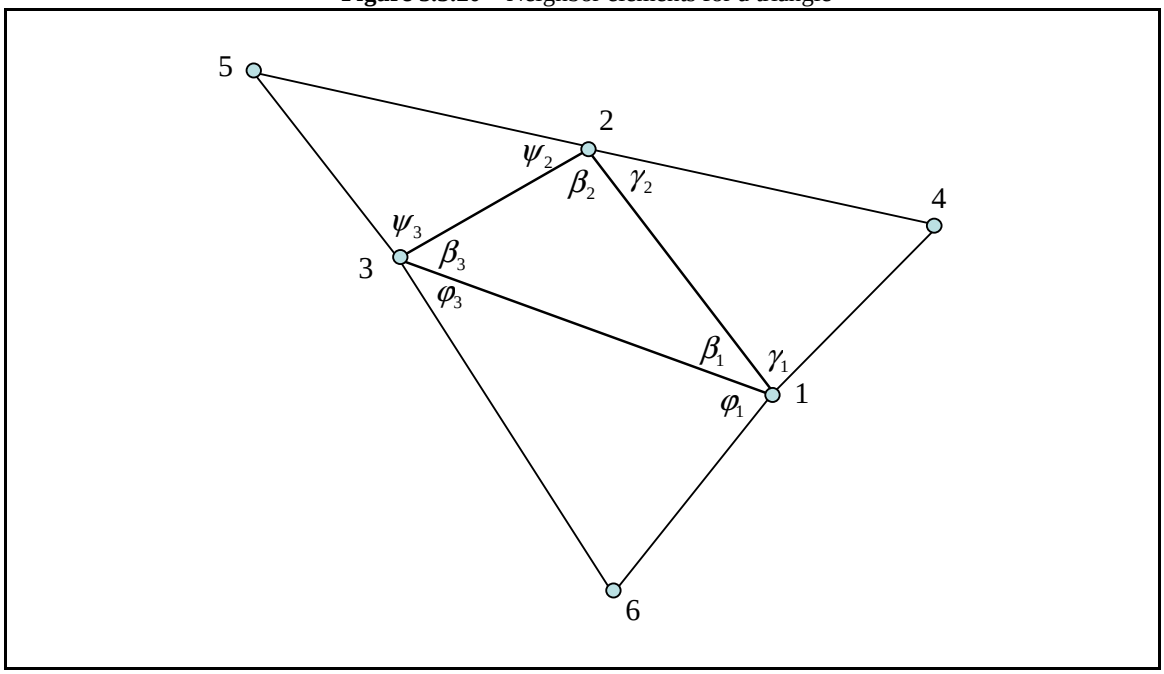

5.3.15.2 Boundary conditions application

As the side rotation of the element is computed using the out-of-plane displacement of the neighbor elements, the application of clamped or free boundary conditions needs a particular attention. It is natural to consider the boundary conditions on the edges by introducing a virtual and symmetric element outside of the edge as described in Figure 5.3.21. In the case of free rotation at the edge, the normal strain ε_{nk} is vanished. From EQ.5.3.15.4, this leads to:

$$\alpha_k = -\alpha_m \quad \text{EQ.5.3.15.7}$$

In EQ.5.3.15.5 the fourth row of the matrix is then changed to:

$$\left[\frac{\cos\beta_2}{h_1} \quad \frac{\cos\beta_1}{h_2} \quad -\frac{1}{h_3} \quad 0 \quad 0 \quad 0\right] \quad \text{EQ.5.3.15.8}$$

The clamped condition is introduced by the symmetry in out-of-plane displacement i.e. $w_m=w_k$. This implies $\alpha_k = \alpha_m$. The fourth row of the matrix in EQ.5.3.15.5 is then changed to:

$$\left[-\frac{\cos\beta_2}{h_1} \quad -\frac{\cos\beta_1}{h_2} \quad -\frac{1}{h_3} \quad 0 \quad 0 \quad 0\right] \qquad \text{EQ.5.3.15.9}$$

Figure 5.3.21 – Virtual element definition for boundary conditions application

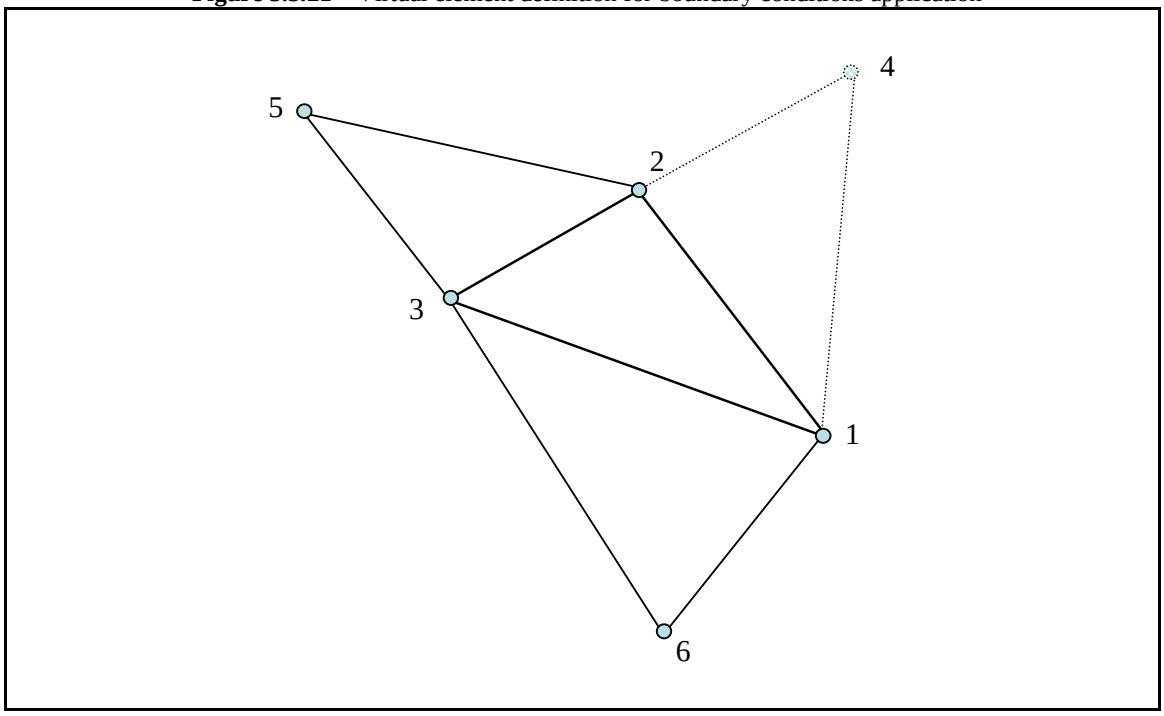

5.4 Solid-Shell Elements

Solid-shell elements form a class of finite element models intermediate between thin shell and conventional solid elements. From geometrical point of view, they are represented by solid meshes with two nodes through the thickness and generally without rotational degree-of-freedom. On the other hand, they account for shell-like behavior in the thickness direction. They are useful for modeling shell-like portions of a 3D structure without the need to connect solid element nodes to shell nodes (Figure 5.4.1).

Figure 5.4.1 Solid-shell elements application

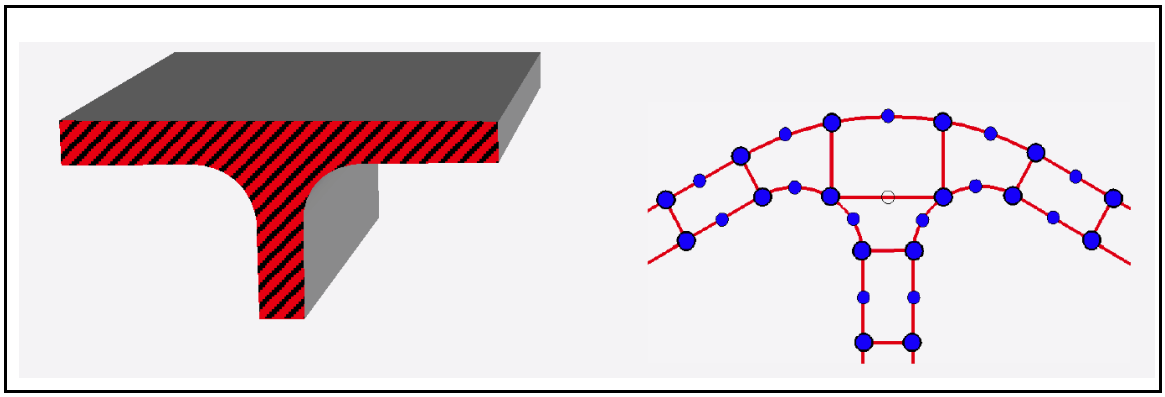

The derivation of solid-shell elements is more complicated than that of standard solid elements since they are prone to the following problems:

- Shear and membrane locking with the hybrid strain formulation [89], [90], the hybrid stress [91], and the Assumed and Enhanced Natural Strain formulations [92], [93], [94], and [95].
- Trapezoidal locking caused by deviation of mid-plane from rectangular shape [8].
- Thickness locking due to Poisson's ratio coupling of the in-plane and transverse normal stresses [89], [90], [92], and [94].

Solid shell elements in RADIOSS are the solid elements with a treatment of the normal stresses in the thickness direction. This treatment consists of ensuring **constant** normal stresses in the thickness by a penalty method. Advantage of this approach with respect to the plane-stress treatment is that it can simulate the normal deformability and exhibits no discernible locking problems. The disadvantage is its possible small time step since it is computed as solid element and the characteristic length is determined often using the thickness.

The solid-shell elements of *RADIOSS* are the following:

- HA8: 8-node linear solid and solid-shell with or without reduced integration scheme,
- HSEPH: 8-node linear thick shell with reduced integration scheme and physical stabilization of hourglass modes,
- PA6: Linear pentahedral element for thick shells,
- SHELL16: 16-node quadratic thick shell.

The thick shell elements HA8 and HSEPH are respectively the solid elements HA8 and HEPH in which the hypothesis of constant normal stress through the thickness is applied by penalty method. The theoretical features of these elements are explained in section 5.1. The thick shell element SHELL16 is described hereby.

5.4.1 Thick Shell Element SHELL16

The element can be used to model thick-walled structures situated between 3D solids and thin shells. The element is presented in Figure 5.4.2. It has 16 nodes with three translational d.o.f's per each node. The element is quadratic in plane and linear through the thickness. The numerical integration through the thickness is carried out by Gauss-Lobatto schemes rise up to 9 integrations to enhance the quality of elasto-plastic behavior. The in-plane integration may be done by a reduced 2x2 scheme or a fully integrated 3x3 points (Figure 5.4.3). A reduced integration method is applied to the normal stress in order to avoid locking problems.

Figure 5.4.2 Thick Shell Element SHELL16

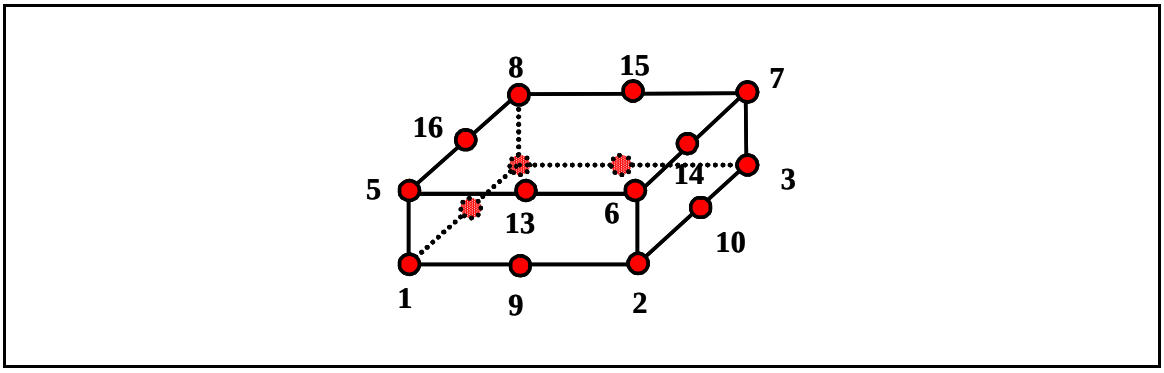

The distribution of mass is not homogenous over the nodes. The internal nodes receive three times more mass than the corner nodes as shown in Figure 5.4.4.

Figure 5.4.3 Integration points for SHELL16

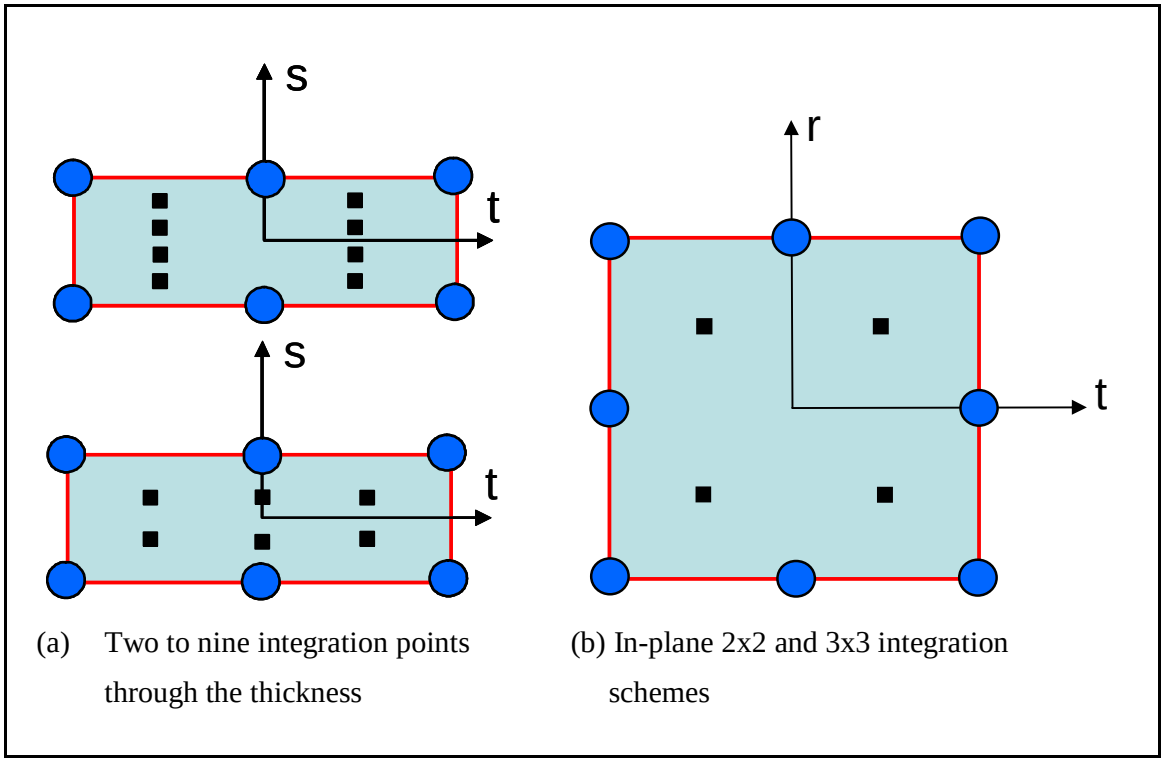

(a) Two to nine integration points through the thickness

(b) In-plane 2x2 and 3x3 integration schemes

Figure 5.4.4 Mass distribution for SHELL16 element

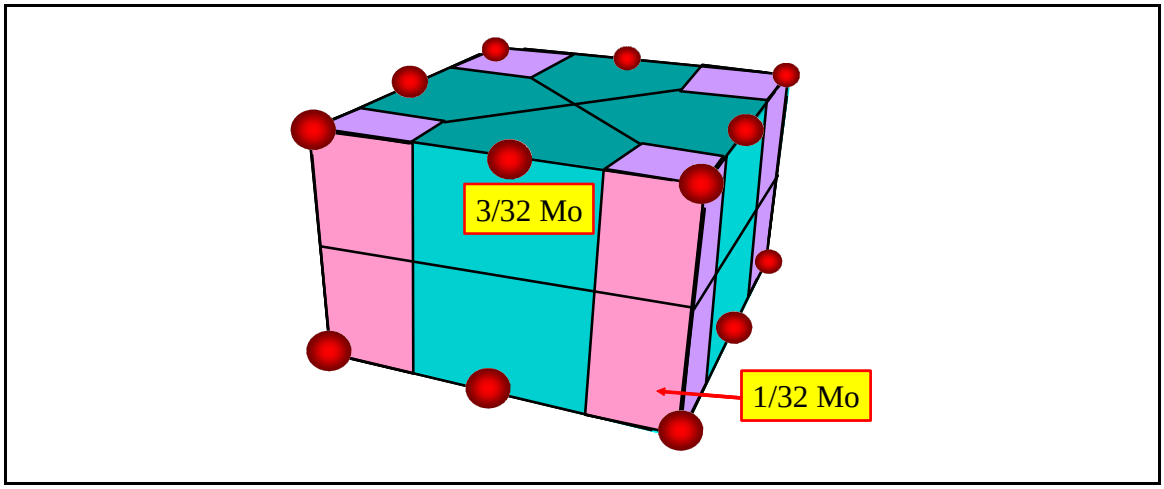

5.5 TRUSS ELEMENTS (TYPE 2)

Truss elements are simple two node linear members that only take axial extension or compression. Figure 5.5.1 shows a truss element.

Figure 5.5.1 Truss Element

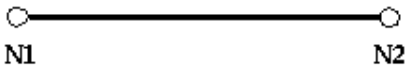

5.5.1 Property input

The only property required by a truss element is the cross sectional area. This value will change as the element is deformed. The cross sectional area is computed using:

$$Area(t) = \frac{Area(t-\Delta t)}{(1-\nu\dot{\varepsilon}_x \Delta t)^2} \qquad \text{EQ. 5.5.1.1}$$

where ν is the Poisson's ratio defined in the material law.

5.5.2 Stability

Determining the stability of truss elements is very simple. The characteristic length is defined as the length of the element, i.e. the distance between N1 and N2 nodes.

$$\Delta t \le \frac{L(t)}{C} \qquad \text{EQ. 5.5.2.1}$$

Where, $L(t)$ is the current truss length and $C = \sqrt{\frac{E}{\rho}}$ is the sound speed.

5.5.3 Rigid body motion

The rigid body motion of a truss element as shown in Figure 5.5.2 shows the different velocities of nodes 1 and 2. It is the relative velocity difference between the two nodes that produces a strain in the element, namely e_x.

Figure 5.5.2 Truss Motion

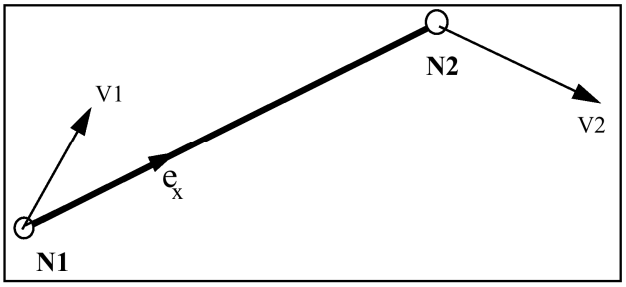

5.5.4 Strain

The strain rate, as shown in Figure 5.5.2, is defined as:

$$\dot{\varepsilon}_x = \frac{\partial v_x}{\partial x} = \frac{\partial\left(\vec{V}\cdot\vec{e}_x\right)}{\partial x} \qquad \text{EQ. 5.5.4.1}$$

5.5.5 Material type

A truss element may only be assigned two types of material properties. These are types 1 and 2, elastic and elasto-plastic properties respectively.

5.5.6 Force calculation

The calculation of forces in a truss element is performed by explicit time integration:

$$F\left(t+\Delta t\right) = F\left(t\right) + \dot{F}\Delta t \qquad \text{EQ. 5.5.6.1}$$

A generalized force-strain graph can be seen in Figure 5.5.3. The force rate under elastic deformation is given by:

$$\dot{F}_x = EA\dot{\varepsilon}_x \qquad \text{EQ. 5.5.6.2}$$

where:

E is the Elastic Modulus,

A is the cross sectional area.

In the plastic region, the force rate is given by:

$$\dot{F}_x = E_t A\dot{\varepsilon}_x \qquad \text{EQ. 5.5.6.3}$$

where E_t is the gradient of the material curve at the deformation point.

Figure 5.5.3 Force-Strain Relationship

(a) without gap (b) with gap

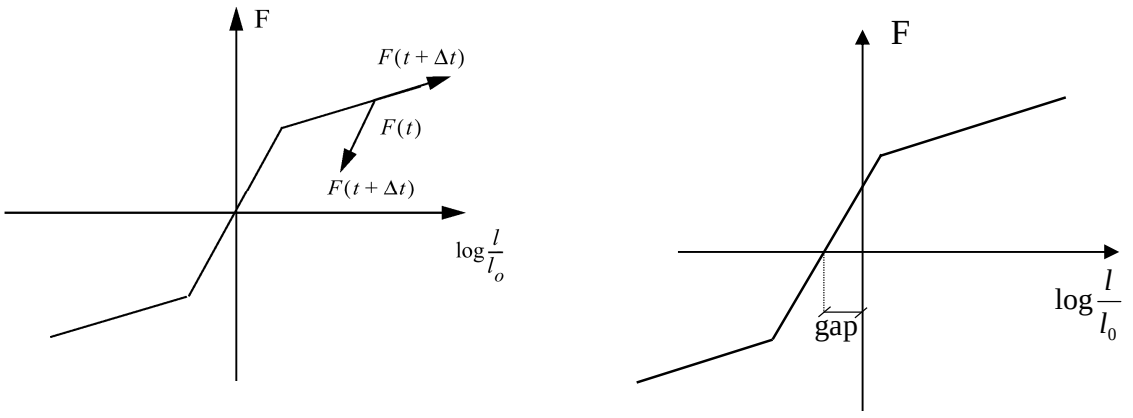

In a general case, it is possible to introduce a gap distance in the truss definition. If gap is not null, the truss is activated when the length of the element is equal to the initial length minus the gap value. This results a force-strain curve shown in Figure 5.5.3(b).

5.6 BEAM ELEMENTS (TYPE 3)

RADIOSS uses a shear beam theory or Timoshenko formulation for its beam elements.

This formulation assumes that the internal virtual work rate is associated with the axial, torsional and shear strains. The other assumptions are:

- No cross section deformation in its plane.
- No cross section warping out of its plane.

With these assumptions, transverse shear is taken into account.

This formulation can degenerate into a standard Euler-Bernoulli formulation (the cross section remains normal to the beam axis). This choice is under user control.

5.6.1 Local coordinate system

The properties describing a beam element are all defined in a local coordinate system.

This coordinate system can be seen in Figure 5.6.1. Nodes 1 and 2 of the element are used to define the local X axis, with the origin at node 1. The local Y axis is defined using node 3, which lies in the local XY plane, along with nodes 1 and 2. The Z axis is determined from the vector cross product of the positive X and Y axes.

The local Y direction is first defined at time t=0 and its position is corrected at each cycle, taking into account the mean rotation of the X axis. The Z axis is always orthogonal to the X and Y axes.

Deformations are computed with respect to the local coordinate system displaced and rotated to take into account rigid body motion. Translational velocities V and angular velocities Ω with respect to the global reference frame are expressed in the local frame.

Figure 5.6.1 Beam Element Local Axis

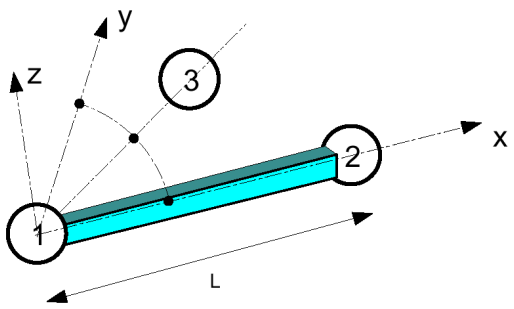

5.6.2 Beam element geometry

The beam geometry is user-defined by:

A: cross section area,

Ix: moment of inertia of cross section about local x axis,

Iy: moment of inertia of cross section about local y axis,

Iz: moment of inertia of cross section about local z axis.

The moments of inertia about the y and z axes are concerned with bending. They can be calculated using the relationships:

$$I_y = \iint_A z^2 dydz \qquad \text{EQ. 5.6.2.1}$$

$$I_z = \iint_A y^2 dydz \qquad \text{EQ. 5.6.2.2}$$

The moment of inertia about the x axis concerns torsion. This is simply the summation of the previous two moments of Ontario:

$$I_x = I_y + I_z \qquad \text{EQ. 5.6.2.3}$$

5.6.3 Minimum time step

The minimum time step for a beam element is determined using the following relation:

$$\Delta t = \frac{aL}{c} \qquad \text{EQ. 5.6.3.1}$$

where:

c is the speed of sound : $\sqrt{E/\rho}$,

$a = 0.5\sqrt{\min(4,1+b/12)}\,F_1\sqrt{b/3}\,F_2$,

$F_1 = \sqrt{(1+2d^2)} - d\sqrt{2}$

$F_2 = \min\left(F_1, \sqrt{(1+2d_s^{\,2})}\right) - d_s\sqrt{2}$

$d_s = d * \max\left(1, \sqrt{\frac{12}{b}} * \sqrt{1+\frac{12*E}{5/6*G}} * b * (1-Ishear)\right)$

$d = \max(d_m, d_f)$

$b = \frac{AL^2}{\max(I_y, I_z)}$

5.6.4 Beam element behavior

RADIOSS beam elements behave in four individual ways:

- Membrane or axial deformation.
- Torsion.
- Bending about the z axis.
- Bending about the y axis.

5.6.4.1 Membrane behavior

Membrane or axial behavior is the extension or compression of the beam element. The forces acting on an element are shown in Figure 5.6.2.

Figure 5.6.2 Membrane Forces

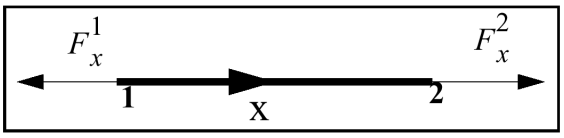

The force rate vector for an element is calculated using the relation:

$$\begin{bmatrix} \dot{F}_{x1} \\ \dot{F}_{x2} \end{bmatrix} = \frac{EA}{l} \begin{bmatrix} +1 & -1 \\ -1 & +1 \end{bmatrix} \begin{bmatrix} v_{x1} \\ v_{x2} \end{bmatrix} \quad \text{EQ. 5.6.4.1}$$

where:

E is the elastic modulus,

l is the beam element length,

v_x is the nodal velocity in x direction.

With the force rate equation, the force vector is determined using explicit time integration:

$$F_x(t+\Delta t) = F_x(t) + \dot{F}_x \Delta t \quad \text{EQ. 5.6.4.2}$$

5.6.4.2 Torsion

Torsional deformation occurs when the beam is loaded with a moment M about the X axis as shown in Figure 5.6.3.

Figure 5.6.3 Torsional Loading

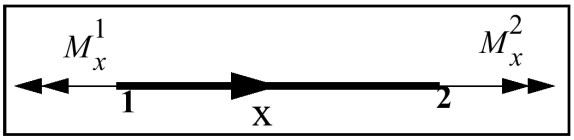

The moment rate vector is computed by:

$$\begin{bmatrix} \dot{M}_{x1} \\ \dot{M}_{x2} \end{bmatrix} = \frac{GI_x}{l} \begin{bmatrix} +1 & -1 \\ -1 & +1 \end{bmatrix} \begin{bmatrix} \dot{\theta}_{x1} \\ \dot{\theta}_{x2} \end{bmatrix} \quad \text{EQ. 5.6.4.3}$$

where:

G is the modulus of rigidity,

$\dot{\theta}_x$ is the angular rotation rate.

The moment about the X axis is found by explicit time integration:

$$M_x(t+\Delta t) = M_x(t) + \dot{M}_x \Delta t \quad \text{EQ. 5.6.4.4}$$

5.6.4.3 Bending about z axis

Bending about the z axis involves a force in the y direction and a moment about the z axis as shown in Figure 5.6.4.

Figure 5.6.4 Bending about the z axis

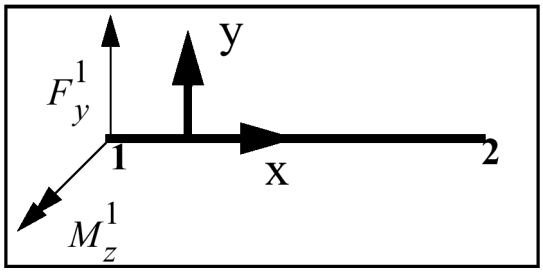

Two vector fields must be solved for forces and moments. The rate equations are:

$$\begin{bmatrix} \dot{F}_{y1} \\ \dot{F}_{y2} \end{bmatrix} = \frac{EI_z}{l^3(1+\phi_y)} \begin{bmatrix} +12 & 6l & -12 & +6l \\ -12 & -6l & +12 & -6l \end{bmatrix} \begin{bmatrix} v_{y1} \\ \dot{\theta}_{z1} \\ v_{y2} \\ \dot{\theta}_{z2} \end{bmatrix} \quad \text{EQ. 5.6.4.5}$$

$$\begin{bmatrix} \dot{M}_{z1} \\ \dot{M}_{z2} \end{bmatrix} = \frac{EI_z}{l^3(1+\phi_y)} \begin{bmatrix} +6l & (4+\phi_y)l^2 & -6l & (2-\phi_y)l^2 \\ +6l & (2-\phi_y)l^2 & -6l & (4+\phi_y)l^2 \end{bmatrix} \begin{bmatrix} v_{y1} \\ \dot{\theta}_{z1} \\ v_{y2} \\ \dot{\theta}_{z2} \end{bmatrix} \quad \text{EQ. 5.6.4.6}$$

where $\phi_y = \frac{144(1+\nu)I_z}{5Al^2}$,

ν is the Poisson's Ratio.

The factor Φ_y takes into account transverse shear.

The time integration for both is:

$$F_y(t+\Delta t) = F_y(t) + \dot{F}_y \Delta t \quad \text{EQ. 5.6.4.7}$$

$$M_z(t+\Delta t) = M_z(t) + \dot{M}_z \Delta t \quad \text{EQ. 5.6.4.8}$$

5.6.4.4 Bending about Y axis

Bending about the Y axis is identical to bending about the Z axis. A force in the Y direction and a moment about the Z axis, shown in Figure 5.6.5, contribute to the elemental bending.

Figure 5.6.5 Bending about Y axis

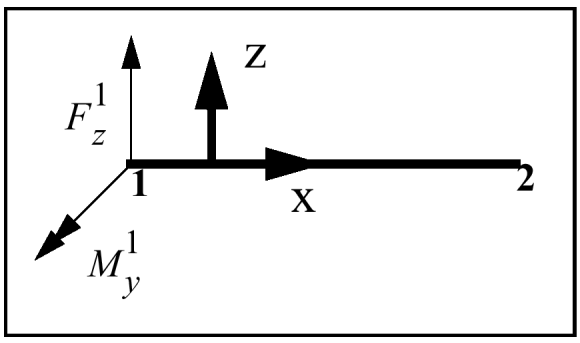

The rate equations are:

$$\begin{bmatrix} \dot{F}_{z1} \\ \dot{F}_{z2} \end{bmatrix} = \frac{El_y}{l^3(1+\Phi_z)} \begin{bmatrix} +12 & 6l & -12+6l \\ -12-6l & +12-6l \end{bmatrix} \begin{bmatrix} v_{z1} \\ \dot{\theta}_{y1} \\ v_{z2} \\ \dot{\theta}_{y2} \end{bmatrix} \quad \text{EQ. 5.6.4.9}$$

$$\begin{bmatrix} \dot{M}_{y1} \\ \dot{M}_{y2} \end{bmatrix} = \frac{El_y}{l^3(1+\Phi_z)} \begin{bmatrix} +6l(4+\Phi_z)l^2 & -6l(2-\Phi_z)l^2 \\ +6l(2-\Phi_z)l^2 & -6l(4+\Phi_z)l^2 \end{bmatrix} \begin{bmatrix} v_{z1} \\ \dot{\theta}_{y1} \\ v_{z2} \\ \dot{\theta}_{y2} \end{bmatrix} \quad \text{EQ. 5.6.4.10}$$

where:

$\Phi_z = \frac{144(1+\nu)I_y}{5Al^2}$.

Like bending about the Z axis, the factor Φ_z introduces transverse shear.

With the time integration, the expression is:

$$F_z(t+\Delta t) = F_z(t) + \dot{F}_z \Delta t \quad \text{EQ. 5.6.4.11}$$

$$M_y(t+\Delta t) = M_y(t) + \dot{M}_y \Delta t \quad \text{EQ. 5.6.4.12}$$

5.6.5 Material properties

A beam element may have two different types of material property:

- Elastic
- Elasto-plastic

5.6.5.1 Elastic Behavior

The elastic beam is defined using material law 1 which is a simple linear material law.

The cross-section of a beam is defined by its area *A* and three moments of inertia I_x , I_y and I_z .

An elastic beam can be defined with these four parameters. For accuracy and stability, the following limitations should be respected:

$$L > \sqrt{A} \quad \text{EQ. 5.6.5.1}$$

$$0.01A^2 < I_y < 100A^2 \quad \text{EQ. 5.6.5.2}$$

$$0.01A^2 < I_z < 100A^2 \quad \text{EQ. 5.6.5.3}$$

$$0.1(I_y + I_z) < I_x < 10(I_y + I_z) \quad \text{EQ. 5.6.5.4}$$

5.6.5.2 Elasto-plastic Behavior

A global plasticity model is used.

The main assumption is that the beam cross section is full and rectangular. Optimal relations between sections and section inertia are:

$$12 I_y I_z = A^4 \quad \text{EQ. 5.6.5.5}$$

$$I_x = I_y + I_z \quad \text{EQ. 5.6.5.6}$$

However, this model also gives good results for the circular or ellipsoidal cross-section. For tubular or H cross-sections, plasticity will be approximated.

Recommendations:

$$L > \sqrt{A} \quad \text{EQ. 5.6.5.7}$$

$$0.1A^4 < 12 I_y I_z < 10A^4 \quad \text{EQ. 5.6.5.8}$$

$$0.01 < I_y / I_z < 100 \quad \text{EQ. 5.6.5.9}$$

$$0.5\left(I_y + I_z\right) < I_x < 2\left(I_y + I_z\right) \quad \text{EQ. 5.6.5.10}$$

5.6.5.3 Global Beam Plasticity

The elasto-plastic beam element is defined using material law 2:

$$\sigma_y = \left(A + B\varepsilon_p^n\right)\left(1 + C \ln \frac{\dot{\varepsilon}}{\dot{\varepsilon}_0}\right) \quad \text{EQ. 5.6.5.11}$$

The increment of plastic strain is:

$$\Delta\varepsilon_p = \frac{\Delta W_{plastic}}{\sigma_y} \quad \text{EQ. 5.6.5.12}$$

The equivalent strain rate is derived from the total energy rate:

$$\dot{\varepsilon} = \frac{\Delta W_{total}}{\sigma_{eq} \Delta t} \quad \text{EQ. 5.6.5.13}$$

Yield stress:

$$\sigma_{eq} = \sqrt{\frac{F_x^2}{A^2} + \frac{3}{A}\left(\frac{M_x^2}{I_{xx}} + \frac{M_y^2}{I_{yy}} + \frac{M_z^2}{I_{zz}}\right)} \quad \text{EQ. 5.6.5.14}$$

If $\sigma_{eq} > \sigma_y$, one performs a radial return on the yield surface:

$$F_x^{pa} = F_x \frac{\sigma_y}{\sigma_{eq}} \quad \text{EQ. 5.6.5.15}$$

and for i= x, y, z:

$$M_i^{pa} = M_i \frac{\sigma_y}{\sigma_{eq}} \quad \text{EQ. 5.6.5.16}$$

5.6.6 Inertia Computation

The computational method of inertia for some kinds of elements as beam is particular as the inertia has to be transferred to the extremities of the beam. The nodal inertias are computed in function of the material density ρ, the cross-section area *S*, the element length *L* and the moments of inertia I_{xx}, I_{yy}, I_{zz}:

$$MAX\left(\left(\frac{\rho SL}{2}\right)\left(\frac{L^2}{12}\right)+\left(\frac{\rho L}{2}\right)\bullet MAX\left(I_{yy} \quad ; \quad I_{zz}\right) \quad ; \quad \left(\frac{\rho L}{2}\right)\bullet I_{xx}\right) \qquad \text{EQ. 5.6.6.1}$$

5.7 ONE DEGREE OF FREEDOM SPRING ELEMENTS (TYPE 4)

One degree of freedom (DOF) spring elements are defined as a type 4 property set. Three variations of the element are possible:

- Spring only
- Dashpot (damper) only
- Spring and dashpot in parallel

These three configurations are shown in Figures 5.7.1 to 5.7.3.

Figure 5.7.1 Spring Only

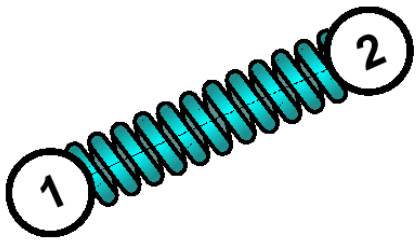

Figure 5.7.2 Dashpot Only

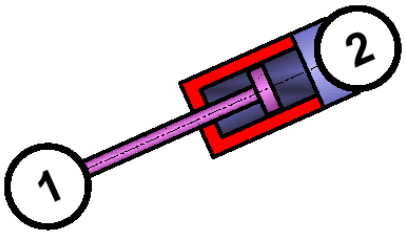

Figure 5.7.3 Spring and Dashpot in Parallel

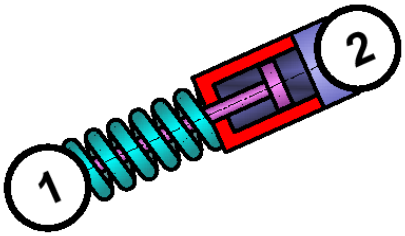

No material data card is required for spring elements. However, the stiffness *k* and equivalent viscous damping coefficient *c* are required. The mass *m* is required if there is any spring translation.

There are three other options defining the type of spring stiffness with the hardening flag:

- Linear Stiffness
- Nonlinear Stiffness
- Nonlinear Elasto-Plastic Stiffness

Likewise, the damping can be either:

- Linear
- Nonlinear

A spring may also have zero length. However, a one DOF spring must have 2 nodes.

The forces applied on the nodes of a one DOF spring are always colinear with direction through both nodes; refer to figure 5.7.4.

Figure 5.7.4 Colinear Forces

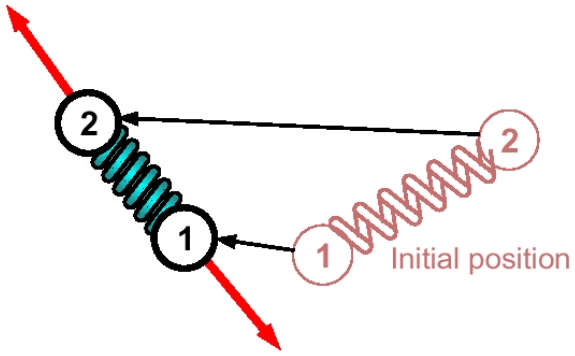

5.7.1 Time step

The time of a spring element depends on the values of stiffness, damping and mass.

For a spring only element:

$$\Delta t = \sqrt{\frac{m}{k}} \qquad \text{EQ. 5.7.1.1}$$

For a dashpot only element:

$$\Delta t = \frac{m}{2c} \qquad \text{EQ. 5.7.1.2}$$

For a parallel spring and dashpot element:

$$\Delta t = \frac{\left(\sqrt{mk + c^2}\right) - c}{k} \qquad \text{EQ. 5.7.1.3}$$

The critical time step ensures that the stability of the explicit time integration is maintained, but it does not ensure high accuracy of spring vibration behavior. Only two time steps are required during one vibration period of a free spring to keep stability. However, if true sinusoidal reproduction is desired, the time step should be reduced by a factor of at least 5.

If the spring is used to connect the two parts, the spring vibration period increases and the default spring time step ensures stability and accuracy.

5.7.2 Linear spring

Function number defining f(δ)

N1=0

The general linear spring is defined by constant mass, stiffness and damping. These are all required in the property type definition. The relationship between force and spring displacement is given by:

$$F = k(l - l_0) + c\frac{dl}{dt}$$ EQ. 5.7.2.1

Figure 5.7.5 Linear Force-Displacement Curve

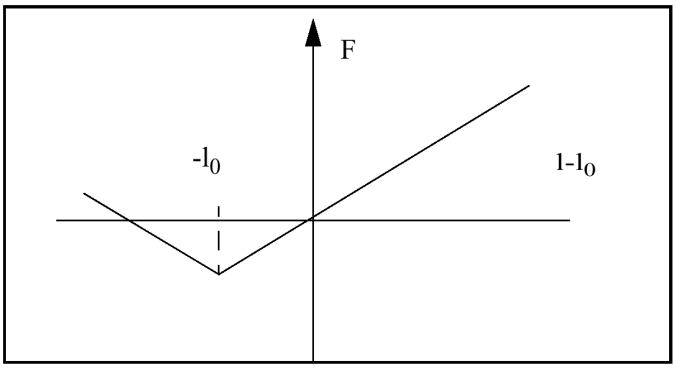

The stability condition is given by equation 5.7.1.3.:

$$\Delta t = \frac{\left(\sqrt{c^2 + km}\right) - c}{k}$$ EQ. 5.7.2.2

5.7.3 Nonlinear elastic spring

Hardening flag

H=0

The hardening flag must be set to 0 for a nonlinear elastic spring. The only difference between linear and nonlinear elastic spring elements is the stiffness definition. The mass and damping are defined as constant. However, a function must be defined that relates the force, *F*, to the displacement of the spring, (l-l_0). It is defined as:

$$F = f(l - l_0) + c\frac{dl}{dt}$$ EQ. 5.7.3.1

Figure 5.7.6 Nonlinear Elastic Force-Displacement Curve

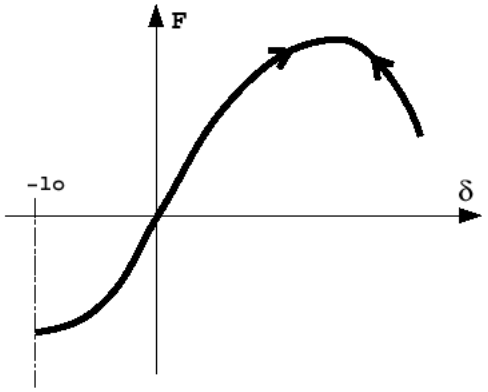

The stability criterion is the same as for the linear spring, but rather than being constant, the stiffness is displacement dependent:

$$\Delta t = \frac{\left(\sqrt{c^2 + k'm}\right) - c}{k'} \qquad \text{EQ. 5.7.3.2}$$

where:

$$k' = \max\left[\frac{\partial}{\partial(l - l_0)} f(l - l_0)\right] \qquad \text{EQ. 5.7.3.3}$$

5.7.4 Nonlinear elasto-plastic spring - Isotropic hardening

H=1

The hardening flag must be set to 1 in this case and f(l-l$_0$) is defined by a function. Hardening is isotropic if compression behavior is identical to tensile behavior:

$$F = f(l - l_0) + C\frac{dl}{dt} \qquad \text{EQ. 5.7.4.1}$$

Figure 5.7.7 Isotropic Hardening Force-Displacement Curve

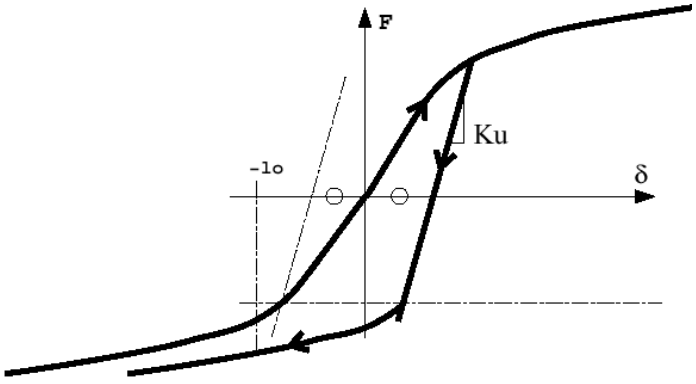

5.7.5 Nonlinear elasto-plastic spring - Decoupled hardening

H=2

The hardening flag is set to 2 in this case and f(l-l$_o$) is defined by a function. The hardening is decoupled for compression and tensile behavior:

$$F = f\left(l - l_0\right) + C\frac{dl}{dt}$$ EQ. 5.7.5.1

Figure 5.7.8 Decoupled Hardening Force-Displacement Curve

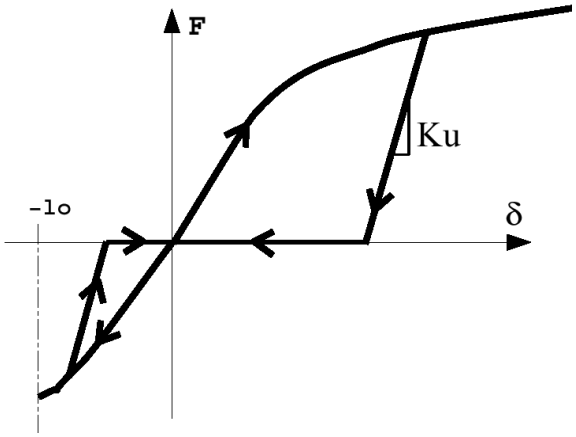

5.7.6 Nonlinear elastic-plastic spring - Kinematic hardening

H=4

The hardening flag is set to 4 in this case and f_1(l-l$_o$) and f_2(l-l$_o$) (respectively maximum and minimum yield force) are defined by a function. The hardening is kinematic if maximum and minimum yield curves are identical:

$$F = f\left(l - l_0\right) + C\frac{dl}{dt}$$ EQ. 5.7.6.1

Figure 5.7.9 Kinematic Hardening Force-Displacement Curve

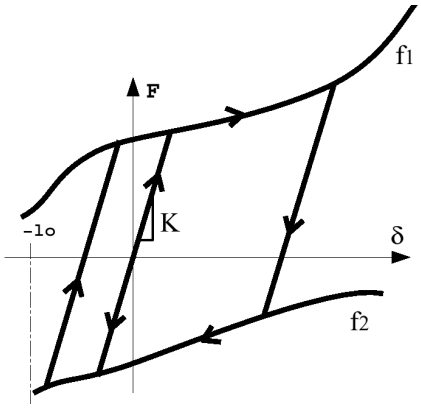

5.7.7 Nonlinear elasto-plastic spring - Nonlinear unloading

H=5

The hardening flag is set to 5 in this case and f(δ) and f2(δ_{max}) (respectively maximum yield force and residual deformation) are defined by a function. Uncoupled hardening in compression and tensile behavior with nonlinear unloading:

$$F = f\left(l - l_0\right) + C\frac{dl}{dt} \qquad \text{EQ. 5.7.7.1}$$

With $\delta = l - l_0$.

Figure 5.7.10 Nonlinear unloading Force-Displacement Curve

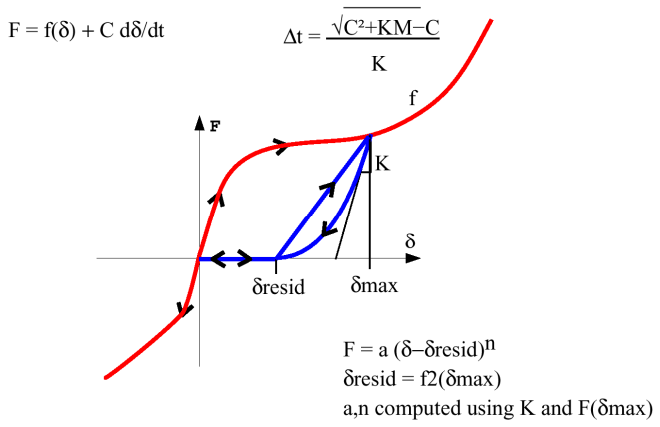

5.7.8 Nonlinear dashpot

The input properties for a nonlinear dashpot are very close to that of a spring. The required values are:

- Mass, *M*.
- A function defining the change in force with respect to the spring displacement. This must be equal to unity:
  $f\left(l - l_0\right) = 1$
- A function defining the change in force with spring displacement rate,
  $g\left(dl/dt\right)$
- The hardening flag in the input must be set to zero.

The relationship between force and spring displacement and displacement rate is:

$$F = f\left(l - l_0\right)g\left(\frac{dl}{dt}\right) = g\left(\frac{dl}{dt}\right) \qquad \text{EQ. 5.7.8.1}$$

A nonlinear dashpot property is shown in Figure 5.7.11.

Figure 5.7.11 Nonlinear Dashpot Force Curve

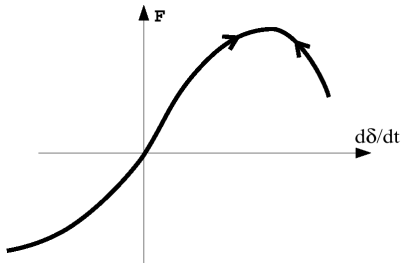

The stability condition for a nonlinear dashpot is given by:

$$\Delta t = \sqrt{\frac{M}{C'}} \qquad \text{EQ. 5.7.8.2}$$

where:

$$C' = \max\left[\frac{\partial}{\partial(dl/dt)} g(dl/dt)\right] \qquad \text{EQ. 5.7.8.3}$$

5.7.9 Nonlinear viscoelastic spring

The input properties for a nonlinear viscoelastic spring are:

- Mass, *M*
- Equivalent viscous damping coefficient *C*
- A function defining the change in force with spring displacement $f(l-l_0)$
- A function defining the change in force with spring displacement rate $g(dl/dt)$

The hardening flag in the input must be set to equal zero. The force relationship is given by:

$$F = f(l-l_0)g\left(\frac{dl}{dt}\right) \qquad \text{EQ. 5.7.9.1}$$

Graphs of this relationship for various values of $g(dl/dt)$ are shown in Figure 5.7.12.

Figure 5.7.12 Visco-Elastic Spring Force-Displacement Curves

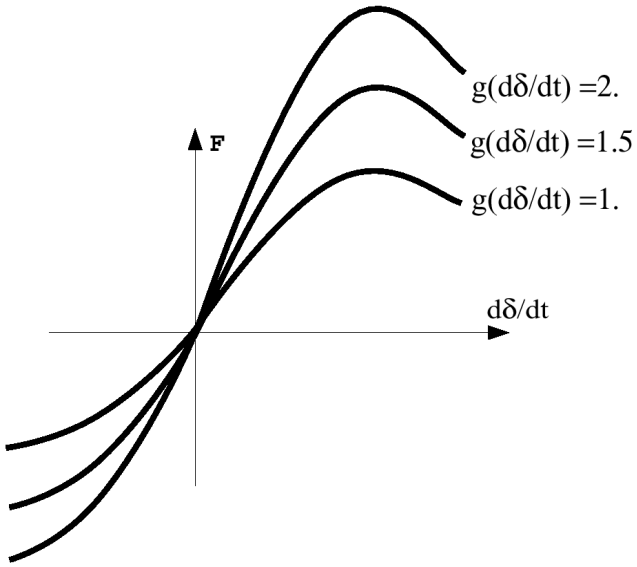

The stability condition is given by:

$$\Delta t = \frac{\left(\sqrt{C'^2 + k'M}\right) - C'}{k'} \qquad \text{EQ. 5.7.9.2}$$

where:

$$K' = \max\left[\frac{\partial}{\partial(l - l_0)} f(l - l_0)\right] \qquad \text{EQ. 5.7.9.3}$$

$$C' = \max\left[\frac{\partial}{\partial(dl/dt)} g(dl/dt)\right] \qquad \text{EQ. 5.7.9.4}$$

5.8 GENERAL SPRING ELEMENTS (TYPE 8)

General spring elements are defined as type 8 element property. They are mathematical elements, which have 6 DOF, three translational displacements and three rotational degrees of freedom. Each DOF is completely independent from the others. Spring displacements refer to either spring extension or compression. The stiffness is associated to each DOF. Directions can either be global or local. Local directions are defined with a fixed or moving skew frame. Global force equilibrium is respected, but without global moment equilibrium. Therefore, this type of spring is connected to the laboratory that applies the missing moments, unless the two defining nodes are not coincident.

5.8.1 Time step

The time step calculation for general spring elements is the same as the calculation of the equivalent type 4 spring (Section 5.7.1).

5.8.2 Linear spring

See section 5.7.2; the explanation is the same as for spring type 4.

5.8.3 Nonlinear elastic spring

See section 5.7.3; the explanation is the same as for spring type 4.

5.8.4 Nonlinear elasto-plastic spring - Isotropic hardening

See section 5.7.4; the explanation is the same as for spring type 4.

5.8.5 Nonlinear elasto-plastic spring - Decoupled hardening

See section 5.7.5; the explanation is the same as for spring type 4.

5.8.6 Nonlinear elasto-plastic spring - Kinematic hardening

See section 5.7.6; the explanation is the same as for spring type 4.

5.8.7 Nonlinear elasto-plastic spring - Nonlinear unloading

See section 5.7.7; the explanation is the same as for spring type 4.

5.8.8 Nonlinear dashpot

See section 5.7.8; the explanation is the same as for spring type 4.

5.8.9 Nonlinear viscoelastic spring

See section 5.7.9; the explanation is the same as for spring type 4.

5.8.10 Skew frame properties

To help understand the use of skew frames, the deformation in the local x direction of the spring will be considered. If the skew frame is fixed, deformation in the local X direction is shown in Figure 5.8.1:

Figure 5.8.1 Fixed Skew Frame

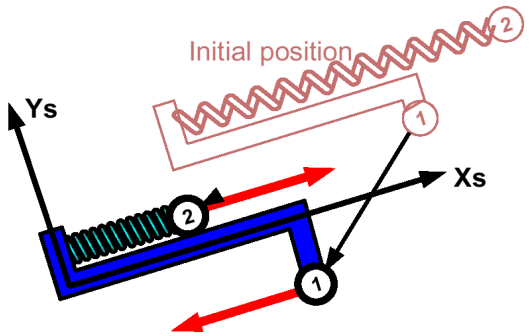

The same local x direction deformation, with a moving skew frame, can be seen in Figure 5.8.2.

Figure 5.8.2 Moving Skew Frame

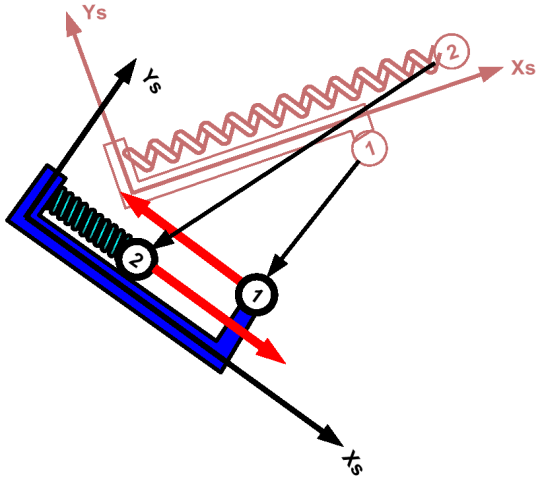

In both cases, the forces are in equilibrium, but the moments are not. If the first two nodes defining the moving skew system are the same nodes as the two spring element nodes, the behavior becomes exactly the same as that of a type 4 spring element. In this case the momentum equilibrium is respected and local Y and Z deformations are always equal to zero.

Fixed Nodes

If one of the two nodes is completely fixed, the momentum equilibrium problem disappears. For example, if node 1 is fixed, the force computation at node 2 is not dependent on the location of node 1. The spring then becomes a spring between node 1 and the laboratory, as shown in Figure 5.8.3.

Figure 5.8.3 Fixed node - Fixed skew frame

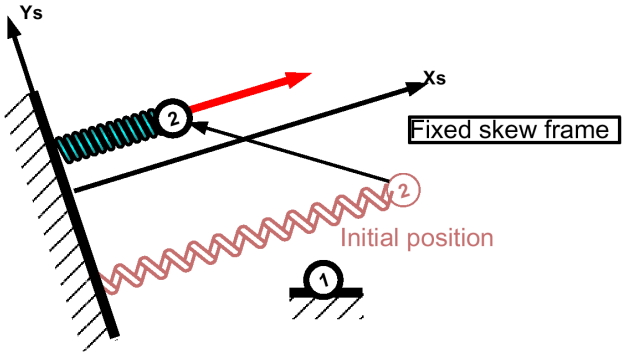

It is generally recommended that a general spring element (type 8) be used only if one node is fixed in all directions or if the two nodes are coincident. If the two nodes are coincident, the translational stiffness' have to be large enough to ensure that the nodes remain near coincident during the simulation.

5.8.11 Deformation sign convention

Positive and negative spring deformations are not defined with the variation of initial length. The initial length can be equal to zero for all or a given direction. Therefore, it is not possible to define the deformation sign with length variation.

The sign convention used is the following. A deformation is positive if displacement (or rotation) of node 2 minus the displacement of node 1 is positive. The same sign convention is used for all 6 degrees of freedom.

$$u_i = u_{i2} - u_{i1}$$ EQ. 5.8.11.1

$$\theta_i = \theta_{i2} - \theta_{i1}$$ EQ. 5.8.11.2

5.8.12 Translational forces

The translational forces that can be applied to a general spring element can be seen in Figure 5.8.4. For each DOF (i = x, y, z), the force is calculated by:

$$F_i = f_i(u_i) + C_i \dot{u}_i$$ EQ. 5.8.12.1

where:

C is the equivalent viscous damping coefficient

$f_i(u_i)$ is a force function related to spring displacement

The value of the displacement function depends on the type of general spring being modeled.

Figure 5.8.4 Translational Forces

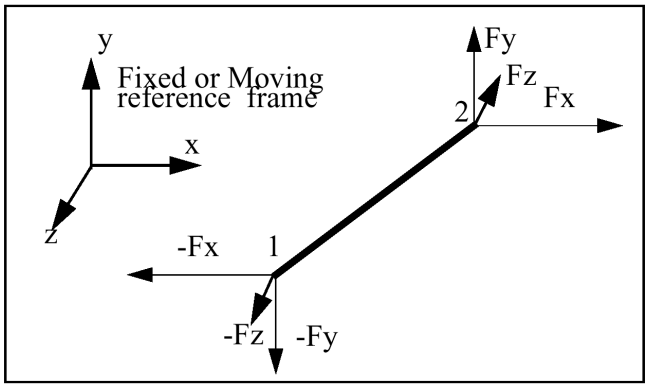

5.8.12.1 Linear Spring

If a linear general spring is being modeled, the translation forces are given by:

$$F_i = K_i u_i + C_i \dot{u}_i$$ EQ. 5.8.12.2

where *K* is the stiffness or unloading stiffness (for elasto-plastic spring)

5.8.12.2 Nonlinear Spring

If a nonlinear general spring is being modeled, the translation forces are given by:

$$F_i = f_i(u_i)\left(A + B\ln\left(\left|\frac{\dot{u}_i}{D}\right|\right) + g(\dot{u}_i)\right) + C_i\dot{u}_i \qquad \text{EQ. 5.8.12.3}$$

where:

$f(u_i)$ is a function defining the change in force with spring displacement

$g(\dot{u}_i)$ is a function defining the change in force with spring displacement rate

A = coefficient. Default = 1.

B = coefficient

D = coefficient. Default = 1.

5.8.13 Moments

Moments can be applied to a general spring element, as shown in Figure 5.8.5. For each DOF (i = x, y, z), the moment is calculated by:

$$M_i = f_i(\theta_i) + C_i\dot{\theta}_i \qquad \text{EQ. 5.8.13.1}$$

where:

C is the equivalent viscous damping coefficient

$f_i(\theta_i)$ is a force function related to spring rotation

The value of the rotation function depends on the type of general spring being modeled. Not all functions and coefficients defining moments and rotations are of the same value as that used in the translational force calculation.

Figure 5.8.5 General Spring Moments

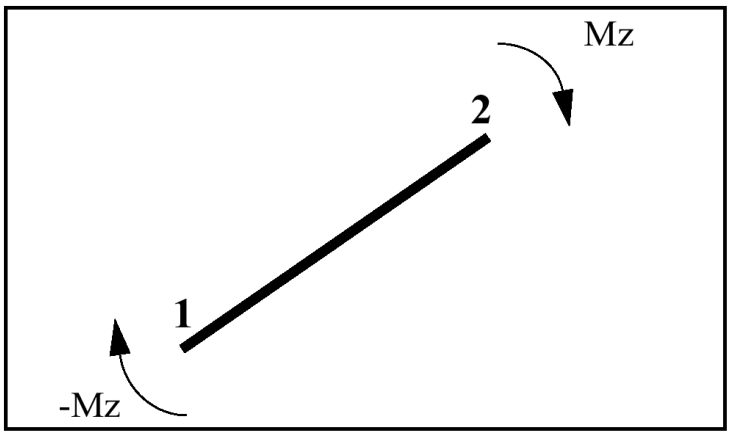

5.8.13.1 Linear Spring

If a linear general spring is being modeled, the moments are given by:

$$M_i = K_i\theta_i + C_i\dot{\theta}_i \qquad \text{EQ. 5.8.13.2}$$

where *K* is the stiffness or unloading stiffness (for elasto-plastic spring).

5.8.13.2 Nonlinear Spring

If a nonlinear general spring is being modeled, the moments are given by:

$$M_i = f\left(\theta_i\right)\left(A + B\ln\left(\left|\frac{\dot{\theta}_i}{D}\right|\right) + g\left(\dot{\theta}_i\right)\right) + C_i\dot{\theta}_i \qquad \text{EQ. 5.8.13.3}$$

where:

$f\left(\theta_i\right)$ is a function defining the change in force with spring displacement

$g\left(\theta_i\right)$ is a function defining the change in force with spring displacement rate

A = coefficient. Default = 1.

B = coefficient.

D = coefficient. Default = 1.

5.8.14 Multidirectional failure criteria

Flag for rupture criteria: Ifail

Ifail=1

The rupture criteria flag is set to 1 in this case:

$$F^2 = D_x^2 + D_y^2 + D_z^2 + D_{xx}^2 + D_{yy}^2 + D_{zz}^2 \qquad \text{EQ. 5.8.14.1}$$

Where:

$D_x = D_{xp}$ is the rupture displacement in positive x direction if $u_x > 0$

$D_x = D_{xn}$ is the rupture displacement in negative x direction if $u_x > 0$

Graphs of this rupture criterion can be seen in Figure 5.8.6.

Figure 5.8.6 Multi-directional failure criteria curves

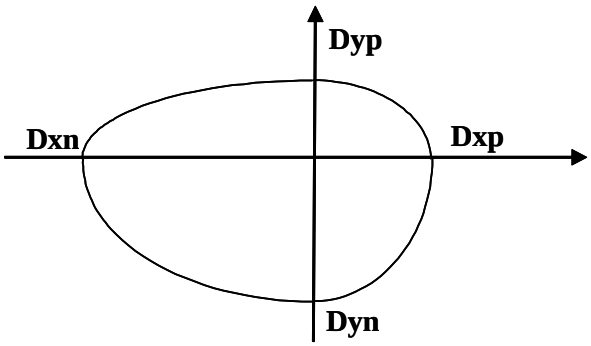

5.9 PULLEY TYPE SPRING ELEMENTS (TYPE12)

Pulley type springs are defined by type 12 element property. A general representation can be seen in Figure 5.9.1. It is defined with three nodes, where node 2 is located at the pulley position. Other properties such as stiffness, damping, nonlinear and plastic effects are the same as for the other spring types, and are defined using the same format.

A deformable "rope" joins the three nodes, with the mass distribution as follows: one quarter at node 1; one quarter at node 3 and one half at node 2.

Coulomb friction can be applied at node 2, which may also take into account the angle between the two rope strands.

The two rope strands have to be long enough to avoid node 1 or node 3 sliding up to node 2 (the pulley). If this occurs, either node 1 or 3 will be stopped at node 2, just as if there were a knot at the end of the rope.

Figure 5.9.1 Pulley Type Spring Element Representation

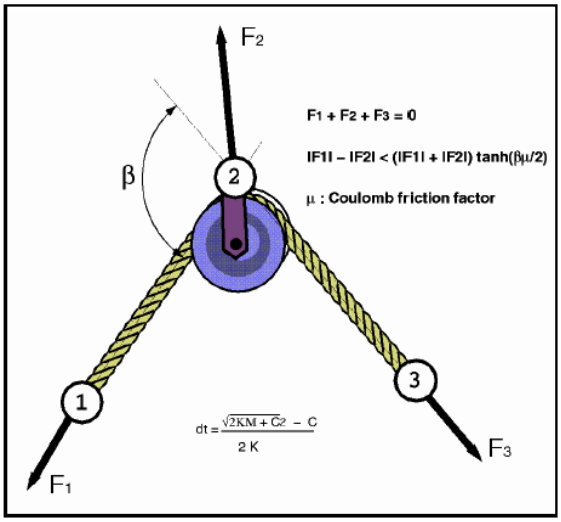

5.9.1 Time step

The time step is calculated using the relation:

$$\Delta t = \frac{\left(\sqrt{2KM + C^2}\right) - C}{2K} \qquad \text{EQ. 5.9.1.1}$$

This is the same as for type 4 spring elements, except that the stiffness is replaced with twice the stiffness to ensure stability with high friction coefficients.

5.9.2 Linear spring

See section 5.7.2; the explanation is the same as for spring type 4.

5.9.3 Nonlinear elastic spring

See section 5.7.3; the explanation is the same as for spring type 4.

5.9.4 Nonlinear elasto-plastic spring - Isotropic hardening

See section 5.7.4; the explanation is the same as for spring type 4.

5.9.5 Nonlinear elasto-plastic spring - Decoupled hardening

See section 5.7.5; the explanation is the same as for spring type 4.

5.9.6 Nonlinear dashpot

See section 5.7.8; the explanation is the same as for spring type 4.

5.9.7 Nonlinear visco-elastic spring

See section 5.7.9; the explanation is the same as for spring type 4.

5.9.8 Friction effects

Pulley type springs can be modeled with or without Coulomb friction effects.

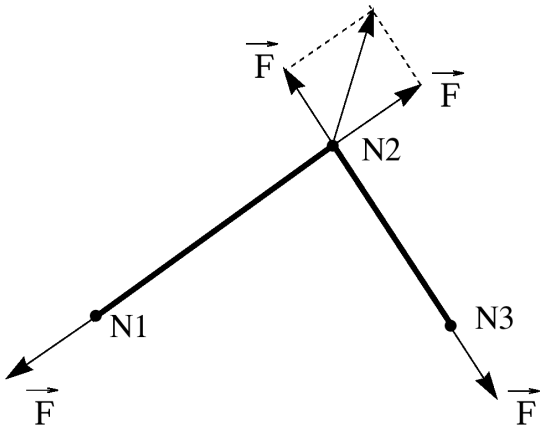

5.9.8.1 Without Friction

Without friction, the forces are computed using:

$$|F_1| = |F_2| = K\delta + C\frac{d\delta}{dt} \qquad \text{EQ. 5.9.8.1}$$

where:

δ is the total rope elongation = $l - l_0$ with $l = l_{12} + l_{23}$

K is the rope stiffness

C is the rope equivalent viscous damping

5.9.8.2 With Coulomb Friction

If Coulomb friction is used, forces are corrected using:

$$F = K(\delta_1 + \delta_2) + C\left(\frac{d\delta_1}{dt} + \frac{d\delta_2}{dt}\right) \qquad \text{EQ. 5.9.8.2}$$

$$\Delta F = \max\left(K(\delta_1 + \delta_2) + C\left(\frac{d\delta_1}{dt} + \frac{d\delta_2}{dt}\right), F\tanh\left(\frac{\beta\mu}{2}\right)\right) \qquad \text{EQ. 5.9.8.3}$$

$$|F_1| = F + \Delta F \qquad \text{EQ. 5.9.8.4}$$

$$|F_3| = F - \Delta F \qquad \text{EQ. 5.9.8.5}$$

$$F_2 = -F_1 - F_3 \qquad \text{EQ. 5.9.8.6}$$

where:

δ1 is the elongation of strand 1-2

δ2 is the elongation of strand 2-3

5.10 BEAM TYPE SPRING ELEMENTS (TYPE13)

Beam type spring elements are defined as property type 13 elements. This type of spring element functions as if it were a beam element. The six independent modes of deformation are:

- Traction / compression
- Torsion
- Bending (two modes)
- Shear (two modes)

Beam type springs only function if their length is not zero. A physical representation of a beam type spring can be seen in Figure 5.10.1.

Figure 5.10.1 Representation of Beam Type Spring

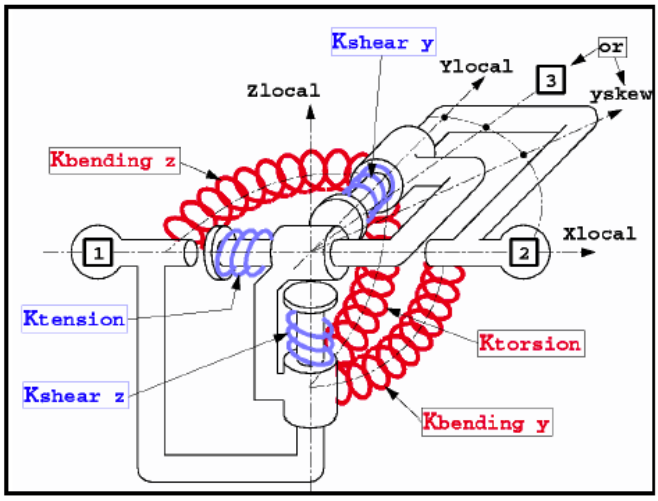

5.10.1 Time step

5.10.1.1 Translational stiffness time step

$$\Delta t_{translational\_stifness} = \frac{\sqrt{mass.\max(Kt) + C_t^2} - C_t}{\max(K_t)}$$

Where, max(Kt) is the maximum translational stiffness
Ct is the translational damping

5.10.1.2 Rotational stiffness time step

$$\Delta t_{rotational\_stifness} = \frac{\sqrt{inertia.K_r^{'} + C_r^{'2}} - C_r^{'}}{K_r^{'}}$$

Kr' is the equivalent rotational stiffness: $K_r^{'} = \max(K_t).L^2 + \max(K_r)$

Where, max(Kt) is the maximum translational stiffness
max(Kr) is the maximum rotational stiffness

Cr' is the equivalent rotational damping: $C_r^{'} = \max(C_t).L^2 + \max(C_r)$

Where,
max(Ct) is the maximum translational damping
max(Cr) is the maximum rotational damping

5.10.2 Linear spring

The properties required to define the spring characteristics are stiffness *K* and damping *C*. Nonlinear and elasto-plastic properties can also be applied, for all degrees of freedom. The properties are of the same form as simple type 4 spring elements (section 5.7).

See section 5.7.2; the explanation is the same as for spring type 4.

5.10.3 Nonlinear elastic spring

See section 5.7.3; the explanation is the same as for spring type 4.

5.10.4 Nonlinear elasto-plastic spring - Isotropic hardening

See section 5.7.4; the explanation is the same as for spring type 4.

5.10.5 Nonlinear elasto-plastic spring - Decoupled hardening

See section 5.7.5; the explanation is the same as for spring type 4.

5.10.6 Nonlinear elasto-plastic spring - Kinematic hardening

See section 5.7.6; the explanation is the same as for spring type 4.

5.10.7 Nonlinear elasto-plastic spring - Nonlinear unloading

See section 5.7.7; the explanation is the same as for spring type 4.

5.10.8 Nonlinear dashpot

See section 5.7.8; the explanation is the same as for spring type 4.

5.10.9 Nonlinear visco-elastic spring

See section 5.7.9; the explanation is the same as for spring type 4.

5.10.10 Skew frame properties

Beam type spring elements are best defined using three nodes (Figure 5.10.2). Nodes 1 and 2 are the two ends of the element and define the local X axis. Node 3 allows the local Y and Z axes to be defined. However, this node does not need to be supplied.

If all three nodes are defined, the local reference frame is calculated by:

$$\vec{x} = \overline{n_1 n_2} \qquad \text{EQ. 5.10.10.1}$$

$$\vec{z} = \vec{x} \times \overline{n_1 n_3} \qquad \text{EQ. 5.10.10.2}$$

$$\vec{y} = \vec{z} \times \vec{x} \qquad \text{EQ. 5.10.10.3}$$

If node 3 is not defined, the local skew frame that can be specified for the element is used to define the Z axis. The X and Y axes are defined in the same manner as before.

$$\vec{z} = \vec{x} \times \vec{y}_{skew} \qquad \text{EQ. 5.10.10.4}$$

If no skew frame and no third node are defined, the global Y axis is used to replace the Y skew axis. If the Y skew axis is collinear with the local X axis, the local Y and Z axes are placed in a totally arbitrary position. The local Y axis is defined at time zero, and is corrected at each cycle, taking into account the mean X axis rotation.

Figure 5.10.2 Element Definition

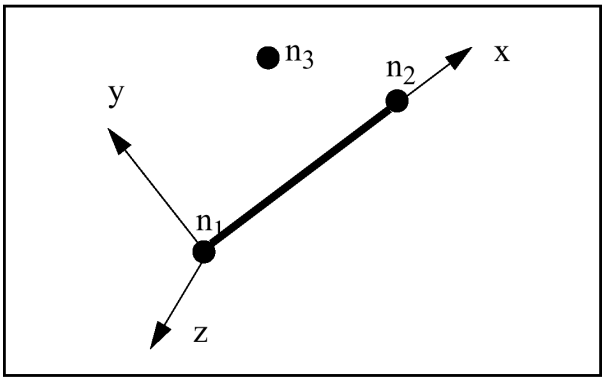

5.10.11 Sign Conventions

The sign convention used for defining positive displacements and forces can be seen in Figure 5.10.3.

Figure 5.10.3 Sign Conventions

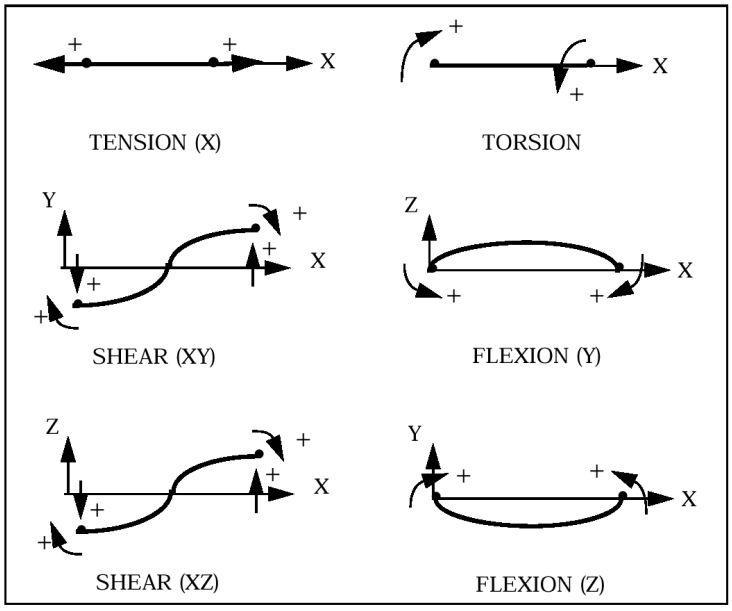

5.10.12 Tension

The tension component of the beam type spring element is independent of other forces. It is shown in Figure 5.10.4. The tension at each node is computed by:

$$F_{x1} = f_x(u_x) + C_x \dot{u}_x \qquad \text{EQ. 5.10.12.1}$$

$$F_{x2} = -F_{x1} \qquad \text{EQ. 5.10.12.2}$$

where

$u_x = u_{x2} - u_{x1}$ is the relative displacement of nodes 1 and 2.

$f_x(u_x)$ is the function defining the force-displacement relationship.

It can be linear or nonlinear (see sections 5.7.2 to 5.7.5.).

Figure 5.10.4 Spring Tension

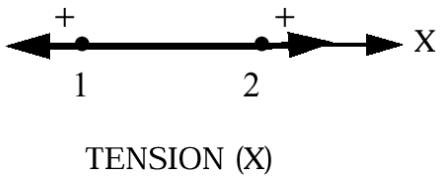

5.10.13 Shear - XY

Shear in the Y direction along the face perpendicular to the X axis is a combination of forces and moments. This can be seen in Figure 5.10.5.

Figure 5.10.5 XY Shear Forces and Moments

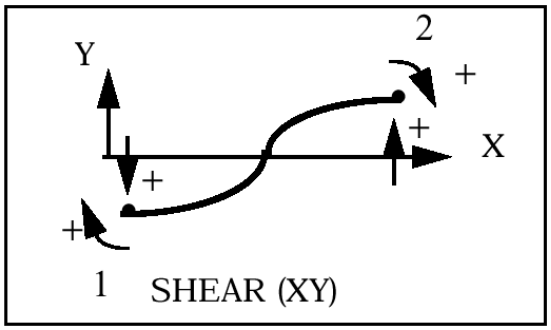

There are two mechanisms that can cause shear. The first is the beam double bending as shown in Figure 5.10.5. The second is shear generated by node displacement, as shown in Figure 5.10.6, where node 2 is displaced.

Figure 5.10.6 Shear due to Node Displacement

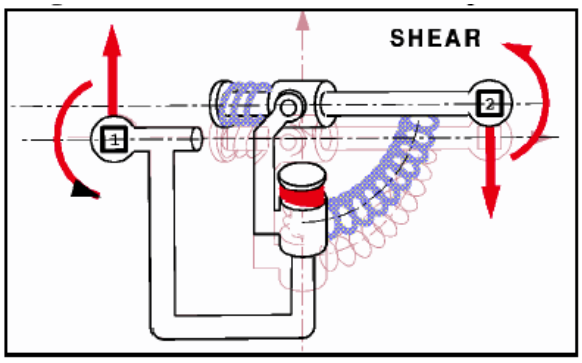

The forces and moments are calculated by:

$$F_{y1} = f_y(u_y) + C_y \dot{u}_y \quad \text{EQ. 5.10.13.1}$$

$$F_{y2} = -F_{y1} \quad \text{EQ. 5.10.13.2}$$

$$M_{z1} = -lF_{y2} \quad \text{EQ. 5.10.13.3}$$

$$M_{z2} = M_{z1} \quad \text{EQ. 5.10.13.4}$$

where:

$$u_y = u_{y2} - u_{y1} - l\left(\frac{\theta_{z2} + \theta_{z1}}{2}\right)$$

$f_y(u_y)$ is the function defining the force-displacement relationship.

5.10.14 Shear - XZ

The XZ shear is orthogonal to the XY shear described in the previous section. The forces and moments causing the shear can be seen in Figure 5.10.7.

Figure 5.10.7 XZ Shear Forces and Moments

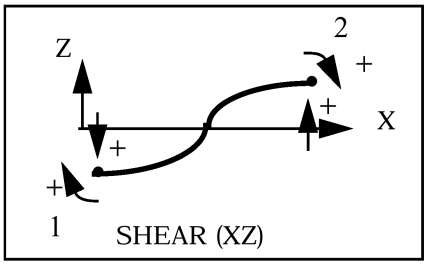

The forces and moments are calculated by:

$$F_{z1} = f_z(u_z) + C_z \dot{u}_z \quad \text{EQ. 5.10.14.1}$$

$$F_{z2} = -F_{z1} \quad \text{EQ. 5.10.14.2}$$

$$M_{y1} = lF_{z2} \quad \text{EQ. 5.10.14.3}$$

$$M_{y2} = M_{y1} \quad \text{EQ. 5.10.14.4}$$

Where,

$$u_z = u_{z2} - u_{z1} + l\left(\frac{\theta_{y2} + \theta_{y1}}{2}\right)$$

$f_z(u_z)$ is the function defining the force-displacement relationship.

5.10.15 Torsion

Torsional forces, shown in Figure 5.10.8, are calculated using the relations:

$$M_{x1} = f_{xx}(\theta_x) + C_{xx}\dot{\theta}_x \quad \text{EQ. 5.10.15.1}$$

$$M_{x2} = -M_{x1} \quad \text{EQ. 5.10.15.2}$$

where:

$\theta_x = \theta_{x2} - \theta_{x1}$ is the relative rotation of node 1 and 2.

$f_{xx}(\theta_x)$ is the function defining the force-displacement relationship.

Figure 5.10.8 Beam Type Spring Torsion

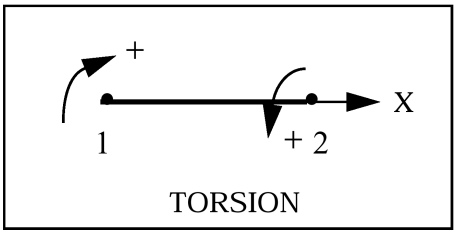

5.10.16 Bending about the Y Axis

Bending about the Y axis can be seen in Figure 5.10.9. The equations relating to the moments being produced are calculated by:

$$M_{y1} = f_{yy}(\theta_y) + C_{yy}\dot{\theta}_y \quad \text{EQ. 5.10.16.1}$$

$$M_{y2} = -M_{y1} \quad \text{EQ. 5.10.16.2}$$

where:

$\theta_y = \theta_{y2} - \theta_{y1}$ is the relative rotation of node 1 and 2.

$f_{yy}(\theta_y)$ is the function defining the force-displacement relationship.

Figure 5.10.9 Bending about Y axis

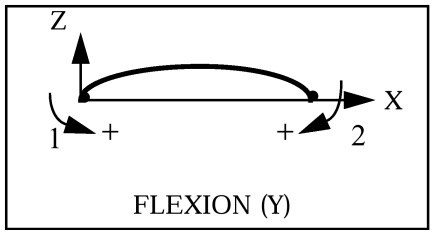

5.10.17 Bending about the Z Axis

The equations relating to the moment generated in a beam type spring element and the beam's displacement, (Figure 5.10.10) is given by:

$$M_{z1} = f_{zz}(\theta_z) + C_{zz}\dot{\theta}_z \quad \text{EQ. 5.10.17.1}$$

$$M_{z2} = -M_{z1} \quad \text{EQ. 5.10.17.2}$$

where $\theta_z = \theta_{z2} - \theta_{z1}$ is the relative rotation of node 1 and 2.

$f_{zz}(\theta_z)$ is the function defining the force-displacement relationship.

Figure 5.10.10 Bending about Z axis

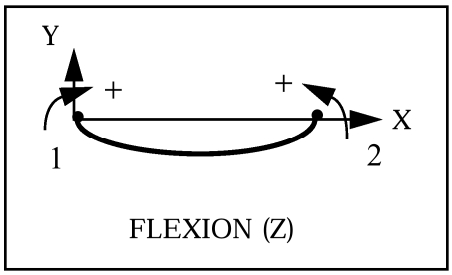

5.10.18 Multidirectional failure criteria

See Section 5.8.14; the explanation is the same as for spring type 8.

5.11 MULTISTRAND ELEMENTS (TYPE 28)

5.11.1 Introducing Multistrand Elements

Multistrand elements are n-node springs where matter is assumed to slide through the nodes. It could be used for belt modelization by taking nodes upon the dummy. Friction may be defined at all or some nodes. When nodes are taken upon a dummy in order to modelize a belt, this allows friction to be modelized between the belt and the dummy.

5.11.2 Internal Forces Computation

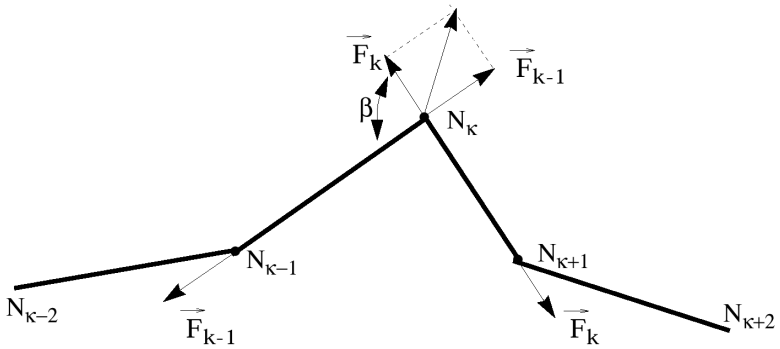

Nodes are numbered from 1 to n, and strands are numbered from 1 to n-1 (strand k goes from node N_k to node N_{k+1}).

5.11.2.1 Averaged force into multistrand element

The averaged force in the multistrand is computed as:

Linear spring $F = \frac{K}{L^0}\delta + \frac{C}{L^0}\dot{\delta}$

Non linear spring $F = f(\varepsilon)\cdot g(\dot{\varepsilon}) + \frac{C}{L^0}\dot{\delta}$

or $F = f(\varepsilon) + \frac{C}{L^0}\dot{\delta}$ if *g* function identifier is 0

or $F = g(\dot{\varepsilon}) + \frac{C}{L^0}\dot{\delta}$ if *f* function identifier is 0

where, ε is engineering strain: $\varepsilon = \frac{L - L^0}{L^0}$

L^0 is the reference length of element.

5.11.2.2 Force into each strand

The force into each strand k is computed as:

$F_k = F + \Delta F_k$

ΔF_k is computed an incremental way:

$$\Delta F_k(t) = \Delta F_k(t-1) + \frac{K}{l_k^0}\delta\varepsilon_k - \frac{K}{L^0}\delta\varepsilon \qquad \text{EQ. 5.11.2.1}$$

with l_k^0 the length of the unconstrained strand k, $\delta\varepsilon = \varepsilon(t) - \varepsilon(t-1)$ and $\delta\varepsilon_k = \delta u_k \cdot (v_{k+1} - v_k)$,

where u_k is the unitary vector from node N_k to node N_{k+1} .

Assuming:

$$\frac{l_k}{l_k^0} = \frac{L}{L^0} \qquad \text{EQ. 5.11.2.2}$$

where l_k is the actual length of strand *k*.

Therefore, EQ. 5.11.2.1 reduces to:

$$\Delta F_k(t) = \Delta F_k(t-1) + \frac{K}{l^0}\left(\delta\varepsilon_k \frac{L}{l_k} - \delta\varepsilon\right) \qquad \text{EQ. 5.11.2.3}$$

5.11.2.3 Friction

Friction is expressed at the nodes: if μ is the friction coefficient at node *k*, the pulley friction at node N_k is expressed as:

$$\left|\Delta F_{k-1} - \Delta F_k\right| \le \left(2F + \Delta F_{k-1} + \Delta F_k\right)\tanh\left(\frac{\beta\mu}{2}\right) \qquad \text{EQ. 5.11.2.4}$$

When equation 5.11.2.4 is not satisfied, $\left|\Delta F_{k-1} - \Delta F_k\right|$ is reset to $\left(2F + \Delta F_{k-1} + \Delta F_k\right)\tanh\left(\frac{\beta\mu}{2}\right)$.

All the ΔF_k (k=1,n-1) are modified in order to satisfy all conditions upon $\Delta F_{k-1} - \Delta F_k$ (k=2,n-1), plus the following condition on the force integral along the multistrand element:

$$\sum_{k=1,n-1} l_k\left(F + \Delta F_k\right) = LF \qquad \text{EQ. 5.11.2.5}$$

This process could fail to satisfy equation 5.11.2.4 after the $\Delta F_k\,(k = 1, n-1)$ modification, since no iteration is made. However, in such a case one would expect the friction condition to be satisfied after a few time steps.

Note: Friction expressed upon strands (giving a friction coefficient μ along strand k) is related to pulley friction by adding a friction coefficient $\mu/2$ upon each nodes N_k and N_{k+1} .

5.11.2.4 Time step

Stability of a multistrand element is expressed as:

$$\Delta t \le \frac{\sqrt{C_k^2 + \rho l_k K_k} - C_k}{K_k}, \forall k \qquad \text{EQ. 5.11.2.6}$$

with $K_k = \dfrac{Mass\ of\ \ the\ multistrand}{L^0}$ and (assuming 9.2.2.2) :

$$K_k = \max\left(\frac{K}{l_k^0}, \frac{F}{l_k - l_k^0}\right) = \max\left(\frac{KL}{l_k L^0}, \frac{FL}{l_k\left(L - L^0\right)}\right) \qquad \text{EQ. 5.11.2.7}$$

$$C_k = \frac{\left(f(\varepsilon)\dfrac{dg}{d\dot{\varepsilon}}(\dot{\varepsilon}) + C\right)}{l_k^0} = \left(f(\varepsilon)\frac{dg}{d\varepsilon}(\dot{\varepsilon}) + C\right)\frac{L}{l_k L^0} \qquad \text{EQ. 5.11.2.8}$$

5.12 SPRING TYPE PRETENSIONER (TYPE 32)

5.12.1 Introducing pretensioners

Pretensioner expected behavior is as follows: before pretensioning, a piston is fixed in its initial position; when activated, the piston is pushed and cannot slide once the piston has reached the end of its slide, it is unable to slide further in any direction in the opposite direction from its actual position.

5.12.2 RADIOSS model for pretensioners

5.12.2.1 Linear model

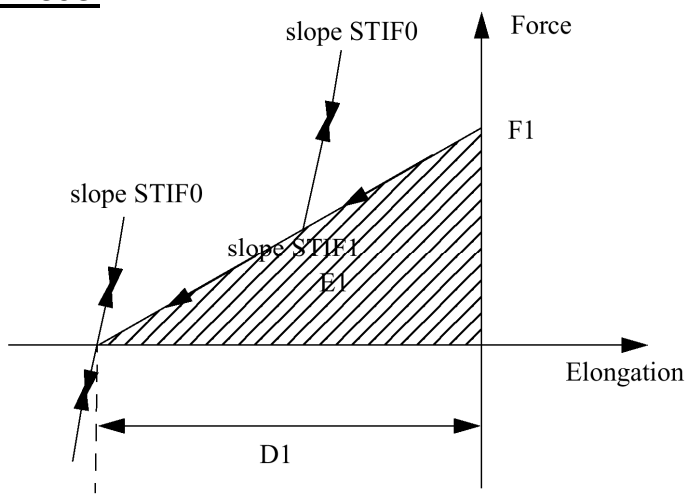

STIF0 is the spring stiffness before sensor activation. At sensor activation, the 2 input coefficients among D1, STIF1, F1 and E1 determine the pretensioner characteristics. Let us recall the following relations between the 4 coefficients:

$$E_1 = \frac{D_1 \cdot F_1}{2}, K_1 = \frac{F_1}{D_1}$$ EQ. 5.12.2.1

STIF0 is also used as unloading stiffness before the end of the piston's slide, and as both loading and unloading stiffness at the end of the piston's slide. STIF0 should be large enough to allow locking.

5.12.2.2 Nonlinear model

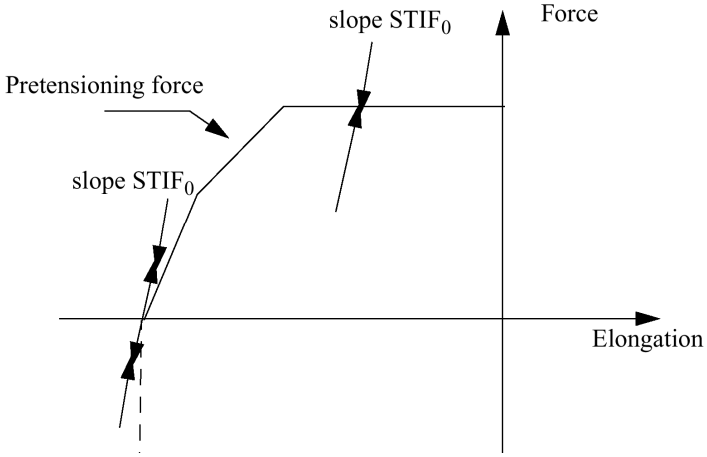

STIF0 is spring stiffness before sensor activation. Depending on the input, pretensioning force is defined as f(L-L_0), with either g(t-t_0), or f(L-L_0).g(t-t_0), with L_0 length of the spring at sensor activation time and at t_0 sensor activation time.

Similar use of $STIF_0$ allows piston locking.

5.12.2.3 Force computation

Let the pretensioning force $F_p(t) = F_1 + STIF_1 \cdot (L(t) - L_0)$ for a linear model,

and $F_p(t) = f(L(t) - L_0)$ or $g(t - t_0)$ or $f(L(t) - L_0) \cdot g(t - t_0)$ for a nonlinear model.

The force into the pretensioner spring is computed as: EQ. 5.12.2.2

if, $F_p(t + dt) \geq 0$

$$F(t + dt) = Max(F_p(t + dt), F(t) + STIF_0 \cdot L(t + dt) - L(t))$$

and $F(t + dt) = F(t) + STIF_0 \cdot (L(t + dt) - L(t))$ otherwise.